



**Calhoun: The NPS Institutional Archive**

---

Theses and Dissertations

Thesis Collection

---

2001-09

## Mine Drop Experiment (MIDEX)

Gilless, Anthony F.

Monterey, California. Naval Postgraduate School

---

<http://hdl.handle.net/10945/1594>



Calhoun is a project of the Dudley Knox Library at NPS, furthering the precepts and goals of open government and government transparency. All information contained herein has been approved for release by the NPS Public Affairs Officer.

**Dudley Knox Library / Naval Postgraduate School**  
**411 Dyer Road / 1 University Circle**  
**Monterey, California USA 93943**

<http://www.nps.edu/library>

# NAVAL POSTGRADUATE SCHOOL Monterey, California



## THESIS

**MINE DROP EXPERIMENT (MIDEX)**

by

Anthony Gilles

September 2001

Thesis Advisor:  
Second Reader:

Peter Chu  
Peter Fleischer

**Approved for public release; distribution is unlimited**

<b>REPORT DOCUMENTATION PAGE</b>			<i>Form Approved OMB No. 0704-0188</i>	
Public reporting burden for this collection of information is estimated to average 1 hour per response, including the time for reviewing instruction, searching existing data sources, gathering and maintaining the data needed, and completing and reviewing the collection of information. Send comments regarding this burden estimate or any other aspect of this collection of information, including suggestions for reducing this burden, to Washington headquarters Services, Directorate for Information Operations and Reports, 1215 Jefferson Davis Highway, Suite 1204, Arlington, VA 22202-4302, and to the Office of Management and Budget, Paperwork Reduction Project (0704-0188) Washington DC 20503.				
<b>1. AGENCY USE ONLY (Leave blank)</b>		<b>2. REPORT DATE</b> September 2001	<b>3. REPORT TYPE AND DATES COVERED</b> Master's Thesis	
<b>4. TITLE AND SUBTITLE:</b> Mine Drop Experiment (MIDEX)			<b>5. FUNDING NUMBERS</b> N0001401WR20239	
<b>6. AUTHOR(S)</b> Gillless, Anthony F.				
<b>7. PERFORMING ORGANIZATION NAME(S) AND ADDRESS(ES)</b> Naval Postgraduate School Monterey, CA 93943-5000			<b>8. PERFORMING ORGANIZATION REPORT NUMBER</b>	
<b>9. SPONSORING / MONITORING AGENCY NAME(S) AND ADDRESS(ES)</b> NAVOCEANO, Stennis Space Center, MS 39522-5001 Institute of Joint Warfare Analysis, NPS, Monterey, CA 93943			<b>10. SPONSORING / MONITORING AGENCY REPORT NUMBER</b>	
<b>11. SUPPLEMENTARY NOTES</b> The views expressed in this thesis are those of the author and do not reflect the official policy or position of the Department of Defense or the U.S. Government.				
<b>12a. DISTRIBUTION / AVAILABILITY STATEMENT</b> Approved for public release, distribution is unlimited.			<b>12b. DISTRIBUTION CODE</b>	
<b>13. ABSTRACT (maximum 200 words)</b>  The Navy's Impact Burial Prediction Model (IMPACT 25) determines the amount of burial a mine experiences upon impacting the marine sediment. Impact burial calculations are derived primarily from the sediment characteristics and from the mine's two-dimensional air and water phase trajectories. Accurate burial prediction requires that the model's air and water phase trajectories reasonably mimic the objects true trajectory. IMPACT 25 assumes that the objects are cylindrical in shape and calculates the air and water phase trajectories entirely from momentum equations.  In order to determine what effect a varying center of mass has on a mine's water phase trajectory, a Mine Drop Experiment was conducted. The experiment consisted of dropping three cylinders of various lengths into a pool where the trajectories were filmed from two angles. The controlled parameters were, the ratio of mine length to diameter, initial velocity, center of mass position and drop angle. Results indicate that center of mass position has the largest influence on the object's trajectory and that accurate trajectory modeling requires the inclusion of both momentum and moment equations.				
<b>14. SUBJECT TERMS</b> Mine Impact Burial, Hydrodynamics, IMPACT 25, Bottom Mine, Mine Countermeasures, Mine Trajectory			<b>15. NUMBER OF PAGES</b> 125	
			<b>16. PRICE CODE</b>	
<b>17. SECURITY CLASSIFICATION OF REPORT</b> Unclassified	<b>18. SECURITY CLASSIFICATION OF THIS PAGE</b> Unclassified	<b>19. SECURITY CLASSIFICATION OF ABSTRACT</b> Unclassified	<b>20. LIMITATION OF ABSTRACT</b> UL	

THIS PAGE INTENTIONALLY LEFT BLANK

Approved for public release; distribution is unlimited

**Mine Drop Experiment (MIDEX)**

Anthony F. Gilles  
Lieutenant, United States Navy  
B.S., United States Naval Academy, 1993

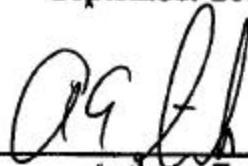
Submitted in partial fulfillment of the  
requirements for the degree of

**MASTER OF SCIENCE IN  
METEOROLOGY AND PHYSICAL OCEANOGRAPHY**

from the

**NAVAL POSTGRADUATE SCHOOL  
September 2001**

Author:

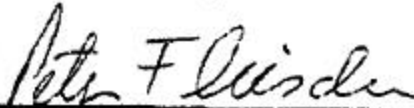


Anthony F. Gilles

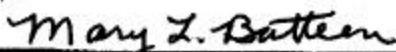
Approved by:



Peter Chu, Thesis Advisor



Peter Fleischer, Second Reader



Mary L. Batteen, Chairman  
Department of Oceanography

THIS PAGE INTENTIONALLY LEFT BLANK

## **ABSTRACT**

The Navy's Impact Burial Prediction Model (IMPACT 25) determines the amount of burial a mine experiences upon impacting the marine sediment. Impact burial calculations are derived primarily from the sediment characteristics and from the mine's two-dimensional air and water phase trajectories. Accurate burial prediction requires that the model's air and water phase trajectories reasonably mimic the objects true trajectory. IMPACT 25 assumes that the objects are cylindrical in shape and calculates the air and water phase trajectories entirely from momentum equations.

In order to determine what effect a varying center of mass has on a mine's water phase trajectory, a Mine Drop Experiment was conducted. The experiment consisted of dropping three cylinders of various lengths into a pool where the trajectories were filmed from two angles. The controlled parameters were, the ratio of mine length to diameter, initial velocity, center of mass position and drop angle. Results indicate that center of mass position has the largest influence on the object's trajectory and that accurate trajectory modeling requires the inclusion of both momentum and moment equations.

THIS PAGE INTENTIONALLY LEFT BLANK



# TABLE OF CONTENTS

I.	INTRODUCTION.....	1
II.	MINE DROP EXPERIMENT (MIDEX) .....	5
A.	PREPARATION .....	5
1.	Mine Shapes and Center of Mass Positions .....	5
2.	Model Mine Scaling .....	6
3.	Initial Velocity .....	6
4.	Drop Angle.....	7
5.	Coordinate System.....	7
B.	METHODOLOGY .....	8
III.	DATA RETREIVAL AND ANALYSIS.....	11
A.	DATA RETREIVAL .....	11
B.	SOURCES OF ERROR.....	11
C.	DATA ANALYSIS .....	11
1.	2-D Plots .....	12
2.	Impact Attitude .....	12
3.	Impact Point Locations .....	12
IV.	DYNAMICS OF A CYLYNDRICAL MINE.....	15
A.	TWO COORDINATE SYSTEMS.....	15
B.	HYDRODYNAMIC THEORY OF MINE IMPACT BURIAL .....	15
C.	PHYSICAL CHARACTERISTICS OF MINE.....	19
D.	INITIAL CONDITIONS IN MIDEX.....	19
V.	RESULTS .....	21
A.	TRAJECTORY PATTERNS.....	21
B.	IMPACT ATTITUDE .....	21
C.	IMPACT POINTS .....	24
D.	MULTIPLE LINEAR REGRESSION ANALYSIS .....	24
VI.	DISCUSSION .....	27
VII.	CONCLUSIONS .....	31
	APPENDIX A. 2-D PLOTS.....	33
	APPENDIX B. HISTOGRAM PLOTS .....	108
	APPENDIX C. IMPACT POINTS .....	117
	APPENDIX D. IMPACT DATA TABLES .....	125
	LIST OF REFERENCES .....	131
	INITIAL DISTRIBUTION LIST .....	133

THIS PAGE INTENTIONALLY LEFT BLANK

## LIST OF FIGURES

Figure 1. Littoral Mine Threat. From Rhodes, 1998.....	3
Figure 2. Equipment used. A denotes drop angle device, B mine injector, C infrared light sensor, D output to universal counter, E mine shapes. ....	5
Figure 3. Internal Components of Mine Shape .....	5
Figure 4. Mine Shape Characteristics. The leftmost column indicates COM position 0, while the rightmost indicates COM position 2. ....	6
Figure 5. Earth Coordinate System. ....	7
Figure 6. Mine's Coordinate System. $\psi$ is the attitude or angle in the z-plane .....	8
Figure 7. Background grid. Affixed to x, -z and -y, -z planes. ....	9
Figure 8. Example of Flat Trajectory. ....	13
Figure 9. Impact Angles for all cases.....	13
Figure 10. Impact Points for all cases and conditions. The yellow areas represent the cameras used. ....	14
Figure 11. Mine Coordinate System. The axis $r_3$ originates at CG and comes out of the page towards the viewer. CB is the center of buoyancy (volumetric center) of the mine. ....	15
Figure 12. Mine Motion without Consideration of Moment Equation. ....	16
Figure 13. Mine Motion with Consideration of both Momentum and Moment Equations. ....	17
Figure 14a. Trajectory Examples. ....	22
Figure 14b. Trajectory Examples.....	23
Figure 15. Relationship between COM Position and Impact Attitude. ....	23

THIS PAGE INTENTIONALLY LEFT BLANK

## LIST OF TABLES

Table 1. Number of Drops Conducted by Drop Angle and COM Position.....	9
Table 2. Commonly used non-dimensional COM positions. Non-dimensional COM positions determined using $\frac{2M}{L}$ , where M is given in Figure 4.....	12
Table 3. Description of Mine Coordinate Based Trajectory Patterns .....	21
Table 4. Multiple Linear Regression Analysis Correlation Coefficients.....	24
Table 5a. Observed Trajectory Patterns for COM Position 2.....	27
Table 5b. Observed Trajectory Patterns for COM Position 1.....	28
Table 5c. Observed Trajectory Patterns for COM Position 0.....	28
Table 5d. Observed Trajectory Patterns for Negative COM Cases.....	28
Table 6. IMPACT 25 Derived Impact Angles.....	29

THIS PAGE INTENTIONALLY LEFT BLANK

## TABLE OF SYMBOLS

$CB$	=	Center of buoyancy (volumetric center)
$CG$	=	Center of gravity
$COM$	=	Center of Mass
$D$	=	Mine Circular Diameter
$F_b$	=	Buoyancy Force
$F_d$	=	Drag Force
$g$	=	Gravitational Force
$L$	=	Mine length
$M$	=	Distance from $CB$ to center of internal weight
$M^*$	=	Resultant Moment of Momentum
$r_1, r_2, r_3$	=	Mine coordinate system
$t$	=	time
$t^*$	=	Non-dimensional time
$V_{init}$	=	Mine's initial velocity prior to impacting water
$\beta$	=	Correlation coefficients
$\psi_1, \psi_2, \psi_3$	=	Mine's angle with vertical axis
$\rho_m$	=	Density of mine
$\rho_w$	=	Density of water
$\omega^*$	=	Angular velocity
$J$	=	Moment of gyration

THIS PAGE INTENTIONALLY LEFT BLANK



## **ACKNOWLEDGMENT**

The author gratefully acknowledges the financial support of the Naval Oceanographic Office, Office of Naval Research and the Institute of Joint Warfare Analysis. This work was performed under contract number N0001401WR20239. I would like to acknowledge and thank Prof. Peter Chu for his patience and guidance. Additionally, a special thanks goes out to the many persons who have provided assistance in the conduct of this experiment. Namely, Chenwu Fan, "MATLAB God"; ET1 Adam Dummer, assisted in construction and provided lifeguard services; Marla Stone, provided digital still photography and logistical support; and George Jaksha, who provided last minute mine model changes.

THIS PAGE INTENTIONALLY LEFT BLANK

## I. INTRODUCTION

On December 31, 1991 the Union of Soviet Socialist Republics (USSR) effectively ceased to exist under international law and the Cold War ended (Fischer 1999). In response, the Navy-Marine Corps team developed a new strategic concept, "...From the Sea" (FTS), which provides a framework for Naval operations into the 21<sup>st</sup> century. FTS effectively shifted operational focus from blue water operations to sea-based power projection into regional littoral areas. FTS, the 1994 revision "Forward ... From the Sea" (FFTS) and "Operational Maneuver from the Sea" (OMFTS) all provide guiding principles for sea-based power projection to regional littoral areas of the world.

One of the greatest threats to U.S. sea-based power projection in littoral areas is the naval mine. Mines were first developed in 1776 and have been used in most major conflicts since. Today, an estimated 50 countries possess some sort of mining capability. (Lehr 2000) Mines can be used in both offensive and defensive roles. Offensively, they can be placed in enemy waters or nearby sea-lanes in order to harass military and commercial shipping. Defensively, they can be used to delay or prevent amphibious assaults or to deny command of the sea. The Wonsan Korea Mine Crisis and Iraq's use of mines during Desert Storm provide excellent examples of the value of the naval mine as a defensive weapon. Shortly after the October 1950 Wonsan, Korea mine crisis, then Chief of Naval Operations Admiral Forest Sherman exclaimed,

" ... when you can't go where you want to, when you want to, you haven't got command of the sea. Command of the sea is the bedrock for all of our war plans. We have always been submarine-conscious and air-conscious. We have now commenced to become mine-conscious... beginning last week." (Boorda 1999).

Within the past 15 years three U.S. ships, the USS Samuel B. Roberts (FFG-58), Tripoli (LPH-10) and Princeton (CG-59) have fallen victim to mines. Total ship damages were \$125 million while the mines cost approximately \$30 thousand. (Boorda 1999) Mines have evolved over the years from the dumb "horned" contact mines that damaged the Tripoli and Roberts to ones that are relatively sophisticated - non-magnetic materials, irregular shapes, anechoic coatings, multiple sensors and ship count routines. Despite

their increased sophistication, mines remain inexpensive and are relatively easy to manufacture, upkeep and place. As such, they are an efficient, yet potent, force multiplier and are widely available to any country or group who has a modest ability to purchase them.

Naval mines are characterized by three factors: position in water (bottom, moored, rising, floating), method of delivery (aircraft, surface, subsurface) and method of actuation (acoustic and/or magnetic influence, pressure, contact, controlled). The littoral battlespace is divided into five regions based upon water depth. Within each of these regions naval forces can encounter multiple types of threats (Fig. 1). The littoral regions are:

- Deep Water (DW). Water depths: >300 ft. Threat: mainly moored and rising mines, although a few large bottom mines exist.
- Shallow Water (SW). Water depths: from 40 to 300 ft. Threat: bottom, moored and rising.
- Very Shallow Water (VSW). Water depths: from 10 to 40 ft. Threat: bottom, moored, rising and controlled.
- Surf Zone (SZ). Water depths: < 10 ft. to the beach itself. Threat: same as VSW but land mines and obstacles can also be encountered.
- Craft Landing Zone (CLZ). Water depths: the beach itself. Threat: conventional land mines and obstacles. (U.S. Naval Mine Warfare Plan 2000)

The shift in focus from the blue water to the littoral has brought many new challenges to the warfighter. The greatest is what impact will the highly variable littoral environment have on future operations, particularly mine countermeasures (MCM). The most influential environmental parameter to successful MCM operations is the local bathymetry character of the bottom. This key parameter often determines whether an area should be swept or hunted. Bottom clutter in the form of rock outcrops, coral reefs, man-made debris and irregularities in slope provide false contacts or create shadow zones that increase overall clearance times. Soft bottom sediments such as marine clays and silts cause a high degree of mine burial upon impact. These buried or partially buried bottom mines are of greatest concern to the MCM planner.



Figure 1. Littoral Mine Threat. From Rhodes, 1998.

Environmental data collection in a potential adversaries' littoral region is often hampered by inaccessibility. This lack of accurate data causes a certain degree of uncertainty in MCM planning. As a result, several numerical models for predicting mine impact burial (IB) have been developed. The most promising IB model was originally developed by Arnone and Bowen in 1980. Later improvements by Satkowiak (1987), Hurst (1992) and others have resulted in the current version, IMPACT 25. IMPACT 25 creates a two-dimensional time history of a cylindrical mine as it falls through air, water and sediment phases. IB prediction is largely calculated from the marine sediment characteristics and mine impact orientation and velocity.

Several studies with regard to IB have been conducted over the years. Taber (1999), Smith (2000) and Lott (1995) conducted experiments to verify the IMPACT 25 sediment phase calculations. However, accurate IB prediction also requires that the mine's trajectory through the air and water phases is adequately accounted for. IMPACT 25 approximates mine shape as a cylinder, includes a torque adjustment for cases where COM does not coincide with the center of buoyancy and calculates the air and water phase trajectories entirely from momentum equations. As a result, calculated trajectories tend to be arc shaped and lack movement of the mine about its own axis. In order to

examine what effect a varying center of mass has on a mine's water phase trajectory, the first in a series of Mine Drop Experiments (MIDEX) was conducted in June 2001.

## II. MINE DROP EXPERIMENT (MIDEX)

### A. PREPARATION

MIDEX basically consisted of dropping each of three right cylinders into the water where each drop was recorded underwater from two viewpoints. The controlled parameters for each drop were: center of mass position (COM), initial velocity ( $V_{init}$ ), drop angle and the ratio of mine's length to diameter. Figure 2 depicts the overall setup.

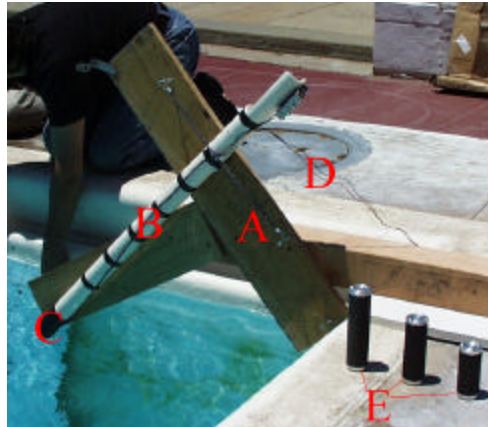


Figure 2. Equipment used. A denotes drop angle device, B mine injector, C infrared light sensor, D output to universal counter, E mine shapes.

#### 1. Mine Shapes and Center of Mass Positions

Three mine shapes were used for the experiment. All had a circular diameter of 4 cm, however the lengths were 15, 12 and 9 cm respectively. The bodies were constructed of rigid plastic with aluminum-capped ends. Inside each was a threaded bolt, running lengthwise across the mine, and an internal weight (Fig 3). The internal weight was used to vary the mine's COM and could be adjusted fore or aft.



Figure 3. Internal Components of Mine Shape

COM positions were denoted using 2, 1, 0, -1, -2. COM 0 cases were identical to the IMPACT 25 model's uniform density assumption (COM = CB). All other cases indicated the relative position of the COM to the CB. Figure 4 displays the various measurements for each COM position.

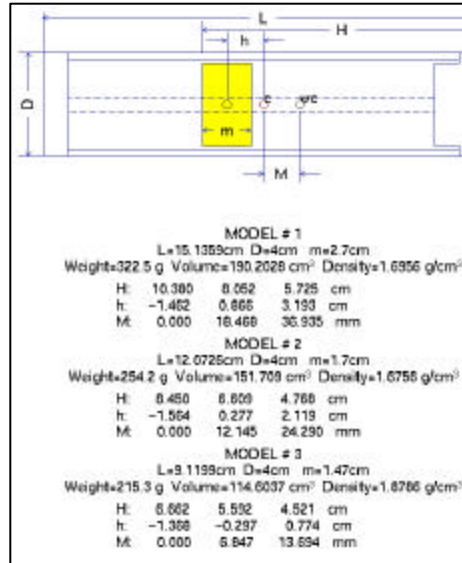


Figure 4. Mine Shape Characteristics. The leftmost column indicates COM position 0, while the rightmost indicates COM position 2.

## 2. Model Mine Scaling

Our goal was to choose a scale that was somewhat representative of the real world ratio of water depth to mine length, but at the same time would be large enough to film and would not damage the pool's bottom. The model mines were based on the realistic assumption that a 3 m mine is laid in water depths of 45 m, thus producing a 15:1 ratio. This ratio was close to our baseline 15 cm mine being dropped into a pool of 2.4 m depth. The addition of a 12 and 9 cm length allowed for later comparison of the sensitivity of water phase trajectory to the ratio of mine length over diameter.

## 3. Initial Velocity

Initial velocity was calculated by using the voltage return of an infrared photo detector located at the base of the mine injector. The infrared sensor produced a square wave pulse when no light was detected due to blockage caused by the mine's passage. The length of the square wave pulse was converted into time by using a universal counter. Dividing the mine's length by the universal counter's time yielded  $V_{init}$ . The



mines were dropped from several positions within the injector mechanism in order to produce a range of  $V_{init}$ .

The method used to determine  $V_{init}$  required that the infrared light sensor be located above the water's surface. This distance was held fixed throughout the experiment at 10 cm.

#### 4. Drop Angle

Drop angle was controlled using the drop angle device. Five screw positions marked the 15, 30, 45, 60, and 75-degree positions. The drop angles were determined from the lay of the pool walkway, which was assumed to be parallel to the water's surface.

A range of drop angles was chosen to represent the various entry angles that air and surface laid mines exhibit. This range produced velocities whose horizontal and vertical components varied in magnitude. This allowed for comparison of mine trajectory sensitivity with the varying velocity components.

#### 5. Coordinate System

Two coordinate systems are used to describe the mine falling through the water column. The first is the earth's coordinate system that follows the right hand rule (Fig 5) and the second is the mine's coordinate system that remains rigidly connected to the mine (Fig 6). Chapter IV provides a more detailed explanation of the coordinate systems used.

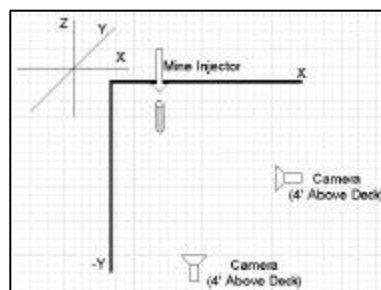


Figure 5. Earth Coordinate System.

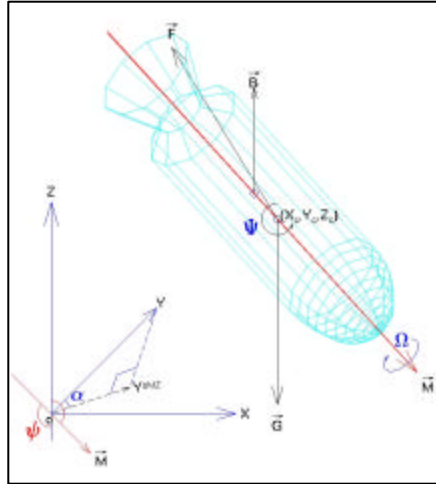


Figure 6. Mine's Coordinate System.  $\psi$  is the attitude or angle in the z-plane

Two 10 cm grids were affixed to each pool wall. Each grid was constructed out of fiberglass and was used to record the mine's position in the x, -z and -y, -z planes (Fig 7).

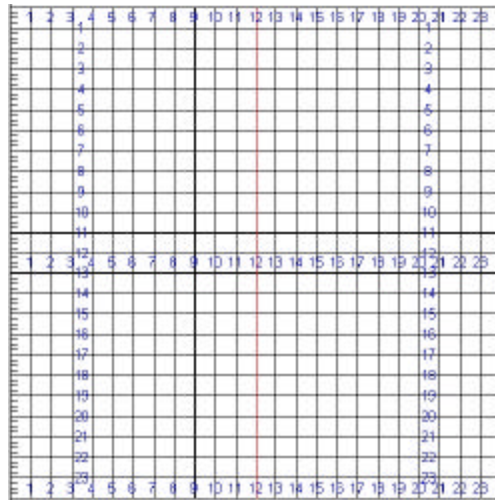


Figure 7. Background grid. Affixed to x, -z and -y, -z planes

## B. METHODOLOGY

For each run the mines were set to a COM position. For positive COM cases, the mines were placed into the injector so that the COM was located below the center of buoyancy. For negative cases, the COM was located above the center of buoyancy prior to release. A series of drops were then conducted in order of decreasing mine length for each angle, starting at  $15^\circ$  (Table 1). Each video camera had a film time of approximately

one hour. At the end of the day, the tapes were replayed in order to determine clarity and optimum camera position.

Drop Angle →	15°	30°	45°	60°	75°
COM Position					
2	13	15	15	15	12
1	9	15	15	15	9
0	12	15	14	18	6
-1	0	6	6	6	0
-2	2	6	6	0	0

Table 1. Number of Drops Conducted by Drop Angle and COM Position

THIS PAGE INTENTIONALLY LEFT BLANK

### **III. DATA RETREIVAL AND ANALYSIS**

#### **A. DATA RETREIVAL**

Upon completion of the drop phase, the video from each camera was converted to digital format. The digital video for each view was then analyzed frame by frame (30 Hz) in order to determine the mine's position in the x, -z and -y, -z planes. The mine's top and bottom positions were input into a MATLAB generated grid, similar to the ones within the pool. The first point to impact the water was always plotted first. This facilitated tracking of the initial entry point throughout the water column. The cameras were not time synced; thus, the first recorded position corresponded to when the full length of the mine was in view.

#### **B. SOURCES OF ERROR**

There were several sources of error that hindered the determination of the mine's exact position within the water column. Locations above or below the camera's focal point were subjected to parallax distortion. Placing the cameras as far back as possible, while still being able to resolve the individual grid squares, minimized this error. Second, the background grids were located behind the mine's trajectory plane. This resulted in the mine appearing larger than normal. This error was minimized by not allowing the plotted points to exceed the particular mine's length. Third, an object injected into the water will generate an air cavity. This air cavity can greatly affect the initial motion, particularly at very high speeds (hydro ballistics). The air cavity effect was deemed to be minimal due to the low inject velocities used.

#### **C. DATA ANALYSIS**

The 2-D data provided by each camera was first used to produce raw 2-D plots of the mine's trajectory. Next, 2-D data from both cameras was then fused to produce a 3-D history. This 3-D history was then made non-dimensional in order to generalize the results. The non-dimensional data was used to generate impact scatter plots and was also used in multiple linear regression calculations. The non-dimensional conversions used were:

$$t^* = \frac{dt}{\sqrt{\frac{L}{g}}}; V_{init}^* = \frac{V_{init}}{\sqrt{gL}}; \frac{L}{D}; COM = \frac{2M}{L}; \frac{(x,y,z)}{L}, \frac{(u,v,w)}{\sqrt{gL}}, \cos(\text{drop angle}), \quad (1)$$

where L = mine length, D = mine diameter, g = gravitational force, (x,y,z) are the mine's earth coordinates and (u,v,w) are the mine's velocities in the x, y and z directions. Table 2 provides a summary of the commonly used non-dimensional COM terms.

Mine Length →	15	12	9
COM Position			
2	0.1939	0.1594	0.1198
1	0.0969	0.0797	0.0599
0	0	0	0
-1	-0.0969	-0.0797	-0.0599
-2	-0.1939	-0.1594	-0.1198

Table 2. Commonly used non-dimensional COM positions. Non-dimensional COM positions determined using  $\frac{2M}{L}$ , where M is given in Figure 4.

### 1. 2-D Plots

The raw 2-D data was plotted in the x, -z and -y, -z planes for two purposes. First, it provided a check on the methodology used for position recording. Second, the 2-D -y, -z data allowed us to develop generalized trajectory patterns that the mine's appeared to follow. Figure 8 depicts an example of a 2-D plot. Trajectory patterns are presented in Chapter 5 and Appendix A.

### 2. Impact Attitude

The mine's final data point was considered to be the impact point. Impact points were grouped by COM position and mine length in order to establish the relationship of COM position to impact attitude. Figure 9 provides a summary of all cases. Further histograms are provided in Appendix B.

### 3. Impact Point Locations

The lateral movement a mine experiences after drop is of extreme importance to

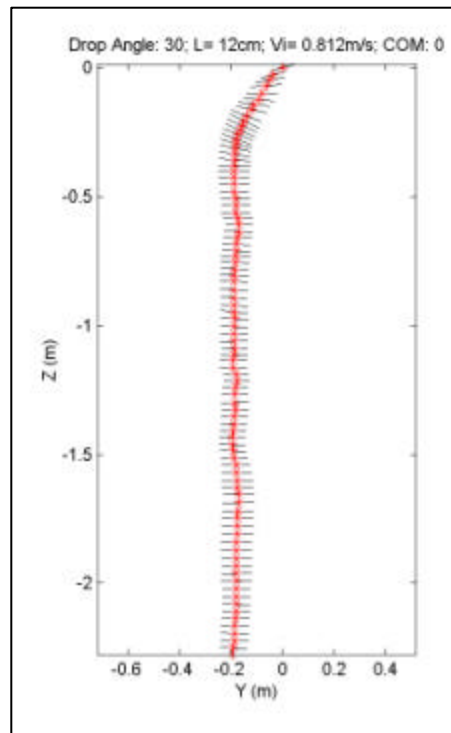


Figure 8. Example of Flat Trajectory.

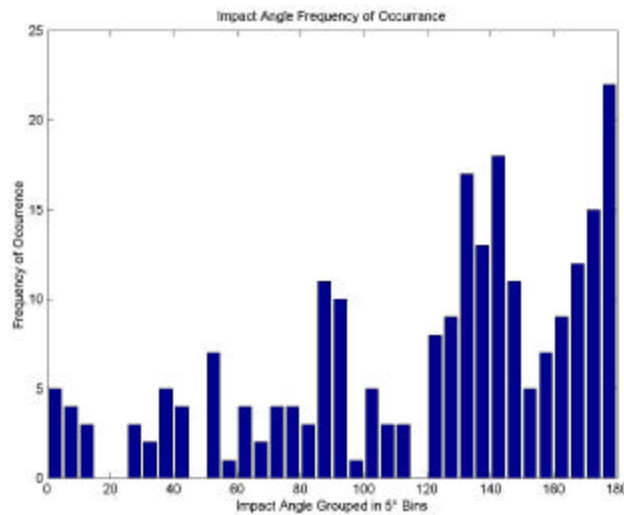


Figure 9. Impact Angles for all cases.

the MCM planner. When the threat of mines exists, a mine danger area is established. The greater the uncertainty in the mine's location, the larger the danger area. Increases in a mine danger area translate into increased clearance times. The impact points were analyzed to determine the lateral movement experienced as influenced by COM position, and drop angle (Fig 10). Additional impact plots can be found in Appendix C.

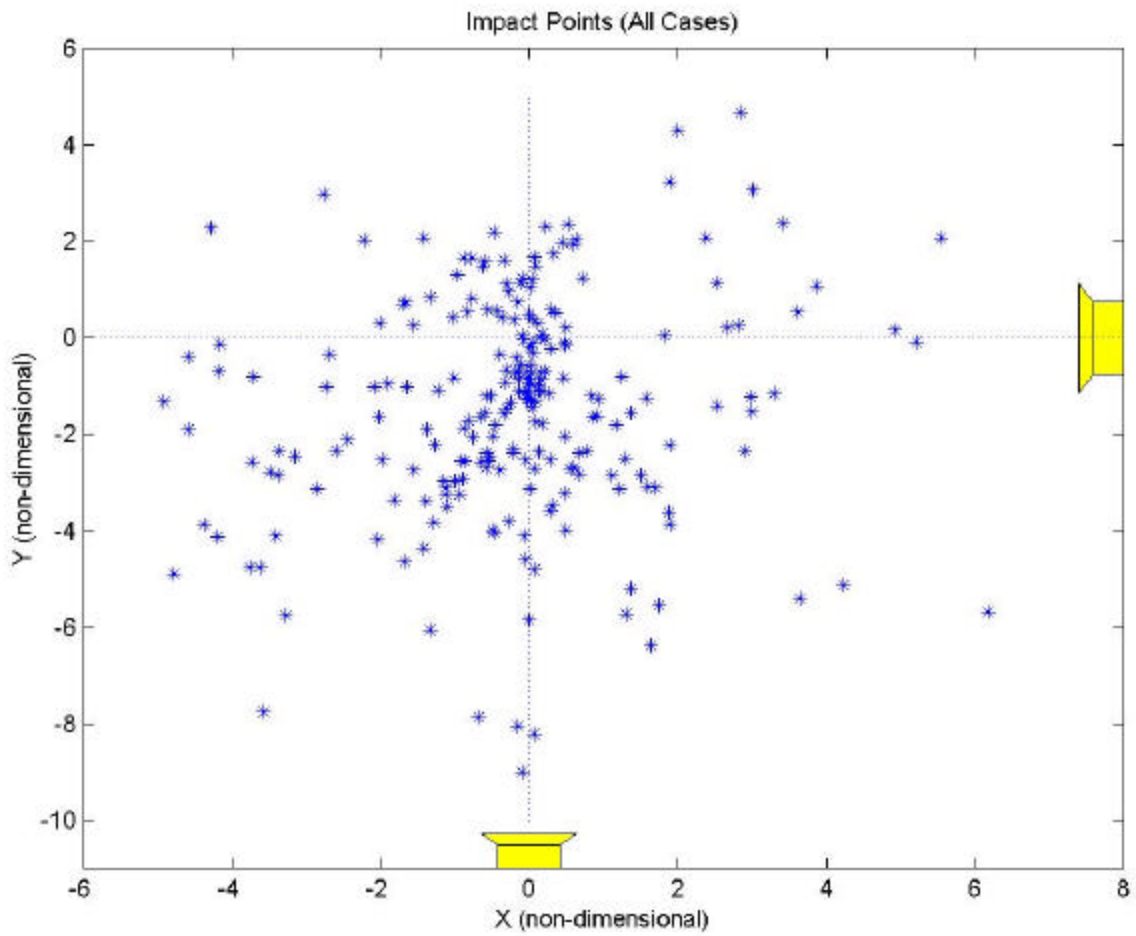


Figure 10. Impact Points for all cases and conditions. The yellow areas represent the cameras used.



## IV. DYNAMICS OF A CYLINDRICAL MINE

### A. TWO COORDINATE SYSTEMS

Two coordinate systems are used to describe a cylindrical mine falling through the water column: earth and body (mine) coordinates. The earth coordinate system is fixed to the swimming pool with horizontal sides as  $x$  and  $y$  axis, and vertical direction as the  $z$ -axis (Fig. 5). The body coordinate is rigidly connected with the cylindrical mine. The origin of the body coordinate system coincides with the center of gravity (CG); the axis- $r_1$  is along the centerline of the cylinder; the axis- $r_2$  is perpendicular to the plane constructed by axes- $r_1$  and axis- $z$  ( $r_1$ - $z$  plane); and the axis- $r_3$  lies in the ( $r_1$ - $z$ ) plane and is perpendicular to axis- $r_1$ . The selection of axes ( $x, y, z$ ) and ( $r_1, r_2, r_3$ ) follows the right-hand rule. The angles that the three axes  $r_1, r_2, r_3$  form with the vertical (upward positive) are called  $\phi_1, \phi_2$ , and  $\phi_3$  (Fig. 11). The angle  $\phi_1$  is usually called the attitude of the mine.

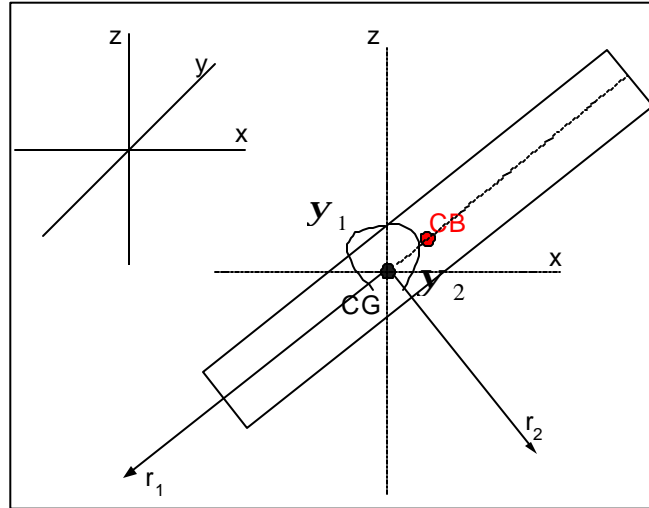


Figure 11. Mine Coordinate System. The axis  $r_3$  originates at CG and comes out of the page towards the viewer. CB is the center of buoyancy (volumetric center) of the mine.

### B. HYDRODYNAMIC THEORY OF MINE IMPACT BURIAL

The essential elements of the mine impact burial model translate into the science and engineering of hydrodynamic processes associated with a falling object and sediment transport. Any solid object falling through a fluid (air and water) should obey two physical principles: (2) momentum balance and (3) moment balance:

$$\rho(d\mathbf{V}^*/dt^*) dm^* = \mathbf{W}^* + \mathbf{F}_b^* + \mathbf{F}_d^* \quad (2)$$

$$\rho[\mathbf{r}^* \times (d\mathbf{V}^*/dt^*)] dm^* = \mathbf{M}^*, \quad (3)$$

where the superscript \* denotes dimensional variables.  $\mathbf{V}^*$  is the velocity of the mine,  $\mathbf{W}^*$  the gravitational force,  $\mathbf{F}_b^*$  the buoyancy force,  $\mathbf{F}_d^*$  the drag force, and  $\mathbf{M}^*$  the resultant moment of momentum. Existing IBPM models only consider the momentum balance of the mine [i.e., Eq. (2)] and disregard the moment balance of the mine [i.e., Eq. (3)]. Such an incomplete hydrodynamics of the model leads to unrealistic prediction of the mine's water phase trajectory (Fig. 12). By considering momentum and moment balance, the falling object should have a spiral-type motion (Fig 13). Without the spiral-type motion, the IBPM may over-predict the impact burial depth (Chu et al. 2000).

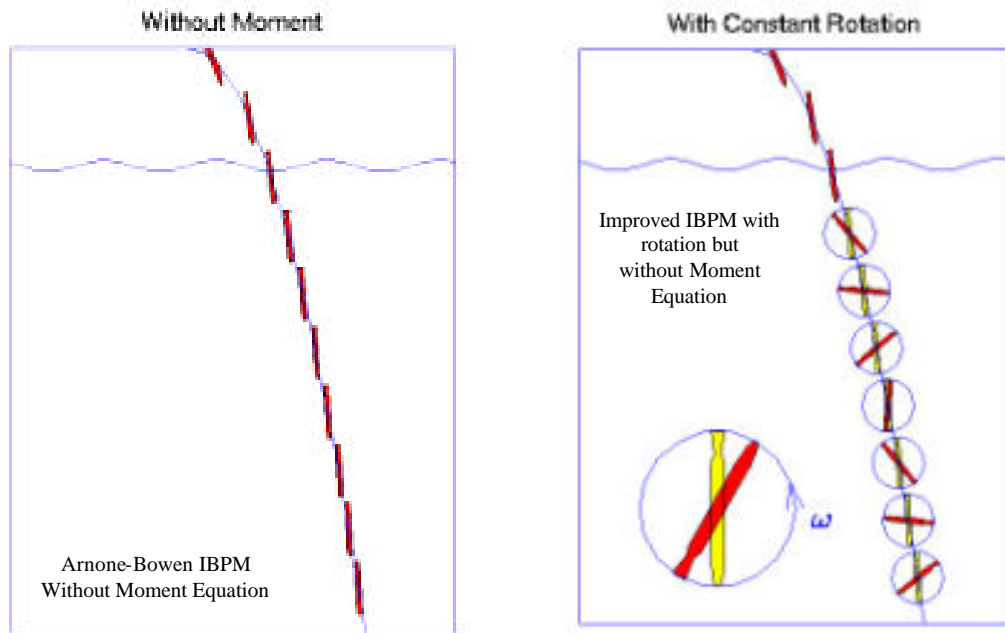


Figure 12. Mine Motion without Consideration of Moment Equation.

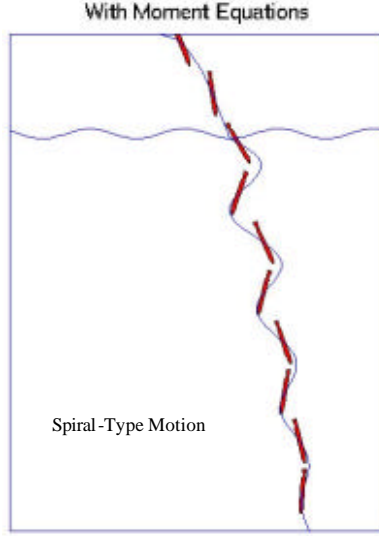


Figure 13. Mine Motion with Consideration of both Momentum and Moment Equations.

Let  $(V_1^*, V_2^*, V_3^*)$  be the three components of the velocity of CG and  $(\mathbf{w}_1^*, \mathbf{w}_2^*, \mathbf{w}_3^*)$  the components of the angular velocity, referring to the direction of the mine-fixed coordinate system. The momentum equation (2) becomes:

$$\frac{dV_1^*}{dt^*} + \mathbf{w}_2^* V_3^* - \mathbf{w}_3^* V_2^* = g \frac{\mathbf{r}_m - \mathbf{r}_w}{r_m} \cos \mathbf{y}_1 - \frac{C_D \mathbf{r}_w}{2L r_m} |\mathbf{V}^*| (V_1^* - V_{w1}^*) \quad (4a)$$

$$\frac{dV_2^*}{dt^*} + \mathbf{w}_3^* V_1^* - \mathbf{w}_1^* V_3^* = g \frac{\mathbf{r}_m - \mathbf{r}_w}{r_m} \cos \mathbf{y}_2 - \frac{C_D \mathbf{r}_w}{2L r_m} |\mathbf{V}^*| (V_2^* - V_{w2}^*) \quad (4b)$$

$$\frac{dV_3^*}{dt^*} + \mathbf{w}_1^* V_2^* - \mathbf{w}_2^* V_1^* = g \frac{\mathbf{r}_m - \mathbf{r}_w}{r_m} \cos \mathbf{y}_3 - \frac{C_D \mathbf{r}_w}{2L r_m} |\mathbf{V}^*| (V_3^* - V_{w3}^*) \quad (4c)$$

where  $C_D$  is the drag coefficient,  $g$  the gravitational acceleration,  $L$  the length of the mine, and  $(V_{w1}^*, V_{w2}^*, V_{w3}^*)$  is the water velocity. The independent and dependent variables are made non-dimensional by:

$$t^* = \sqrt{\frac{L}{g}} t, \quad \mathbf{w}^* = \sqrt{\frac{g}{L}} \mathbf{w}, \quad (V_1^*, V_2^*, V_3^*, V_{w1}^*, V_{w2}^*, V_{w3}^*) = \sqrt{gL} (V_1, V_2, V_3, V_{w1}, V_{w2}, V_{w3}). \quad (5)$$

The momentum equations (4a)-(4c) become:

$$\frac{dV_1}{dt} + \mathbf{w}_2 V_3 - \mathbf{w}_3 V_2 = -\frac{C_D \mathbf{r}_w}{2 \mathbf{r}_m} |\mathbf{V}| (V_1 - V_{w1}) + \frac{\mathbf{r}_m - \mathbf{r}_w}{\mathbf{r}_m} \cos \mathbf{y}_1 \quad (6a)$$

$$\frac{dV_2}{dt} + \mathbf{w}_3 V_1 - \mathbf{w}_1 V_3 = -\frac{C_D \mathbf{r}_w}{2 \mathbf{r}_m} |\mathbf{V}| (V_2 - V_{w2}) + \frac{\mathbf{r}_m - \mathbf{r}_w}{\mathbf{r}_m} \cos \mathbf{y}_2 \quad (6b)$$

$$\frac{dV_3}{dt} + \mathbf{w}_1 V_2 - \mathbf{w}_2 V_1 = -\frac{C_D \mathbf{r}_w}{2 \mathbf{r}_m} |\mathbf{V}| (V_3 - V_{w3}) + \frac{\mathbf{r}_m - \mathbf{r}_w}{\mathbf{r}_m} \cos \mathbf{y}_3. \quad (6c)$$

The non-dimensional equation of the moment of momentum (3) becomes:

$$J_1 \frac{d\mathbf{w}_1}{dt} + (J_3 - J_2) \mathbf{w}_2 \mathbf{w}_3 - J_{31} \left( \frac{d\mathbf{w}_3}{dt} + \mathbf{w}_1 \mathbf{w}_2 \right) = \frac{LM_1^*}{g} \quad (7a)$$

$$J_2 \frac{d\mathbf{w}_2}{dt} + (J_1 - J_3) \mathbf{w}_3 \mathbf{w}_1 - J_{31} (\mathbf{w}_3^2 - \mathbf{w}_1^2) = \frac{LM_2^*}{g} \quad (7b)$$

$$J_3 \frac{d\mathbf{w}_3}{dt} + (J_2 - J_1) \mathbf{w}_1 \mathbf{w}_2 - J_{31} \left( \frac{d\mathbf{w}_1}{dt} - \mathbf{w}_2 \mathbf{w}_3 \right) = \frac{LM_3^*}{g}, \quad (7c)$$

where  $J_1$ ,  $J_2$ , and  $J_3$  are the three moments of gyration,

$$J_1 = \int (r_2^2 + r_3^2) dm^*, \quad J_2 = \int (r_3^2 + r_1^2) dm^*, \quad J_3 = \int (r_1^2 + r_2^2) dm^* \quad (8)$$

and the moment of deviation (or inertia products of second order),

$$J_{31} = \int r_3 r_1 dm^* \quad (9)$$

The orientation of the mine ( $\phi_1$ ,  $\phi_2$ ,  $\phi_3$ ) is determined by

$$\frac{d}{dt} \cos \mathbf{y}_1 = \mathbf{w}_3 \cos \mathbf{y}_2 - \mathbf{w}_2 \cos \mathbf{y}_3 \quad (10a)$$

$$\frac{d}{dt} \cos \mathbf{y}_2 = \mathbf{w}_1 \cos \mathbf{y}_3 - \mathbf{w}_3 \cos \mathbf{y}_1 \quad (10b)$$

$$\frac{d}{dt} \cos \mathbf{y}_3 = \mathbf{w}_2 \cos \mathbf{y}_1 - \mathbf{w}_1 \cos \mathbf{y}_2. \quad (10c)$$

The nine non-dimensional equations (6a-c), (7a-c), and (10a-c) are the basic system for describing the mine movement in the water column.

### C. PHYSICAL CHARACTERISTICS OF MINE

For a cylindrical mine, two characteristics are important for the prediction of mine movement in the water column: the ratio between length and diameter ( $L/D$ ) and the ratio  $M/2L$  with  $M$  being the distance between the centers of gravity and buoyancy. Positive (negative) values of  $M$  refers to the center of gravity below (above) the center of buoyancy. In MIDEX,  $L/D = 15/4, 12/4,$  and  $9/4$ ;  $M/2L$  values are provided in Table 2.

### D. INITIAL CONDITIONS IN MIDEX

During the experiment, the initial conditions were initial velocity and entry angle. Thus, for the dynamical system (6a-c), (7a-c), and (10a-c), the initial conditions at  $t = 0$  were:

$$V_1 = \frac{V_{int}^*}{\sqrt{gL}}, V_2 = 0, V_3 = 0, \gamma_1 = \gamma_2 = \gamma_3 = 0, \mathbf{f}_1 = \text{Drop Angle}, \mathbf{f}_2 = \mathbf{f}_3 = 0. \quad (11)$$

THIS PAGE INTENTIONALLY LEFT BLANK

## V. RESULTS

### A. TRAJECTORY PATTERNS

By analyzing the 2-D -y, -z planar plots we were able to develop seven general trajectory patterns. Pattern names are based upon the mine coordinate system. The -y, -z planar plots were chosen for trajectory analysis, as this plane was parallel to the direction of mine drop. The generalized trajectory patterns are described in Table 3 and Figures 14a and b. Appendix A contains all of the remaining analyzed 2-D plots.

Mine Trajectory Pattern	Description
Straight or Slant	Mine exhibited little angular change about z-axis. For straight mine attitude remained nearly parallel with z-axis ( $\pm 15^\circ$ ). For slant, mine attitude was $45^\circ$ off z-axis ( $\pm 15^\circ$ ).
Spiral	Mine experienced rotation about z-axis throughout its water phase trajectory.
Flip	Initial water entry point rotated at least $180^\circ$ during mine motion.
Flat	Mine's angle with vertical near $90^\circ$ for most of the trajectory.
Seesaw	Similar to the flat pattern except that mine's angle with vertical would oscillate between greater (less) than $90^\circ$ and less (greater) than $90^\circ$ - like a seesaw.
Combination	Complex trajectory where mine exhibited several of the above patterns.

Table 3. Description of Mine Coordinate Based Trajectory Patterns

### B. IMPACT ATTITUDE

IB is largely determined from the impact attitude of the mine. Mines whose impact attitudes are perpendicular ( $\Psi_1 \cong 0$  or  $180^\circ$ ) to the sediment interface will experience the largest degree of IB. (Taber 1999). It is therefore important to analyze the relationship between impact attitude and the controlled parameters, drop angle,  $V_{init}$ , L/D and COM position. Both L/D and  $V_{init}$  had little influence on impact attitude. COM position and drop angle, however, were the largest determinants of mine impact attitude.

From Figure 9 it is apparent that there are several peaks centered near  $90^\circ$ ,  $140^\circ$  and  $180^\circ$ . Further analysis reveals that these peaks correspond to COM positions 0, 1 and 2 respectively (Fig. 15). COM positions -1 and -2 followed the same trend as their positive counterparts. In our coordinate system the attitude is measured with respect to

the mine's first entry point. When looking into the  $-y, -z$  plane, a mine with a  $0^\circ$  or  $40^\circ$  attitude will look the same as a mine with a  $180^\circ$  or  $140^\circ$  attitude.

Although drop angle was not the most influential parameter, variations did induce changes in impact orientation. As drop angle increased, the likelihood of any lateral movement decreased. This allowed for impact angles that were more vertically orientated. This is primarily due to the fact that the vertical components of velocity were greater than those at shallow angles. Thus, the time to bottom and time for trajectory alteration was less.

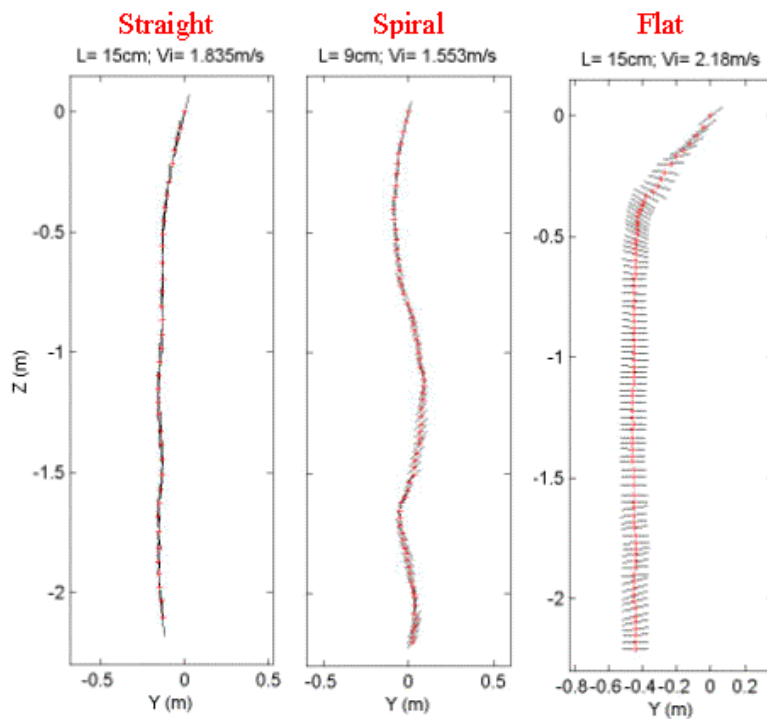


Figure 14a. Trajectory Examples.



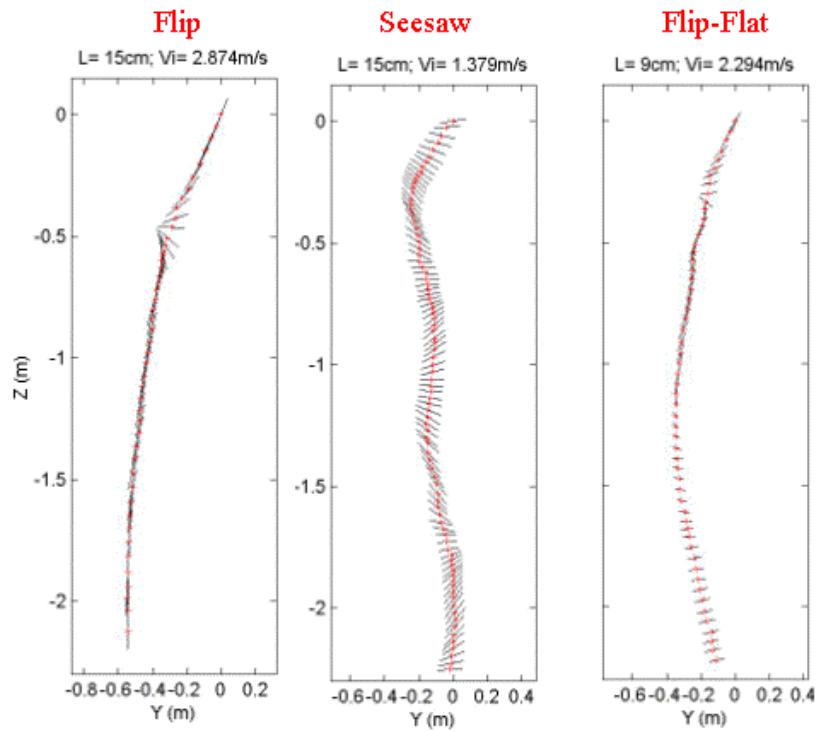


Figure 14b. Trajectory Examples

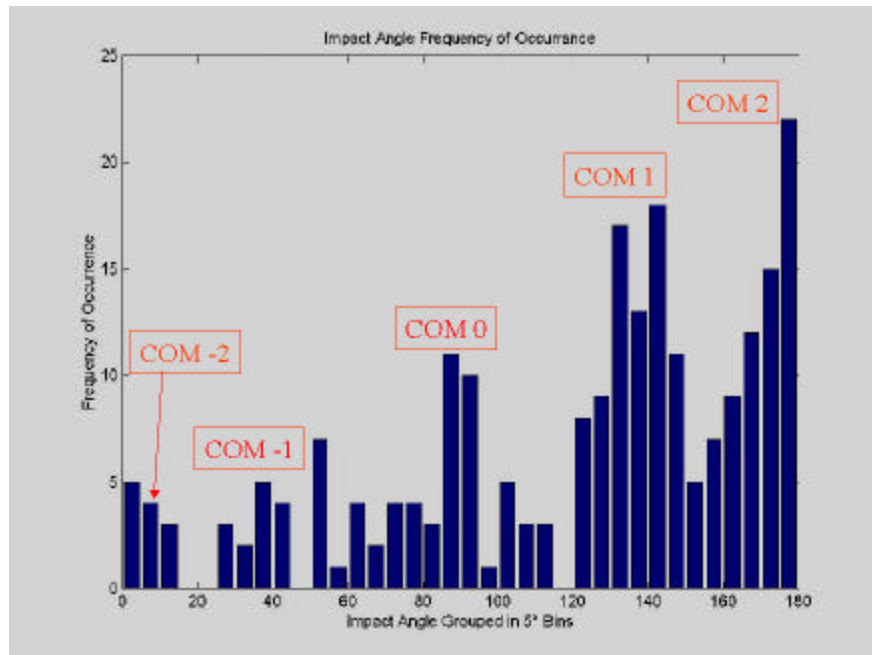


Figure 15. Relationship between COM Position and Impact Attitude.

### C. IMPACT POINTS

Using a methodology similar to that used in impact attitude analysis, impact point scatter plots were analyzed by the controlled parameters, drop angle,  $V_{init}$  and COM position. Impact point scatterplots are provided in Appendix C. COM 2 and 0 cases fell near the drop point greater than 90% of the time while COM 1 cases displayed the most variability. Additionally, the flip experienced in negative COM cases induces a greater degree of lateral movement than in positive COM cases.

### D. MULTIPLE LINEAR REGRESSION ANALYSIS

Multiple linear regression analysis was performed on the last recorded points (impact points) using a least squares technique as outlined by Walpole (1998). The purpose of this was to establish a relationship between the input non-dimensional parameters; drop angle, COM position,  $V_{init}$  and  $L/D$ , and output variables;  $(x_m, y_m)$ ,  $(u, v, w)$  and  $\psi_1$  (Table 4). The basic equation used was:

$$f_i = \beta_0 + \beta_1 x_{1_i} + \beta_2 x_{2_i} + \beta_3 x_{3_i} + \beta_4 x_{4_i} + e_i \quad (12)$$

where  $f_i$  is the desired output parameter,  $(x_m, y_m, \psi_1, u, v, w)$ , betas are the correlation coefficients,  $x_1$  is drop angle,  $x_2$  is  $L/D$ ,  $x_3$  is  $V_{init}$  and  $x_4$  is COM position. The results

	$x_m$	$y_m$	$\psi_1$	$u$	$v$	$w$
$\beta_0$	-.0746	-.0546	102.5691	.0040	-.0135	-.9481
$\beta_1$	.1190	-.0828	-13.3508	-.0075	-.0106	-.1080
$\beta_2$	-.0469	-.0798	-.5009	-.0011	.0005	.0295
$\beta_3$	.0372	.0622	1.0437	.0025	.0011	-.0221
$\beta_4$	.2369	.4330	472.2135	-.0090	.0537	-1.2467

Table 4. Multiple Linear Regression Analysis Correlation Coefficients.

indicate that COM position has the largest influence on all output variables. As a check we determined  $\psi_1$  for a case where  $L/D = 3.75$ , Drop angle =  $15^\circ$ , COM = .1939 and  $V_{init} = 3\text{m/s}$ . After non-dimensionalizing drop angle and  $V_{init}$  we found that the impact attitude

was  $181.2^\circ$ , in good agreement with observations. Similarly, for  $COM = .0969$  and  $0$  we found that the impact attitudes were  $136.1^\circ$  and  $90.4^\circ$  respectively. This is also in good agreement with observations and follows the trends established in the histogram analysis. Impact point data tables can be found in Appendix D.

THIS PAGE INTENTIONALLY LEFT BLANK

## VI. DISCUSSION

The water phase trajectory a mine experiences ultimately determines the impact orientation. In MIDEX, the categorizing of trajectories into general patterns served two purposes. First, the pattern name gives a sense of impact attitude. Second, it allowed for a visualization of the motion a mine experiences about its own axis. Observed trajectories were found to be most sensitive to COM position, drop angle and mine length. As COM distance increased from the CB the mine tended to follow a straight pattern. As COM was moved closer to the CB the mine's trajectory tended towards being more parallel with the pool's bottom (Tables 5a-d). At steep drop angles, the mine experienced little lateral movement and tended towards a straight pattern. Additionally, as mine length decreased more complex trajectory patterns developed. This included significant rotation about the vertical axis and increased lateral movement.

	COM Position: 2		
Mine Length:	15	12	9
Drop Angle: 15°	Straight	Straight	Straight-Slant
	Slant-Straight	Spiral	Spiral
	Slant-Straight	Slant-Straight	Slant-Straight
	Slant-Straight	Slant-Straight	Spiral
Drop Angle: 30°	Slant-Straight	Slant	Spiral
	Straight	Spiral	Spiral
	Slant-Straight	Straight	Spiral
	Slant-Straight	Slant-Straight	Spiral
Drop Angle: 45°	Slant-Straight	Slant-Straight	Spiral
	Slant	Spiral	Spiral
	Straight-Spiral	Straight-Spiral	Spiral
	Straight	Straight	Spiral
Drop Angle: 60°	Slant	Slant-Straight	Slant-Spiral
	Straight	Straight-Slant	Spiral
	Straight	Straight	Spiral
	Straight	Straight-Spiral	Straight-Spiral
Drop Angle: 75 °	Straight	Straight	Spiral
	Straight	Straight-Spiral	Slant
	Straight	Straight	Spiral
	Straight	Straight-Spiral	Straight-Spiral
	Straight	Straight-Spiral	Straight-Spiral

Table 5a. Observed Trajectory Patterns for COM Position 2.

	COM Position: 1		
Mine Length:	15	12	9
Drop Angle: 15°	Slant	Spiral	Straight-Spiral
	Slant-Spiral	Slant-Spiral	Spiral
Drop Angle: 30°	Slant	Slant	Spiral
	Slant	Slant-Spiral	Spiral
	Slant	Straight-Slant	Spiral
	Slant	Slant	Spiral
Drop Angle: 45°	Straight-Slant	Slant	Spiral
	Slant	Slant-Spiral	Spiral
	Slant	Slant	Spiral
	Slant	Slant	Slant-Spiral
	Slant	Straight	Slant-Spiral
Drop Angle: 60°	Straight	Straight-Spiral	Spiral
	Slant	Straight	Spiral
	Slant	Straight	Straight-Spiral
	Slant	Straight	Straight-Spiral
	Slant	Slant	Straight-Slant
Drop Angle: 75°	Straight	Straight	Straight-Spiral
	Straight	Straight	Straight-Spiral
	Straight	Straight-Spiral	Slant-Spiral
	Straight	Straight-Spiral	Slant-Spiral

Table 5b. Observed Trajectory Patterns for COM Position 1.

	COM Position: 0		
Mine Length:	15	12	9
Drop Angle: 15°	Seesaw	Flat	Flat-Seesaw
	Seesaw	Seesaw	Seesaw
	Seesaw	Seesaw	Flat-Seesaw
Drop Angle: 30°	Flat	Spiral-Seesaw	Spiral-Seesaw
	Seesaw	Flat	Spiral-Seesaw
	Flat	Flat-Spiral	Flat-Spiral
	Flat-Spiral	Flat-Spiral	Flat-Spiral
	Flat	Flat-Spiral	Flat-Spiral
Drop Angle: 45°	Slant-Seesaw	Spiral-Flat-Seesaw	Flat
	Seesaw	Flat-Spiral	Spiral-Seesaw
	Flat-Spiral	Straight-Flat	Straight-Flat
	Straight	Straight-Flat	Straight-Flat-Spiral
Drop Angle: 60°	Straight-Flat-Spiral	Seesaw	Seesaw
	Spiral-Seesaw	Straight-Seesaw	Straight-Flat
	Straight-Spiral-Seesaw	Straight-Spiral-Seesaw	Straight-Flat
	Straight-Spiral-Seesaw	Straight-Flat-Spiral	Straight-Seesaw
	Slant	Straight-Flat	Straight-Spiral-Flat
	Straight-Flat-Spiral	Straight	Straight-Seesaw-Spiral
Drop Angle: 75°	Straight-Spiral-Seesaw	Straight-Spiral-Seesaw	Straight-Seesaw
	Straight-Seesaw	Straight-Flat	Straight-Spiral-Seesaw
	Straight-Spiral-Seesaw	Straight	Straight-Flat-Spiral

Table 5c. Observed Trajectory Patterns for COM Position 0.

	COM Position: -2		
Mine Length:	15	12	9
Drop Angle: 30°	Flip-Straight	Flip-Slant	Flip-Straight-Spiral
	Flip-Straight	Flip-Straight	Flip-Straight-Spiral-Flip
Drop Angle: 45°	Flip-Straight	Flip-Straight-Spiral	Flip-Straight
	Flip-Straight	Flip-Straight	Flip-Straight-Spiral
	COM Position: -1		
Drop Angle: 30°	Flip-Straight	Flip-Slant	Straight-Flip-Seesaw
	Flip-Slant	Flip-Straight	Flip-Straight-Spiral
Drop Angle: 45°	Flip-Spiral-Slant	Flip-Slant	Flip-Spiral
	Flip-Slant	Flip-Slant	Flip-Spiral
Drop Angle: 60°	Flip-Straight	Flip-Straight	Flip-Spiral-Seesaw
	Straight-Flip	Slant-Flip-Slant	Flip-Spiral

Table 5d. Observed Trajectory Patterns for Negative COM Cases.

In order to evaluate the validity of the IMPACT 25 water phase trajectory patterns, a comparison between our results and the model's was performed. The mine shape characteristics (length, diameter, COM distance), drop angle, release altitude (.1 m), water temperature (23.8°C) and initial velocities (converted into horizontal and vertical components) were entered into IMPACT 25. Model output was organized by COM position, mine length, drop angle and impact angle (Table 6).

		Mine Length	
COM Position: 2	15 cm	12 cm	9 cm
Drop Angle: 15°	184.8°	187.8°	184.0°
30°	185.1°	187.8°	185.6°
45°	185.8°	187.6°	187.5°
60°	186.1°	187.1°	187.8°
75°	185.8°	186.0°	186.8°
COM Position: 1			
15°	148.3°	152.8°	178.6°
30°	151.9°	156.7°	177.3°
45°	158.0°	162.0°	178.6°
60°	166.9°	169.2°	182.5°
75°	174.9°	174.9°	185.9°
COM Position: 0			
15°	98.8°	98.3°	98.7°
30°	111.5°	111.6°	112.2°
45°	126.8°	126.9°	127.8°
60°	143.1°	143.0°	143.6°
75°	160.1°	160.1°	160.4°
COM Position: -1			
30°	43.1°	38.9°	42.8°
45°	61.1°	54.9°	58.4°
60°	104.6°	93.2°	94.8°
COM Position: -2			
30°	5.5°	358.3°	4.7°
45°	19.3°	168.0°	15.8°

Table 6. IMPACT 25 Derived Impact Angles. Output has been converted into the coordinate system used during MIDEX.

Overall, the IMPACT 25 model decreased the impact angle as COM distance decreased. This agreed with the observed trend in the histogram analysis. Additionally, the model predicted impact angle for COM 2 cases and the flip for negative cases fairly well. However, significant deviation between observed and model output occurred for COM cases 1 and 0. This deviation was primarily due to the fact that the trajectories are calculated using only momentum equations. This caused the model to be more sensitive to drop angle, which resulted in the impact angles being more vertical as drop angle increased. As such, the model tended to be slow in predicting alterations in trajectory caused by moving the COM closer to the CB. Furthermore, the IMPACT 25 patterns tended to be more arc shaped and did not include the spiraling motion frequently observed for the 9 cm mine.

THIS PAGE INTENTIONALLY LEFT BLANK



## VII. CONCLUSIONS

MIDEX is the first step in an ongoing process to better understand and predict the various parameters that effect a mine's motion. Although the crudeness of the experiment precluded development of prediction equations, it did prove one key point. COM position has the largest influence on mine water-phase trajectories.

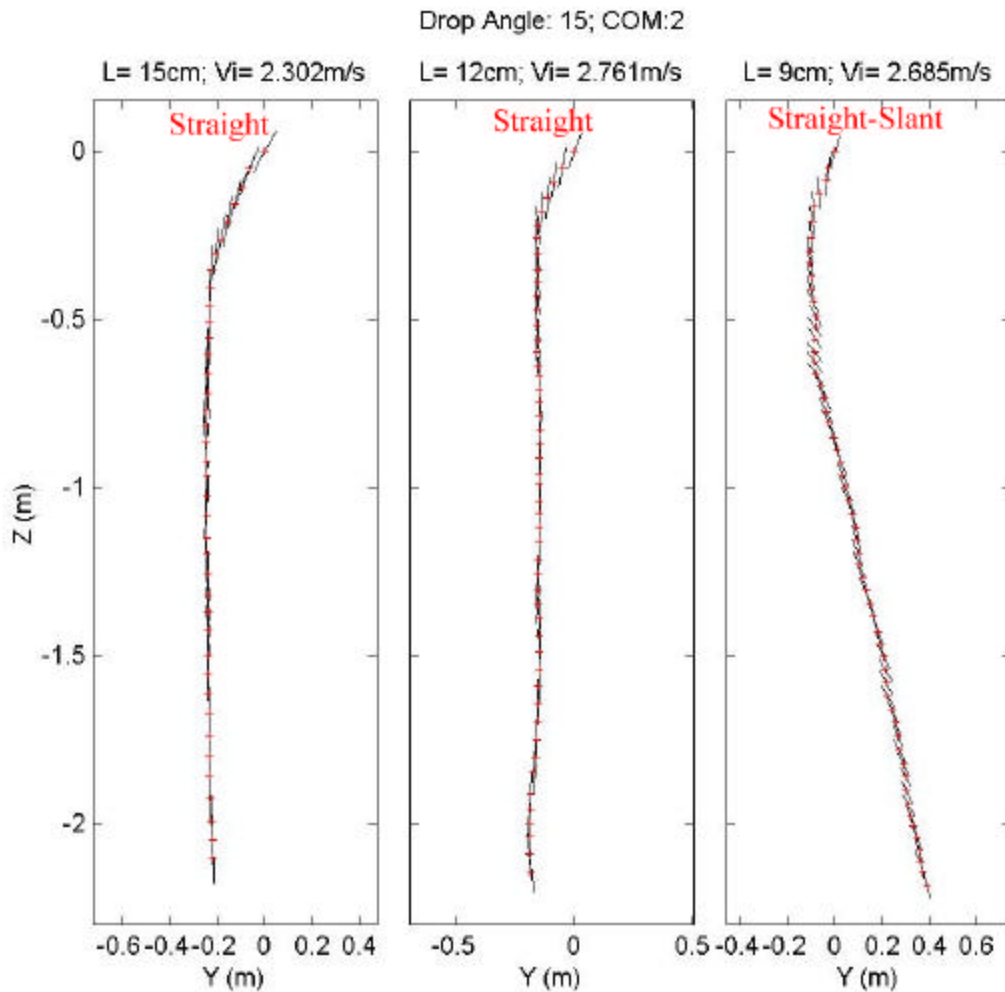
The observed trajectories were far more complex than those theorized by using only the momentum and rotation equations. Simply entering the initial attitude and rotation rate into the model will not satisfy the needs of the modern naval warfighter. At a minimum, updates to the IMPACT 25 model should include the more realistic moment equations.

Further research on mine hydrodynamics is needed. The research needs to expand beyond the simple cylindrical shaped mine to those that are irregularly shaped (Rockan and Manta types). Additionally, the utilization of scaled down versions should be explored. A smaller mine that can be modeled as accurately as its real counterpart will save time, money and will require less logistical support.

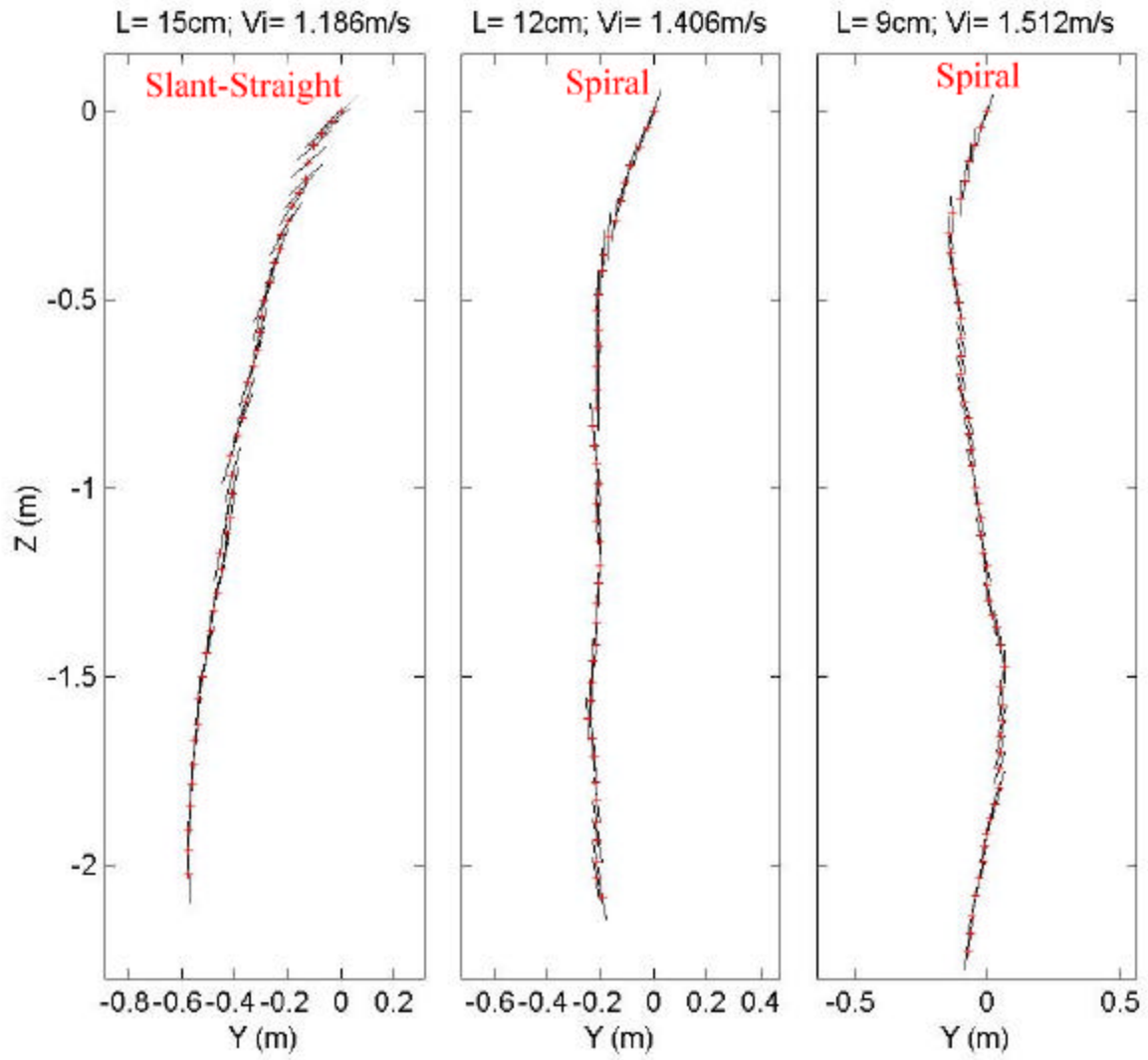
THIS PAGE INTENTIONALLY LEFT BLANK

## APPENDIX A. 2-D PLOTS

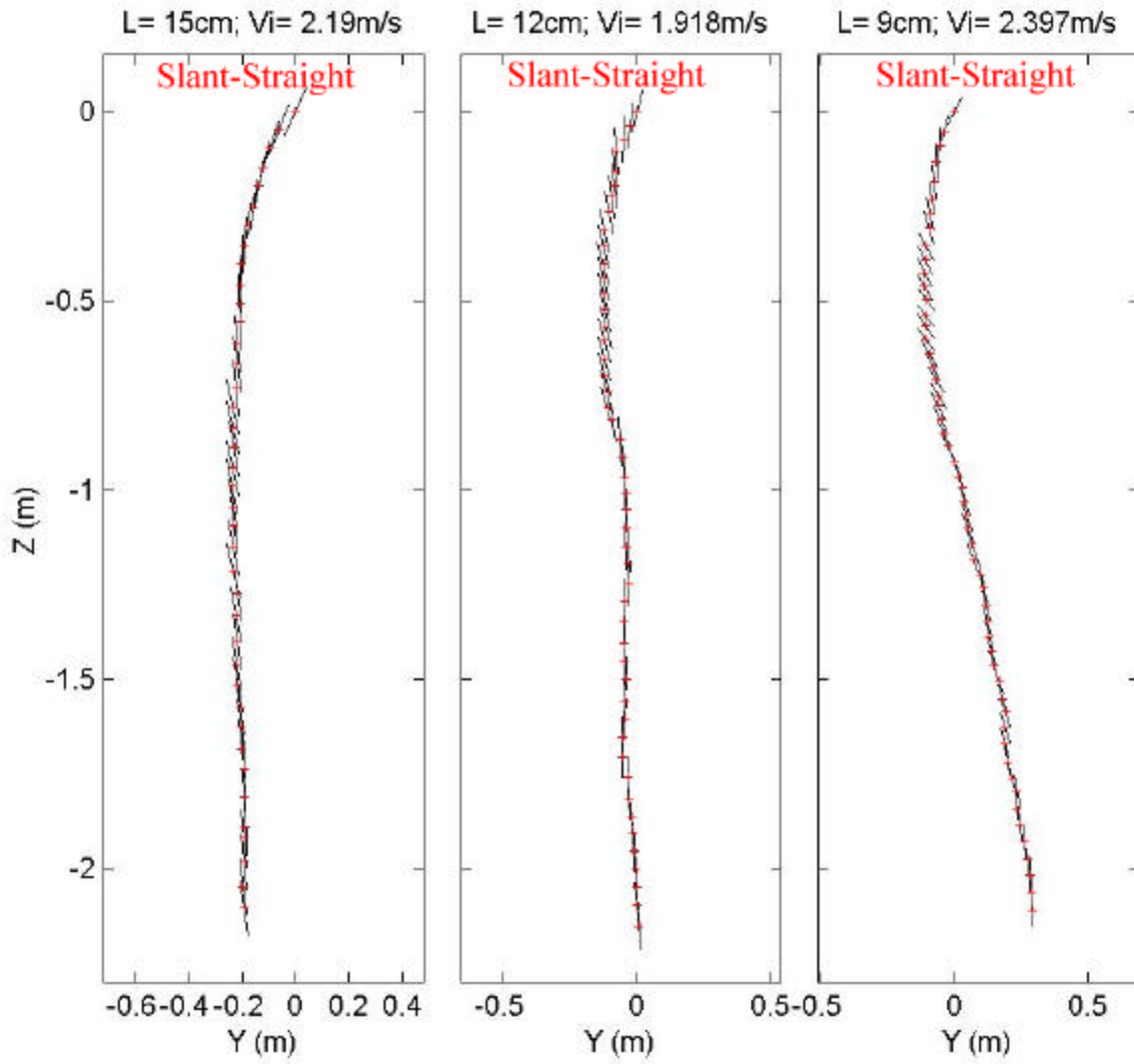
Appendix A contains all of the 2-D -y, -z plots that were used to establish generalized trajectory patterns. The scales have been left in dimensional units and the camera viewpoint is perpendicular to the mine's drop direction (-y axis). The pattern names were chosen based upon the general shape of the trajectory pattern in mine coordinates (straight, slant, spiral, flip, flat, seesaw or combination).



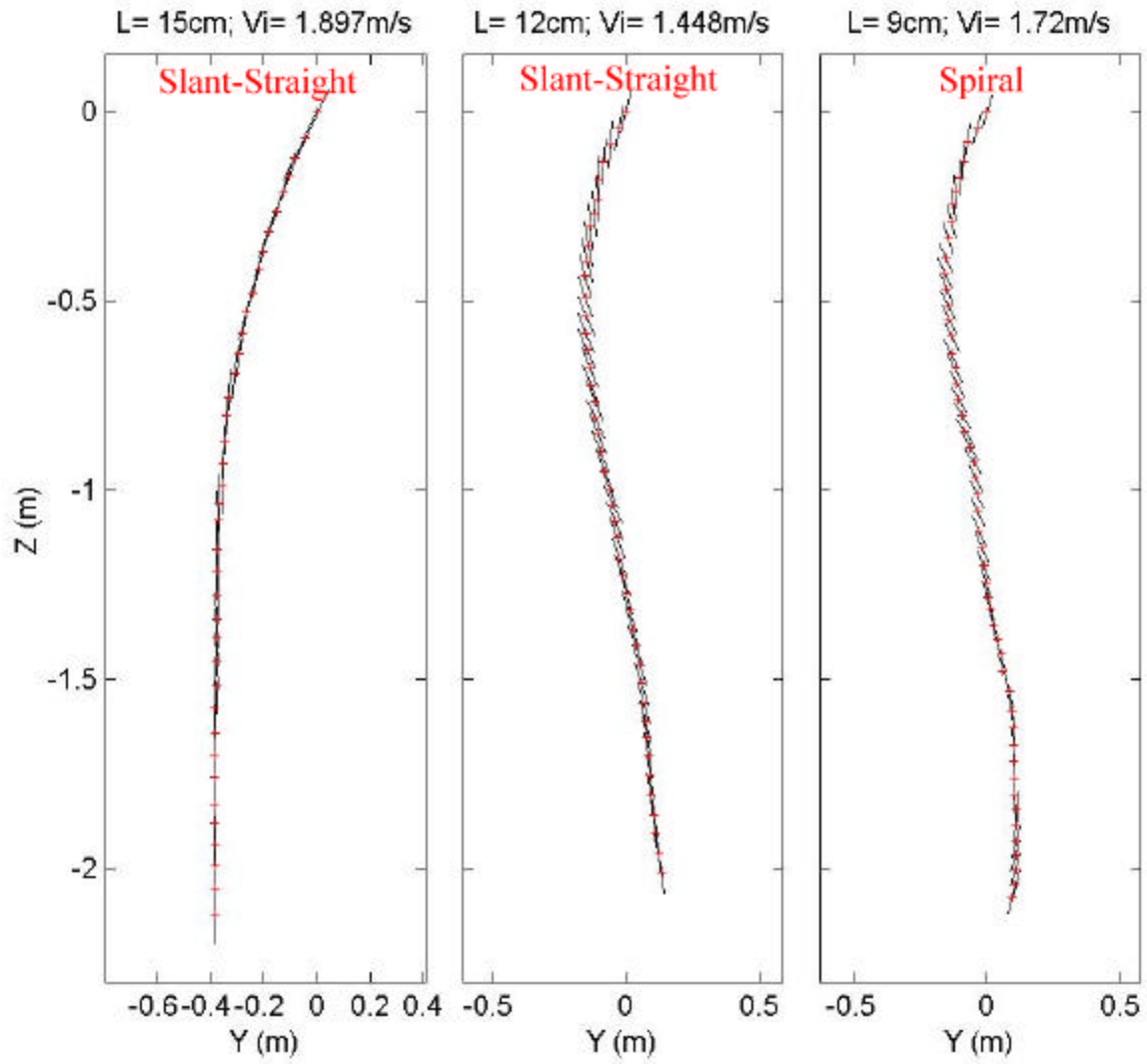
Drop Angle: 15; COM:2



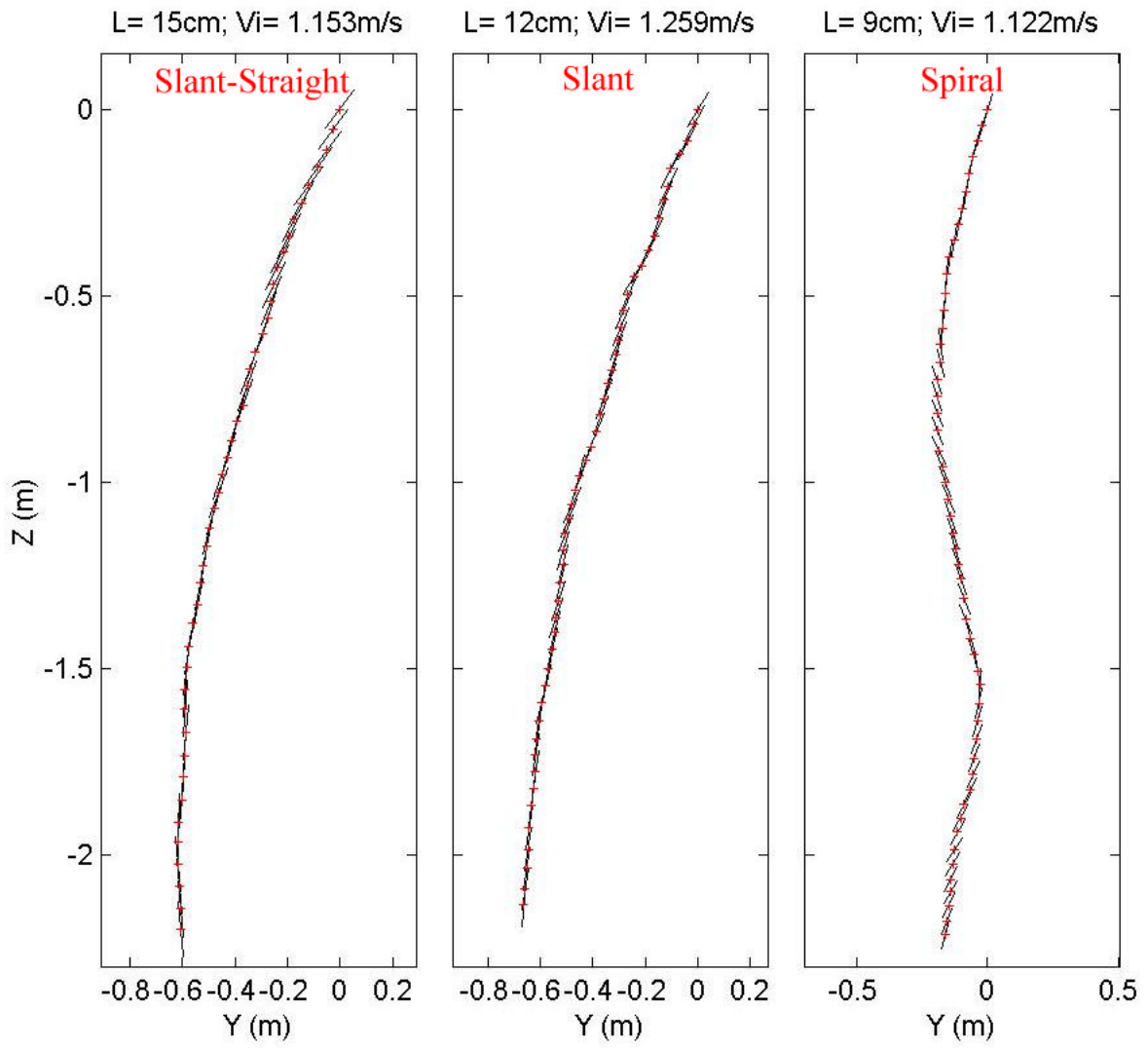
Drop Angle: 15; COM:2



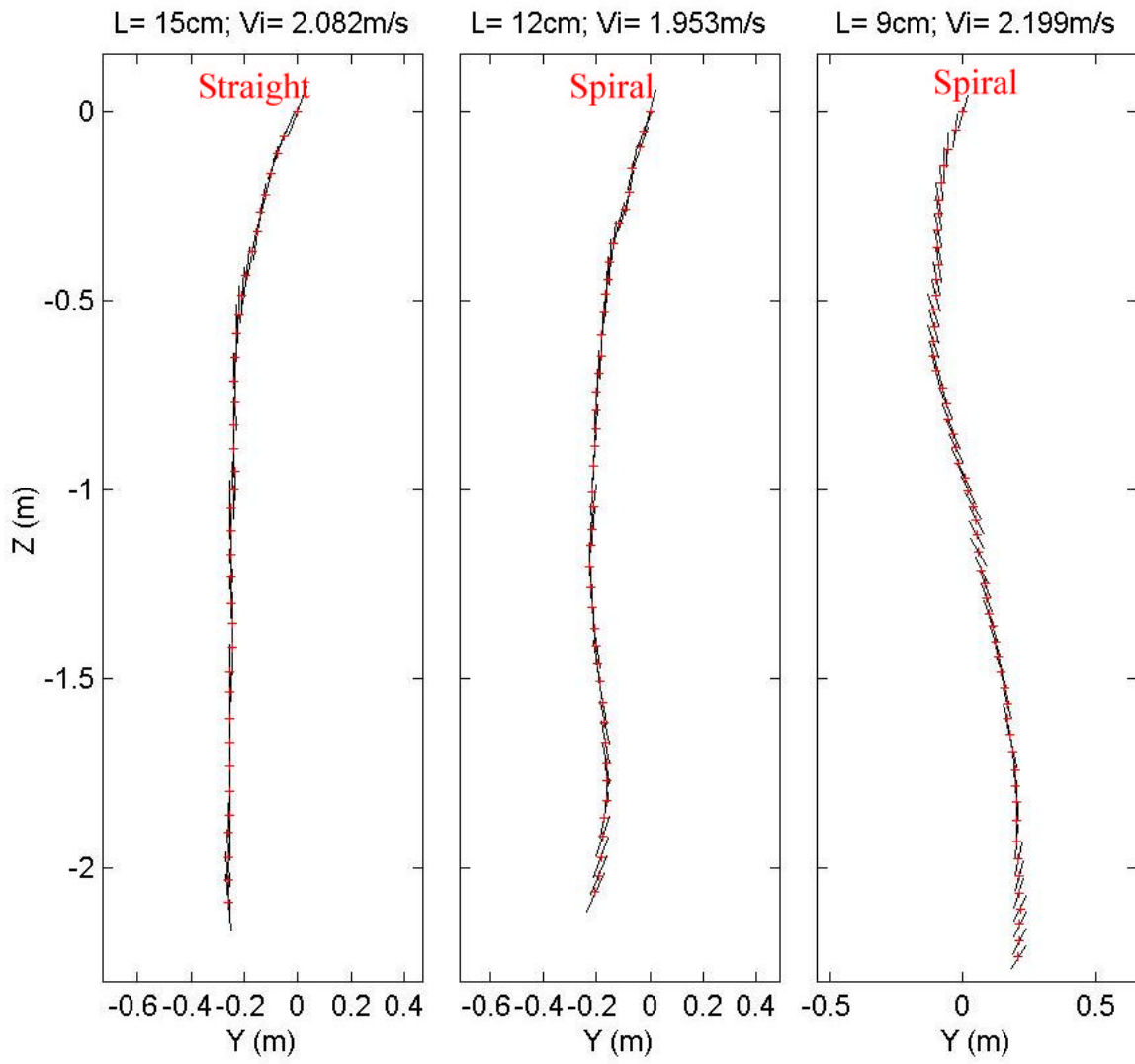
Drop Angle: 15; COM:2



Drop Angle: 30; COM:2

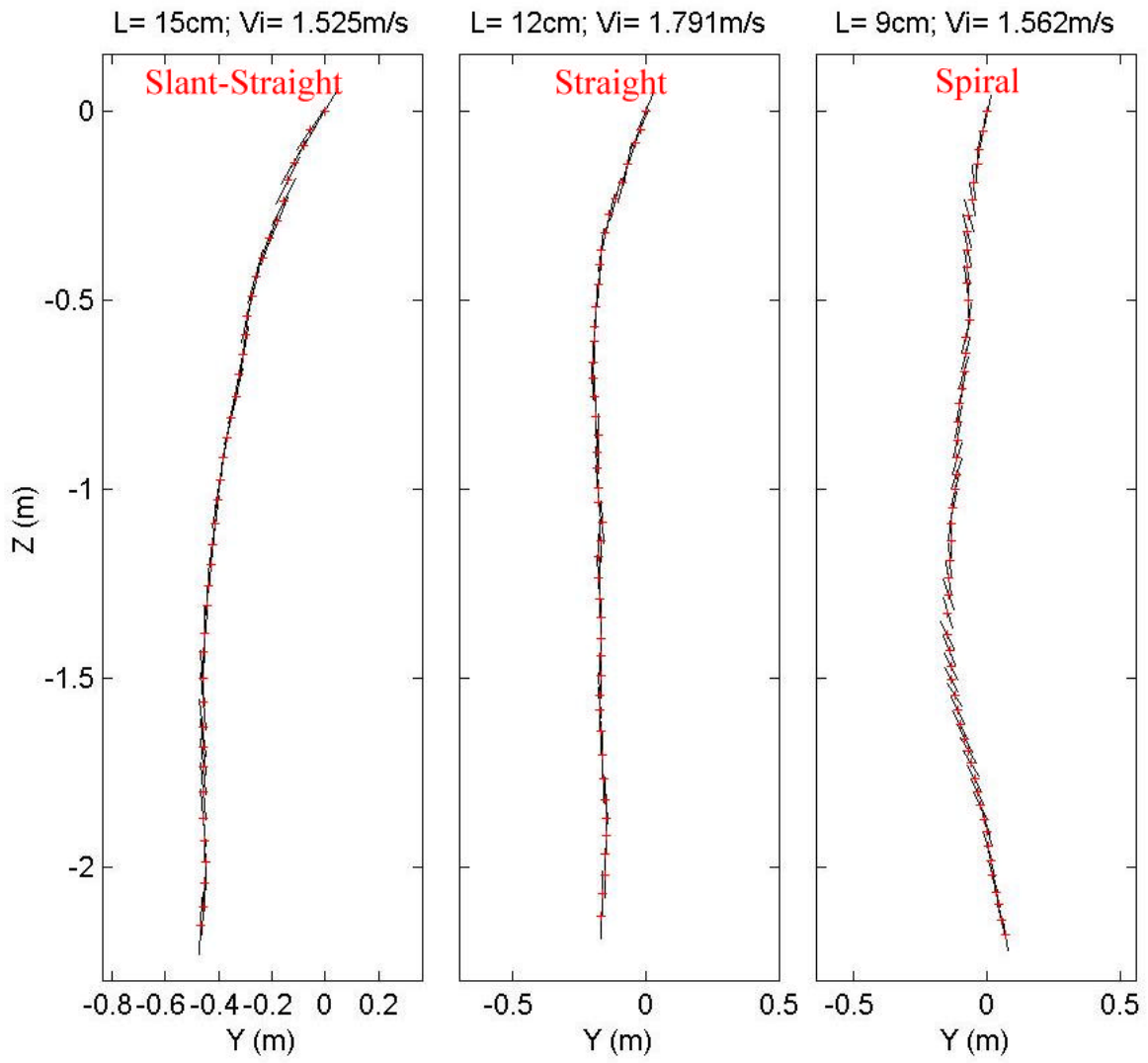


Drop Angle: 30; COM:2

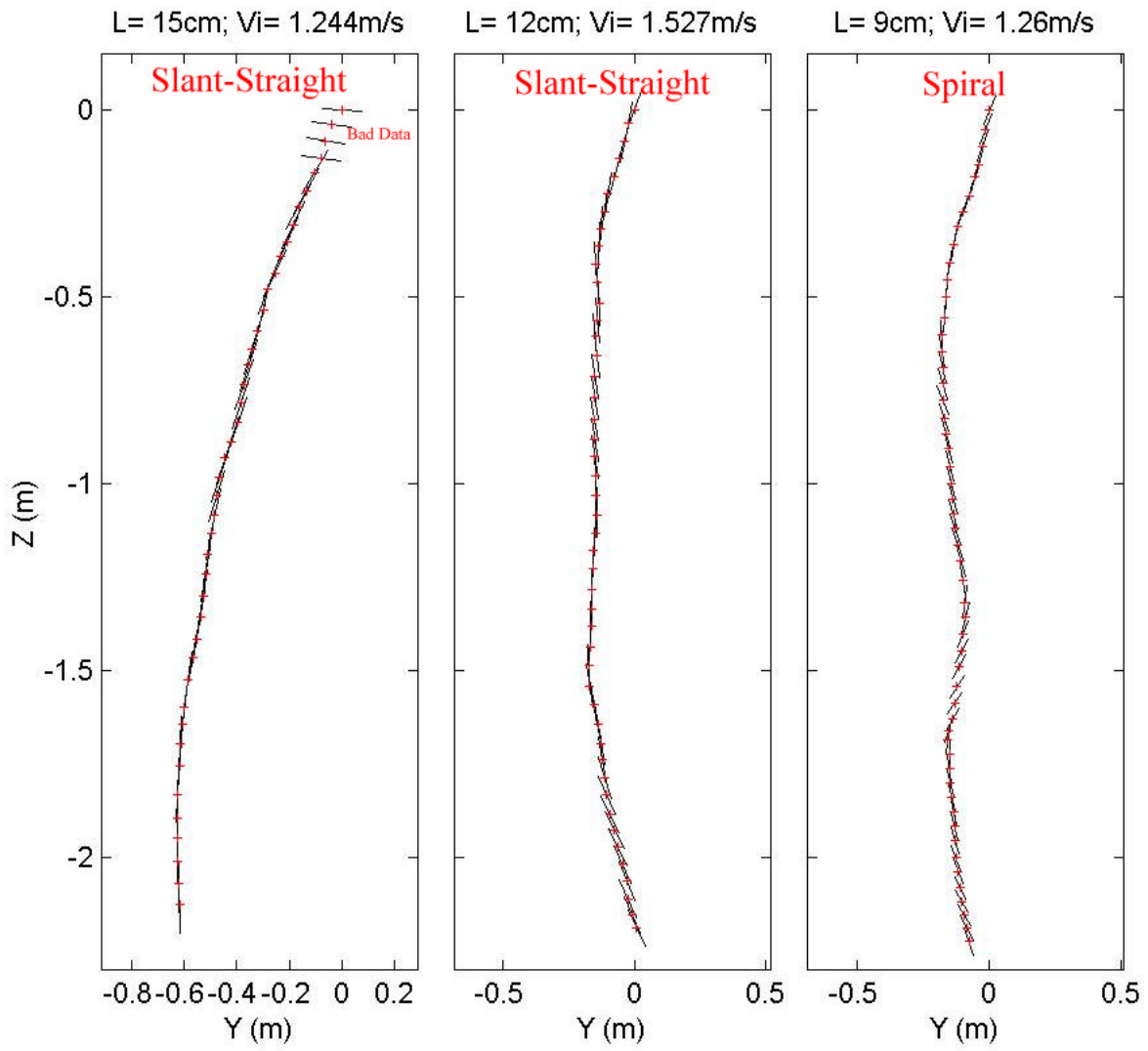




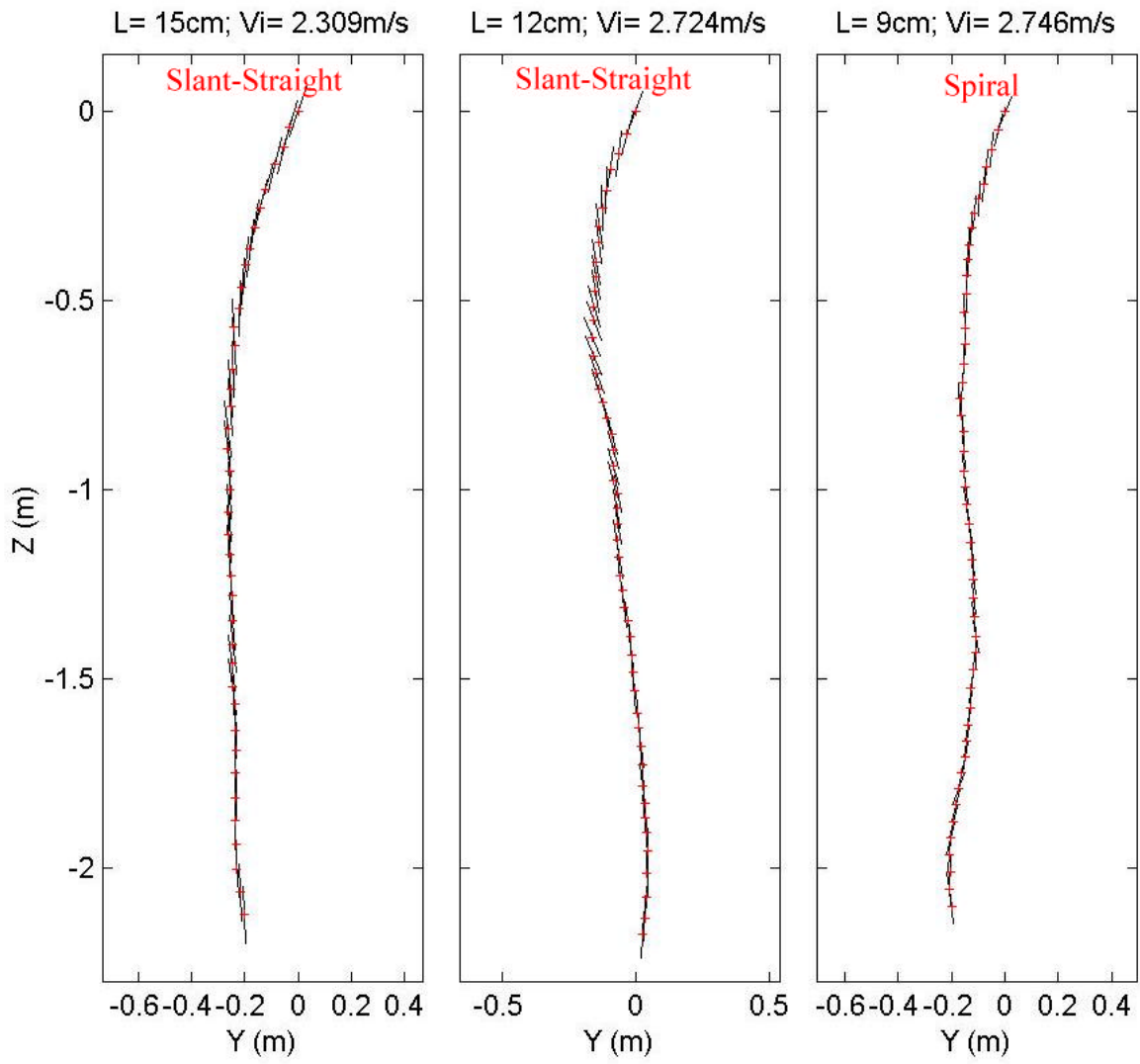
Drop Angle: 30; COM:2



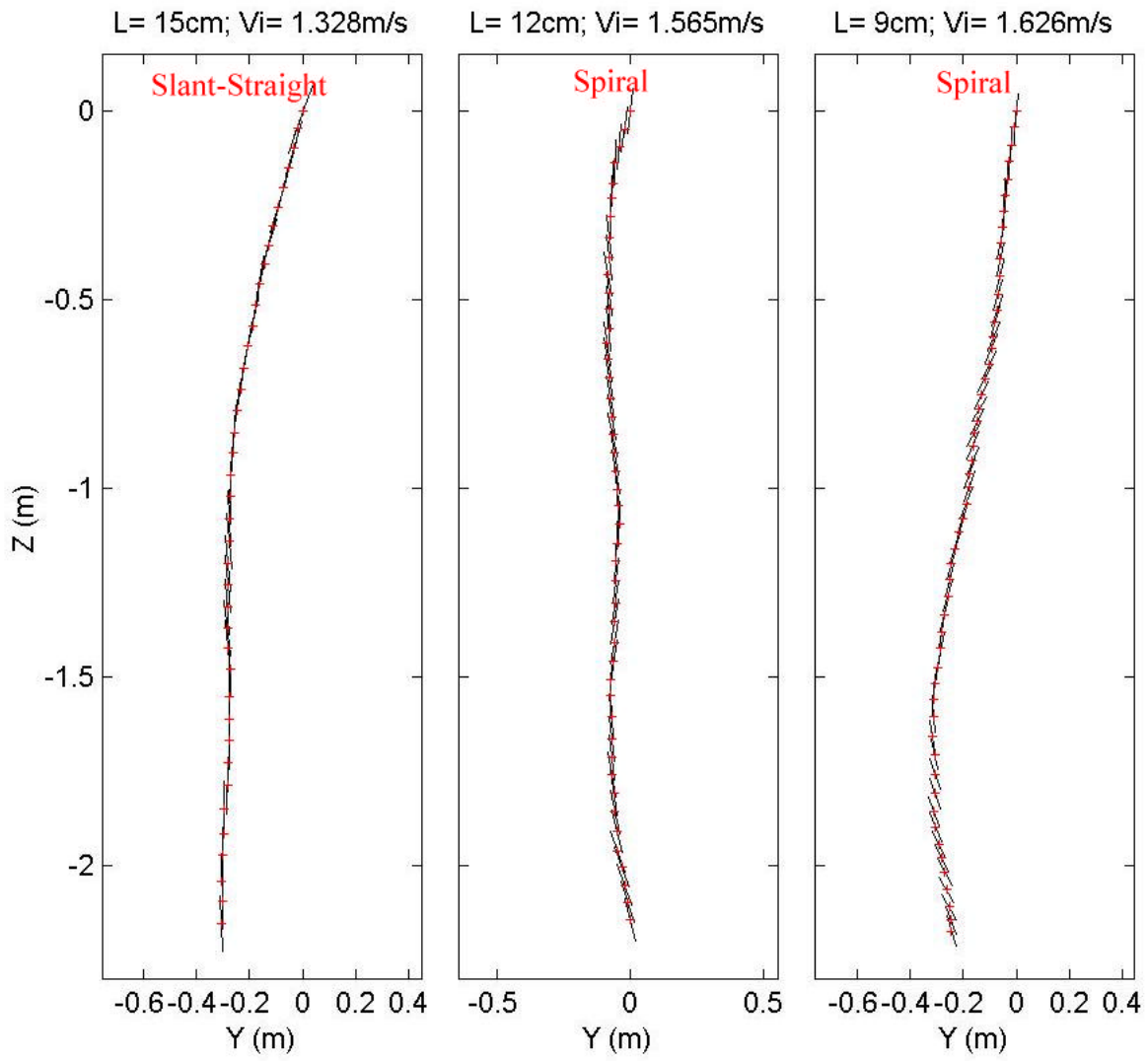
Drop Angle: 30; COM:2



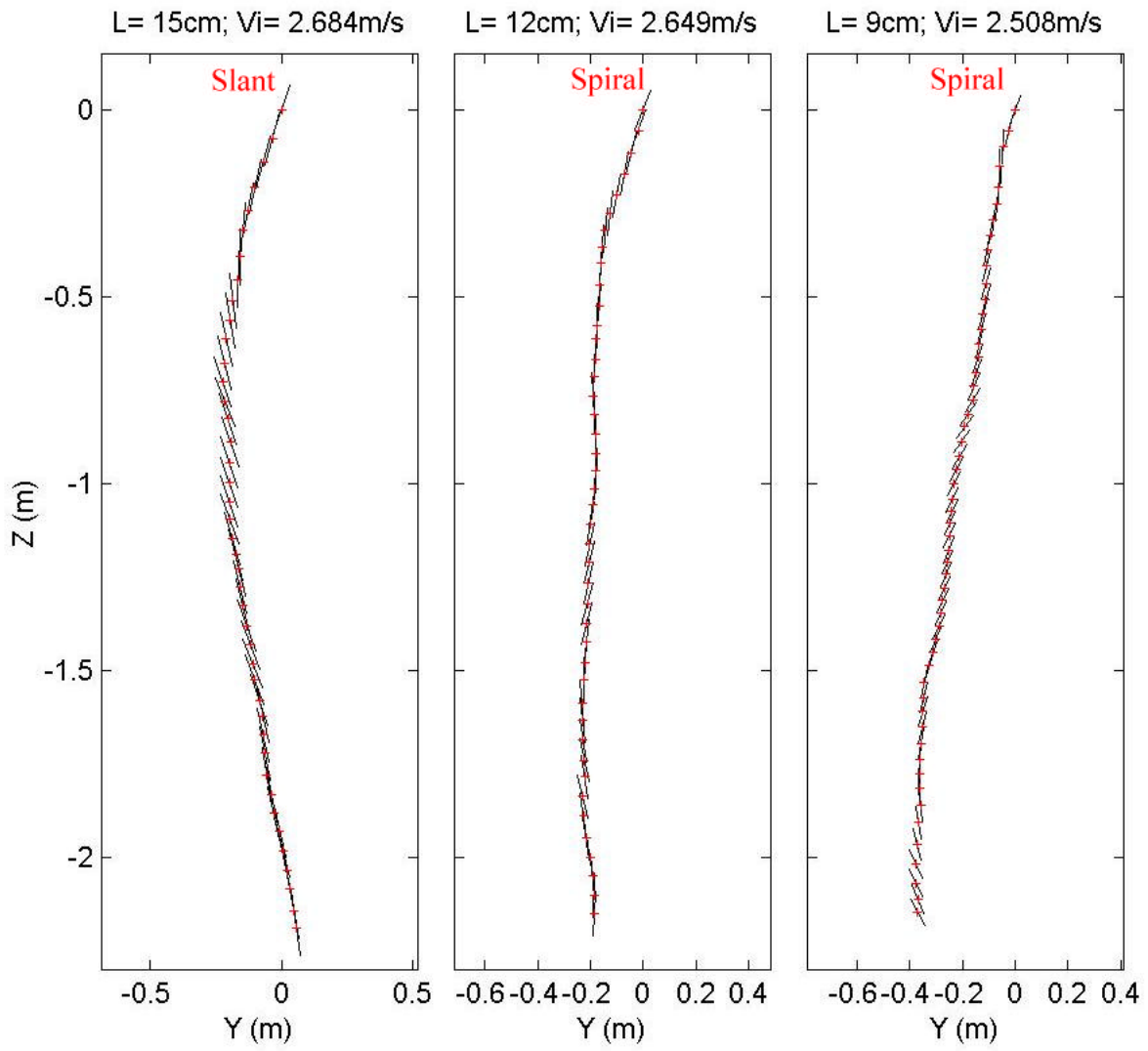
Drop Angle: 30; COM:2



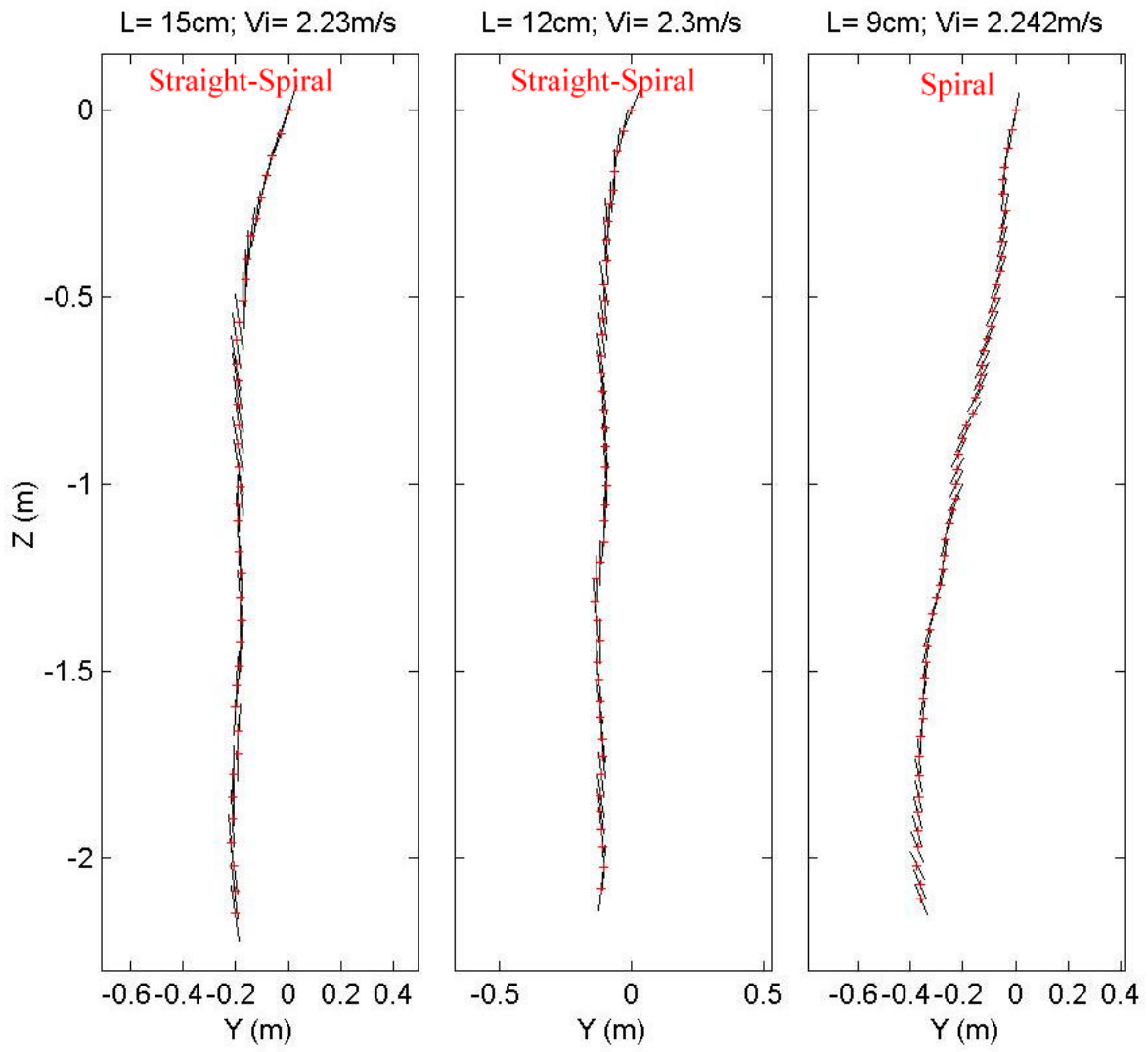
Drop Angle: 45; COM:2



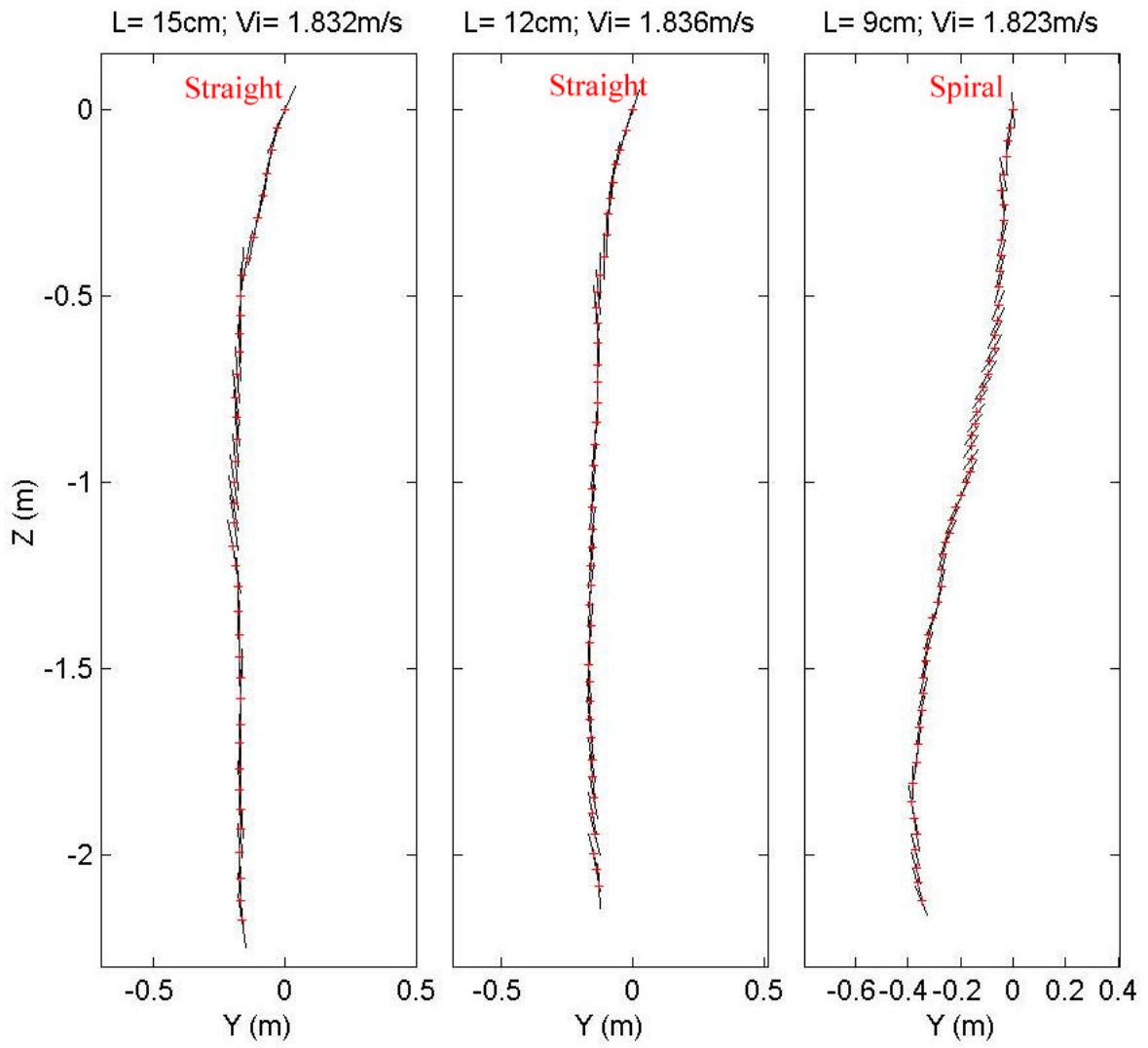
Drop Angle: 45; COM:2



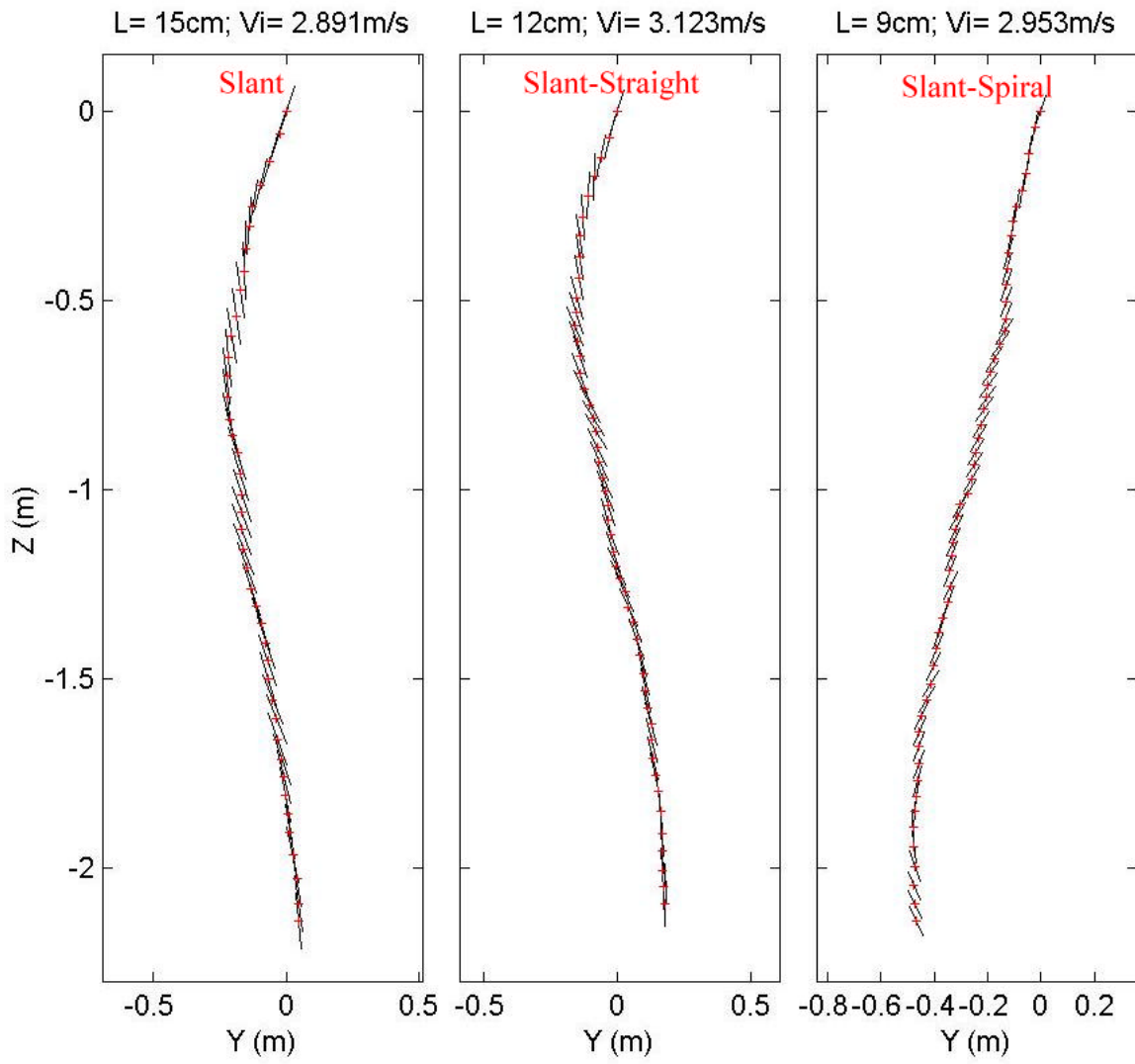
Drop Angle: 45; COM:2



Drop Angle: 45; COM:2

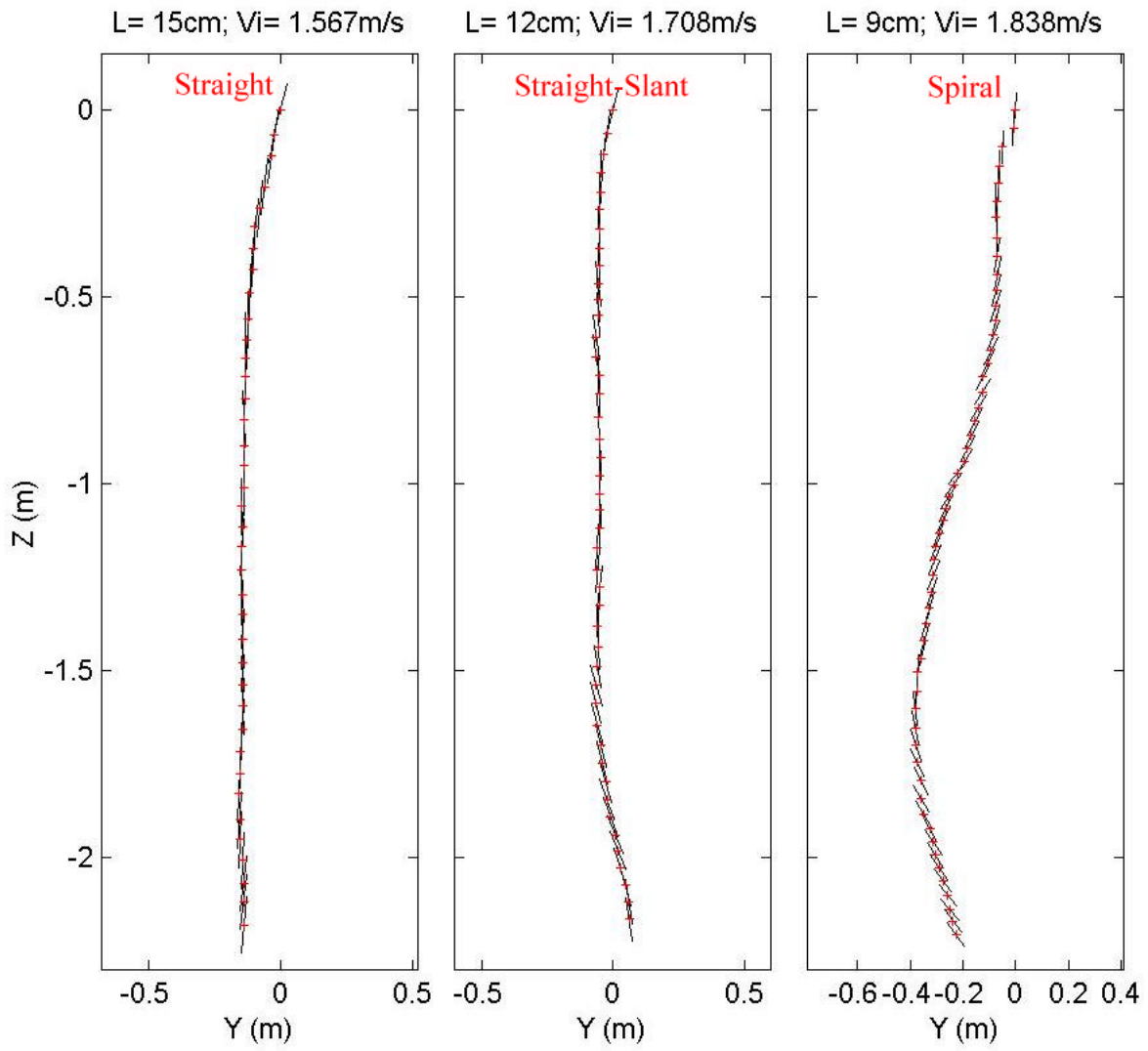


Drop Angle: 45; COM:2

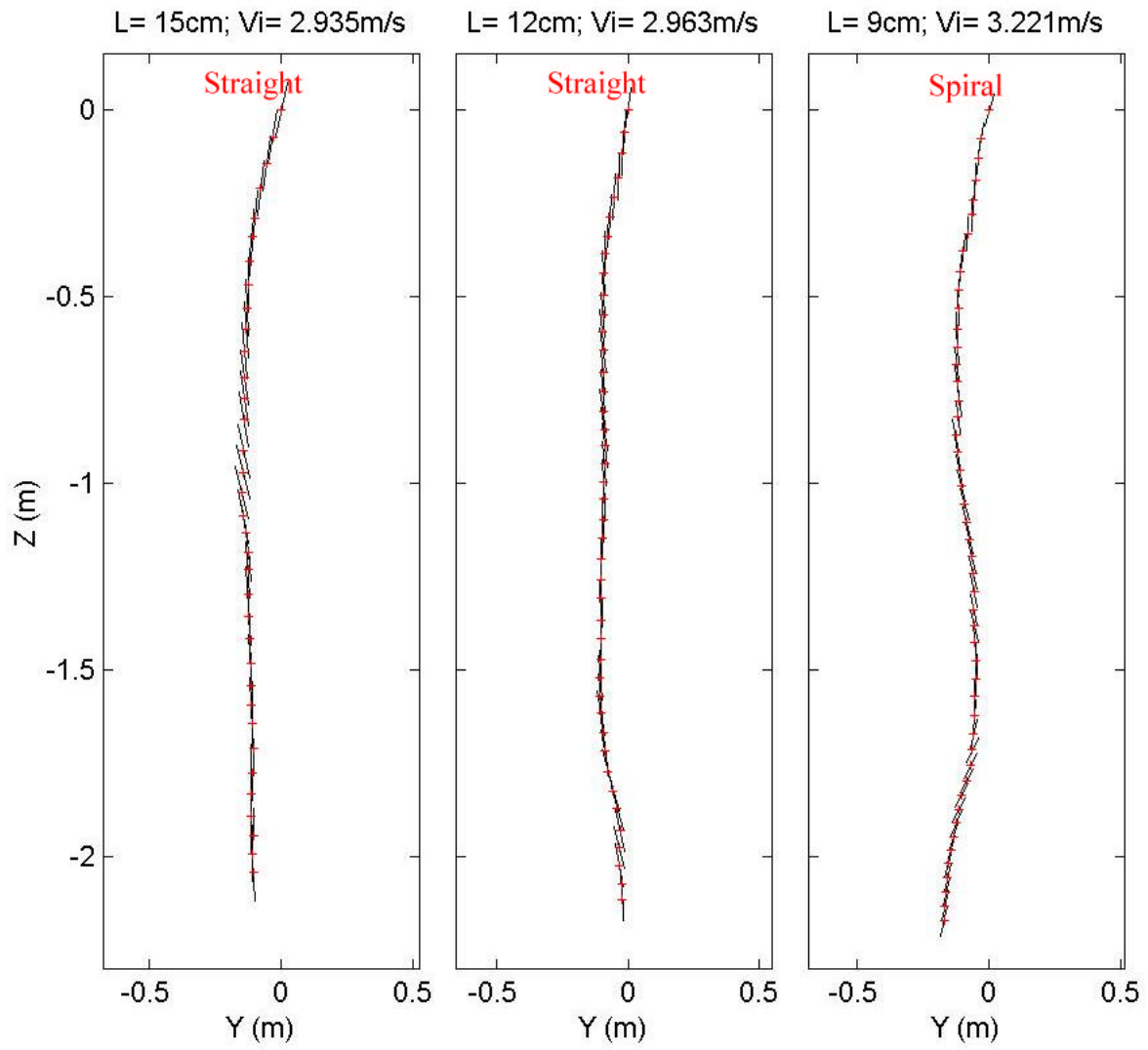




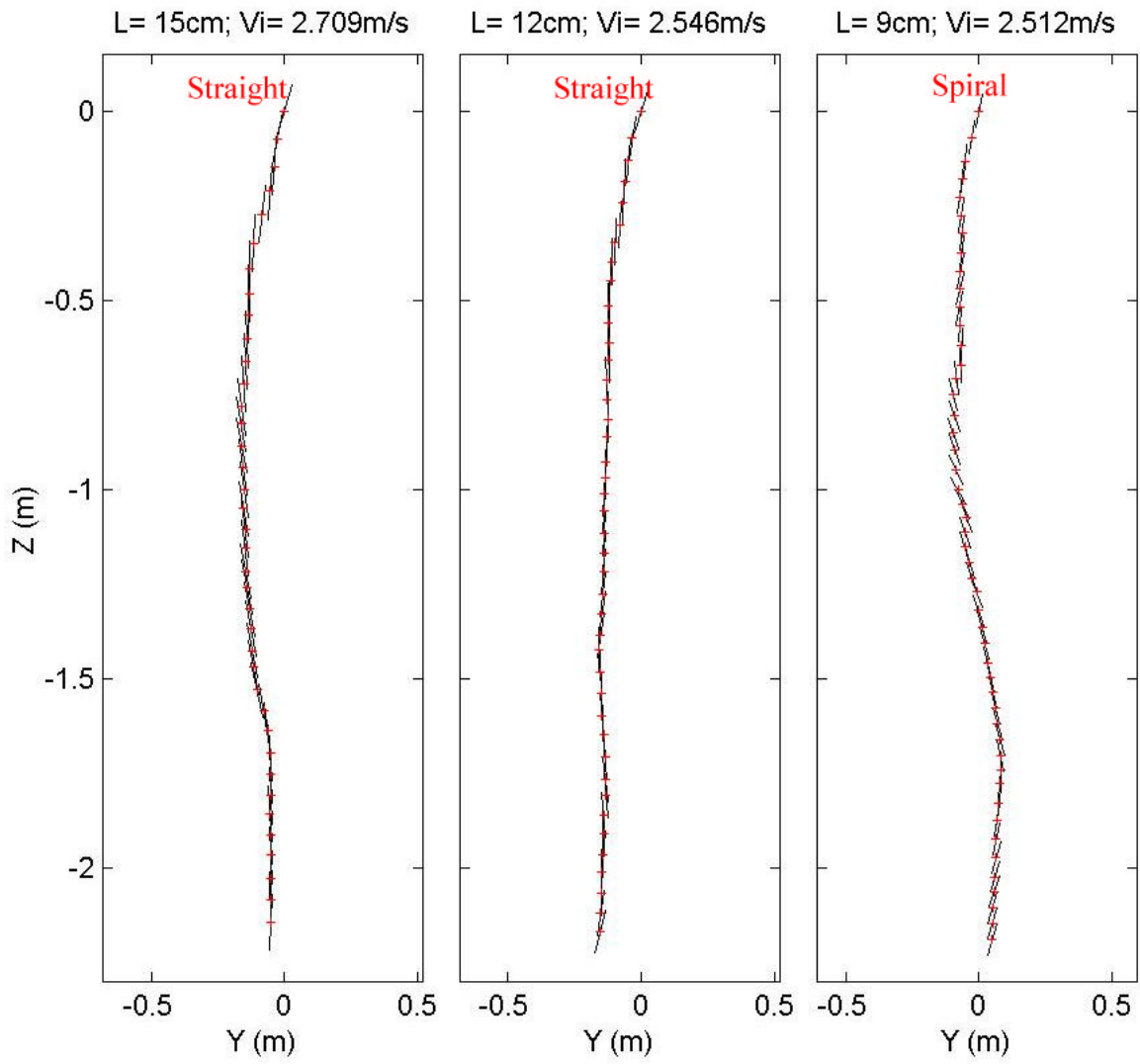
Drop Angle: 60; COM:2



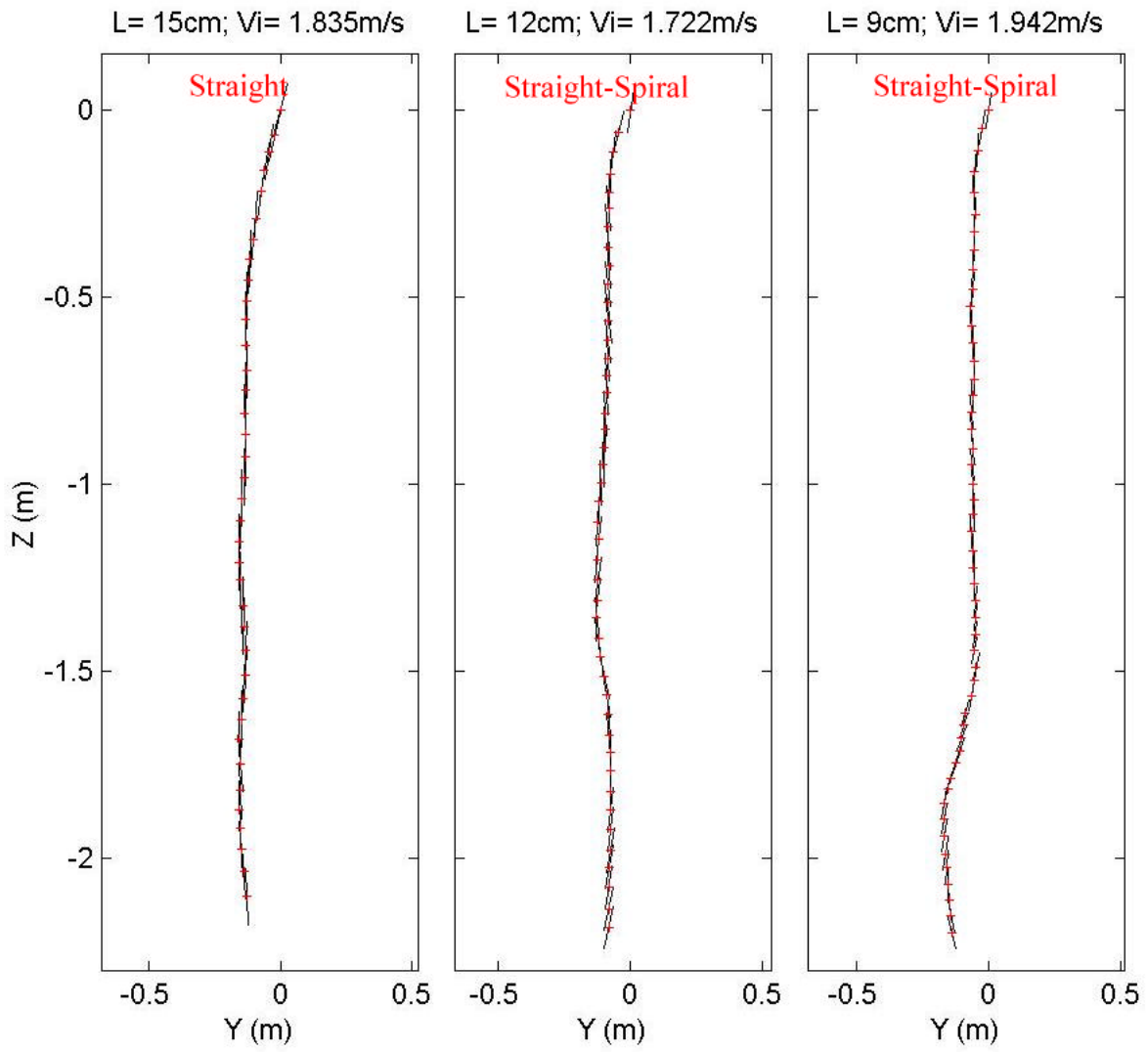
Drop Angle: 60; COM:2



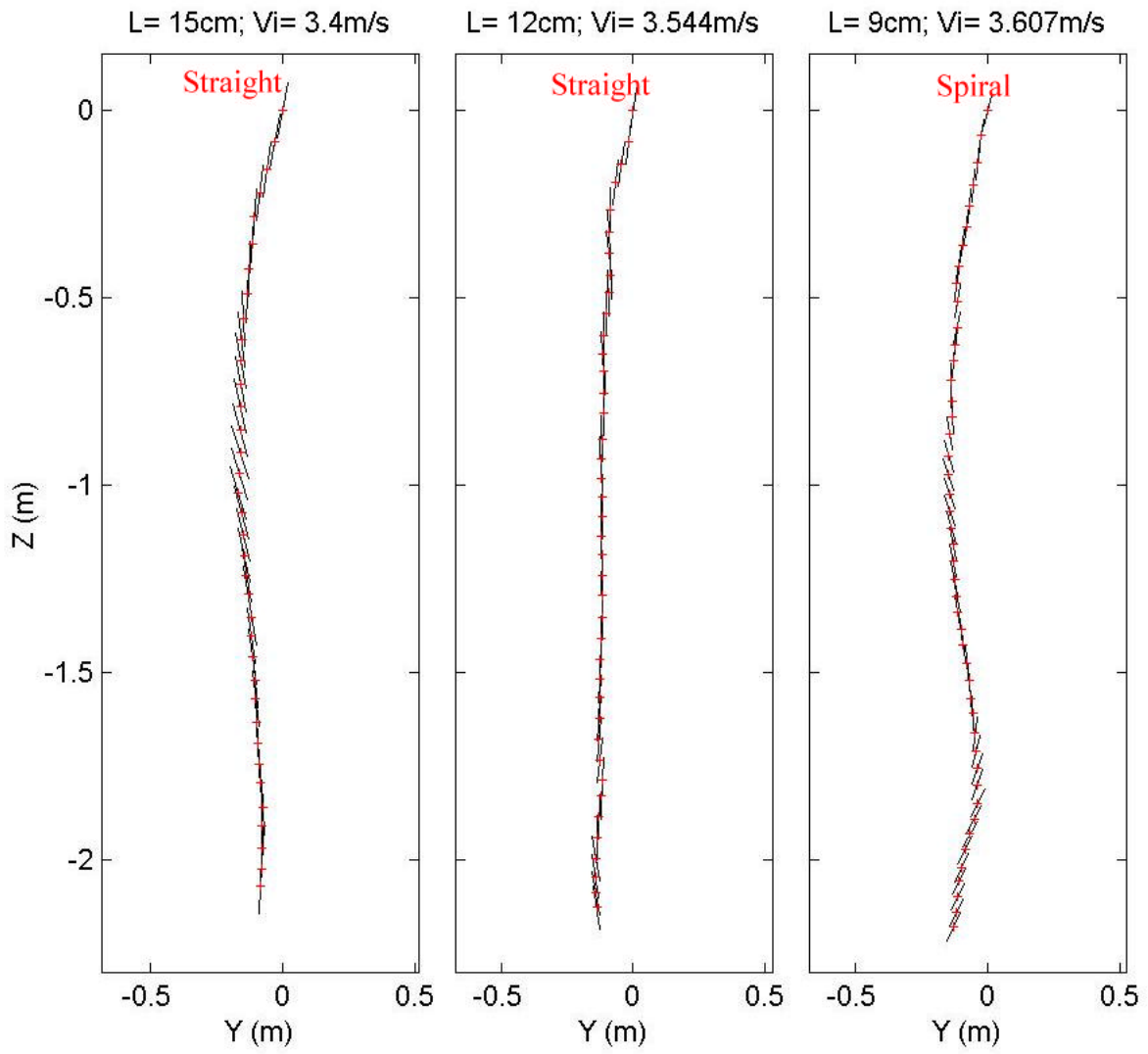
Drop Angle: 60; COM:2



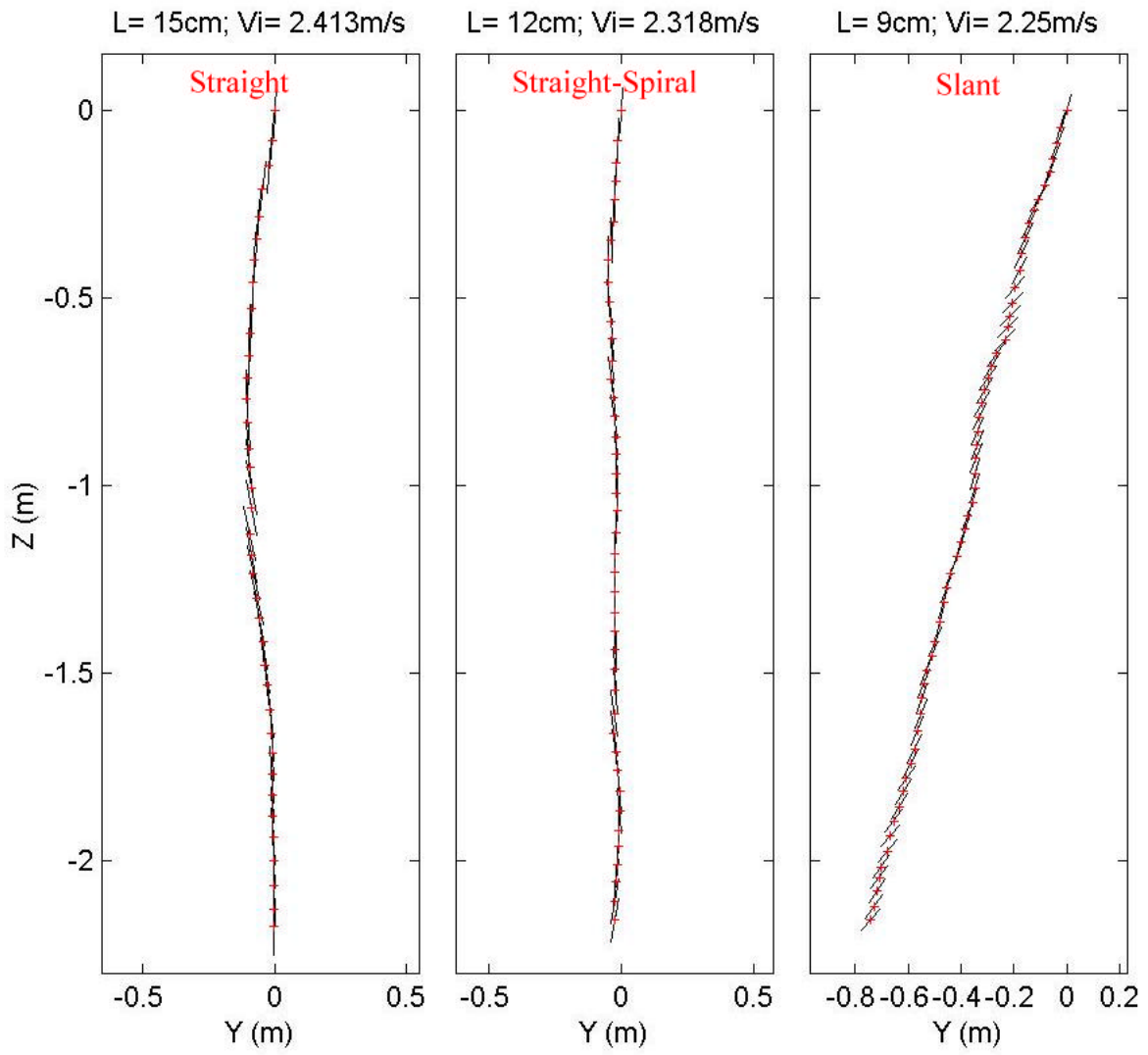
Drop Angle: 60; COM:2



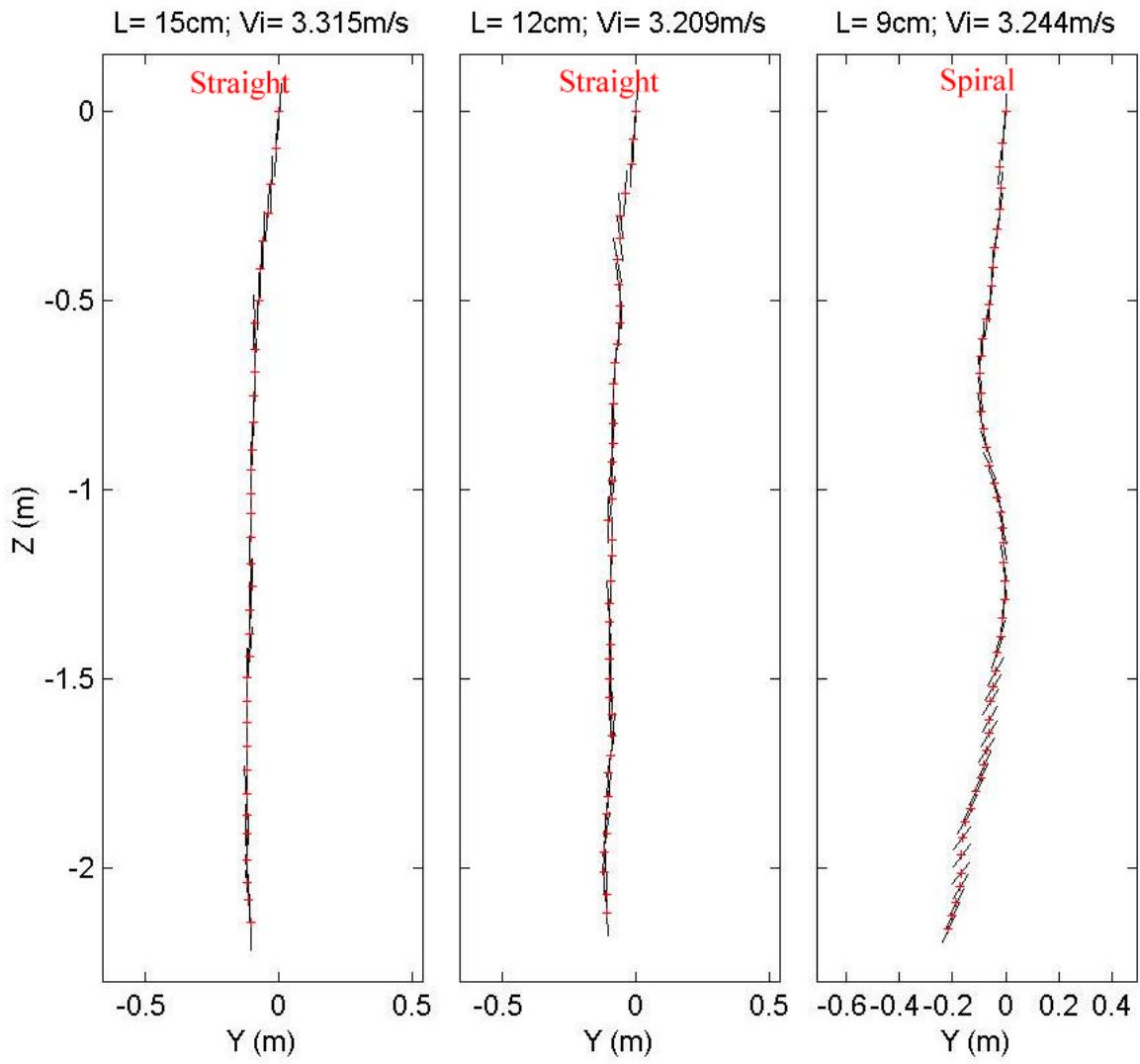
Drop Angle: 60; COM:2



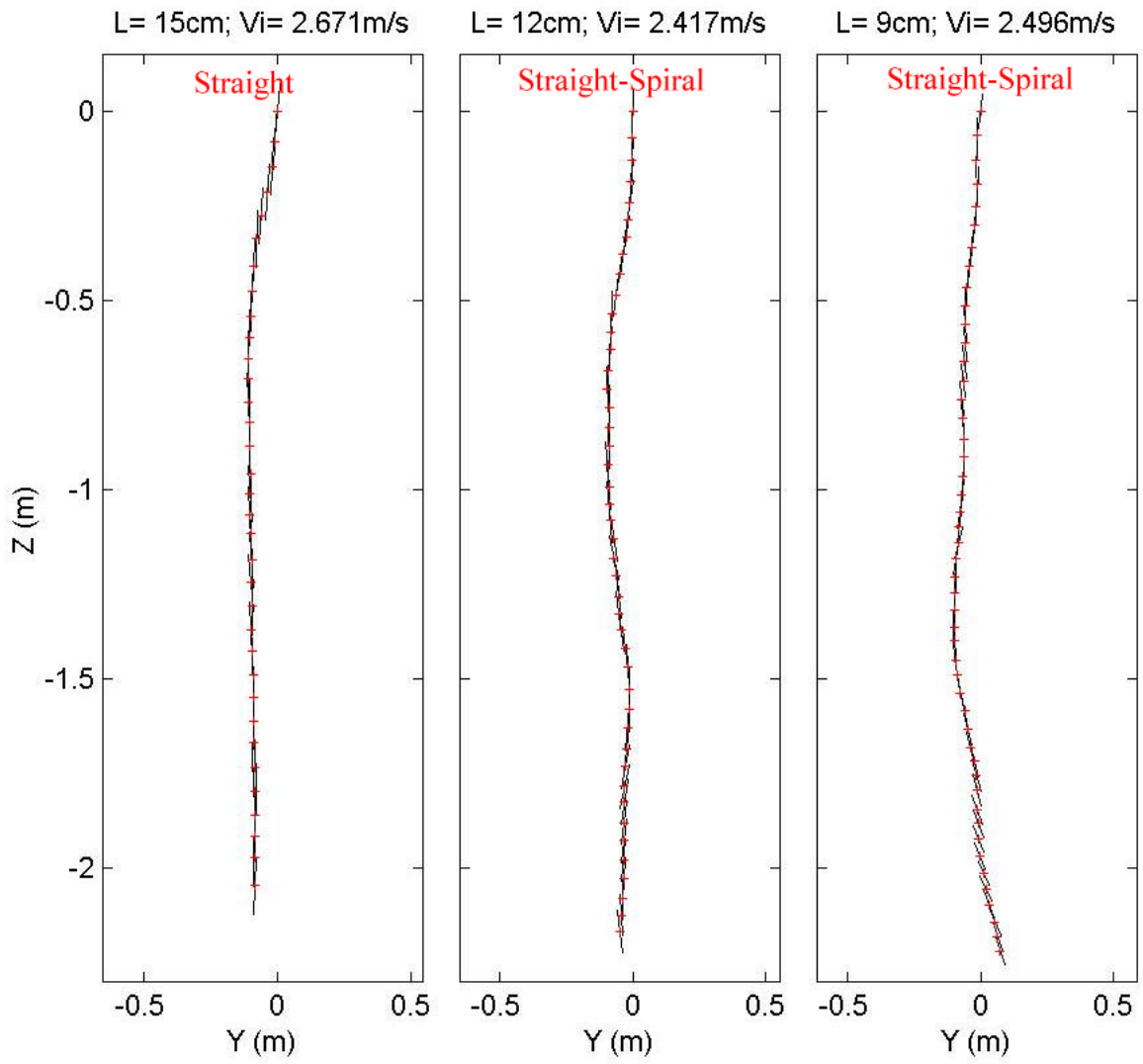
Drop Angle: 75; COM:2



Drop Angle: 75; COM:2

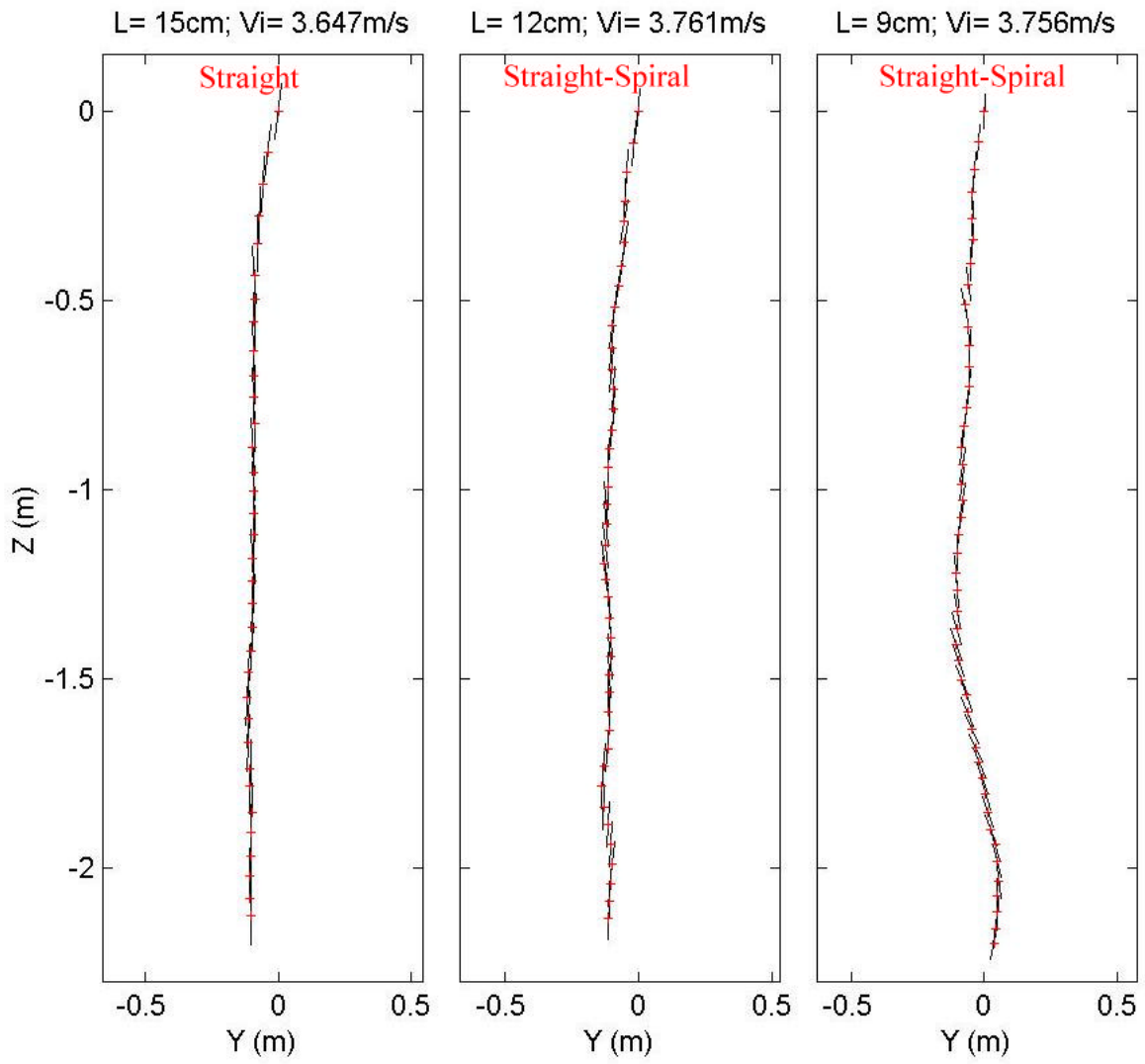


Drop Angle: 75; COM:2

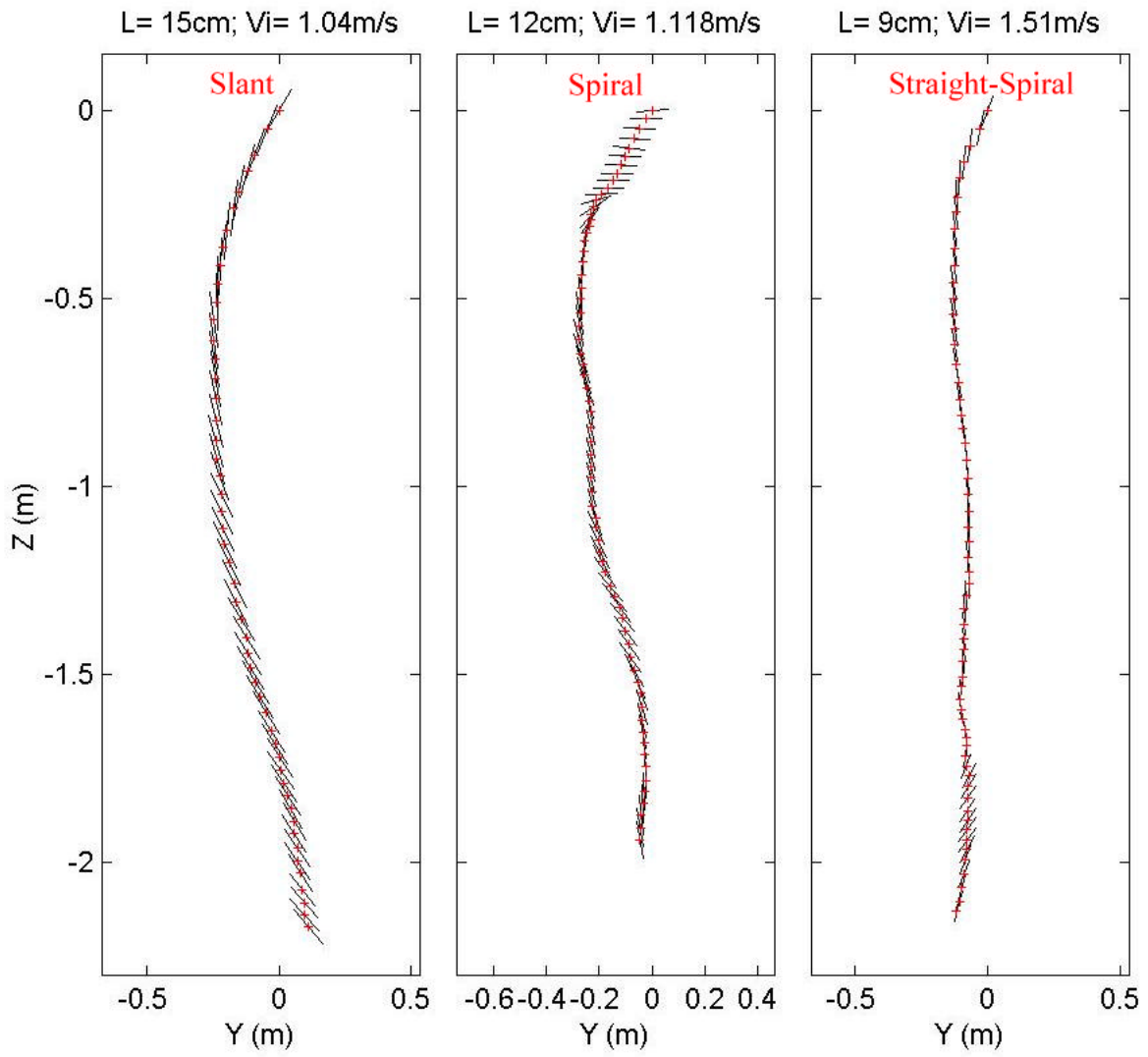




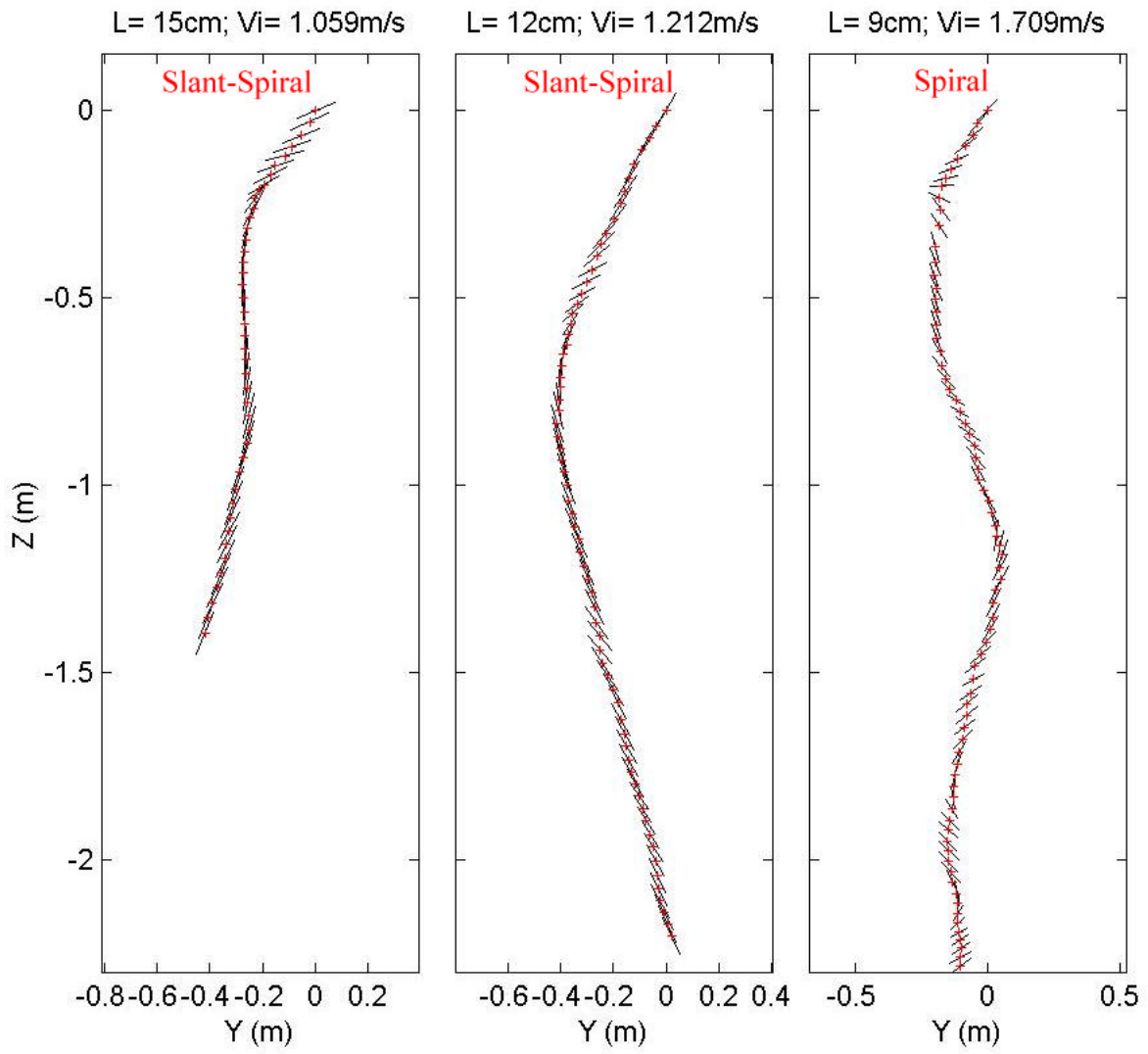
Drop Angle: 75; COM:2



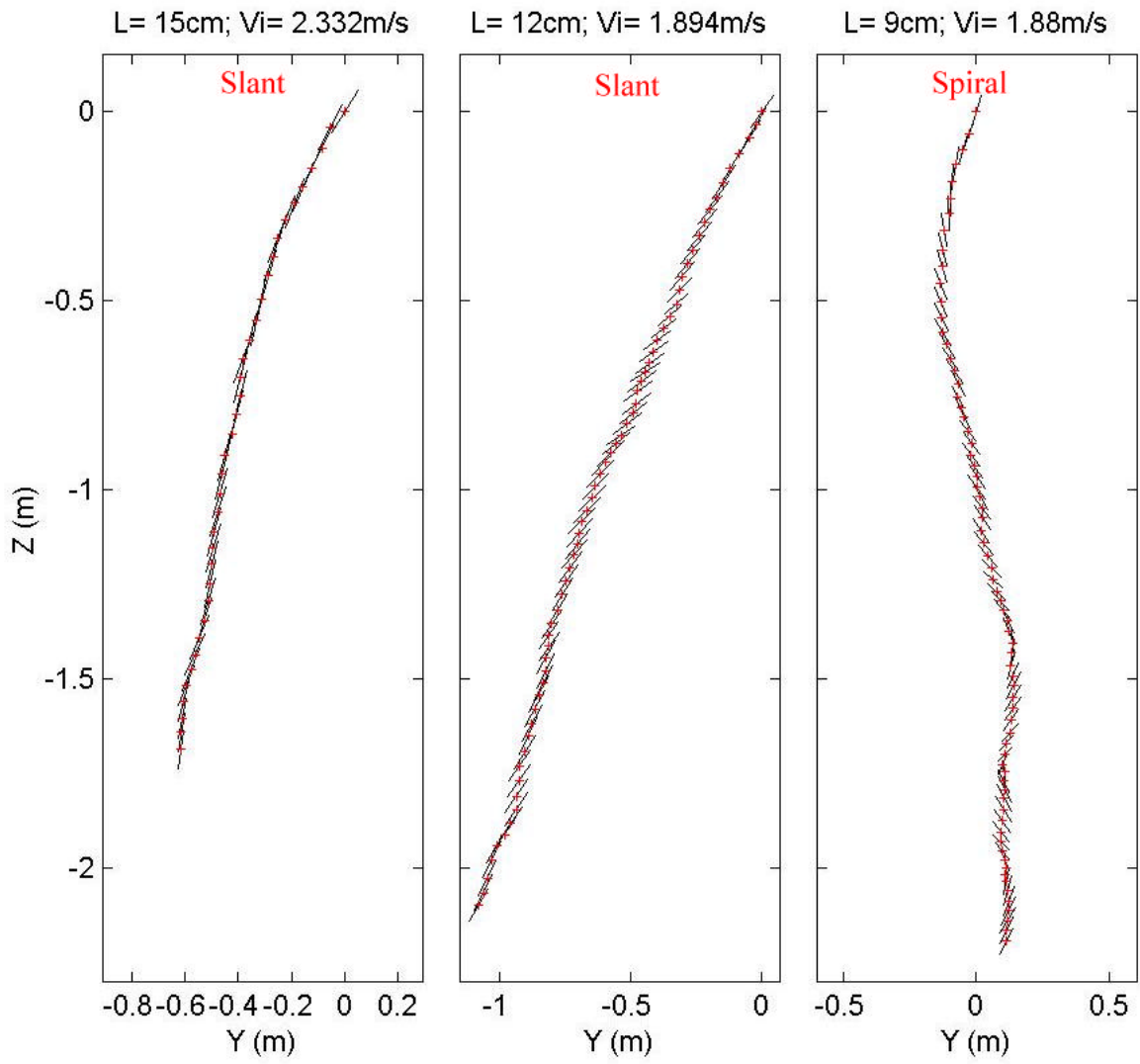
Drop Angle: 15; COM:1



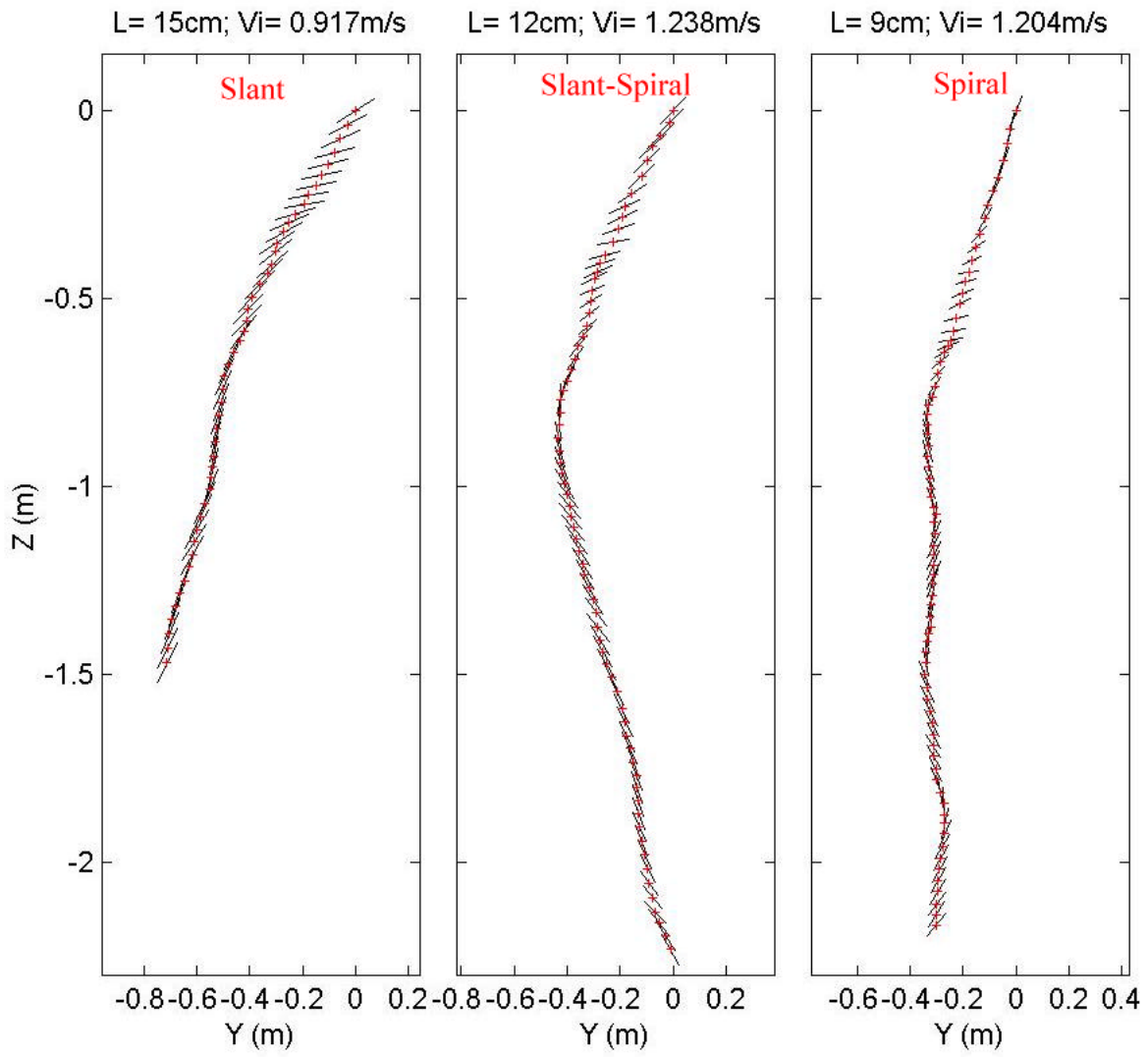
Drop Angle: 15; COM:1



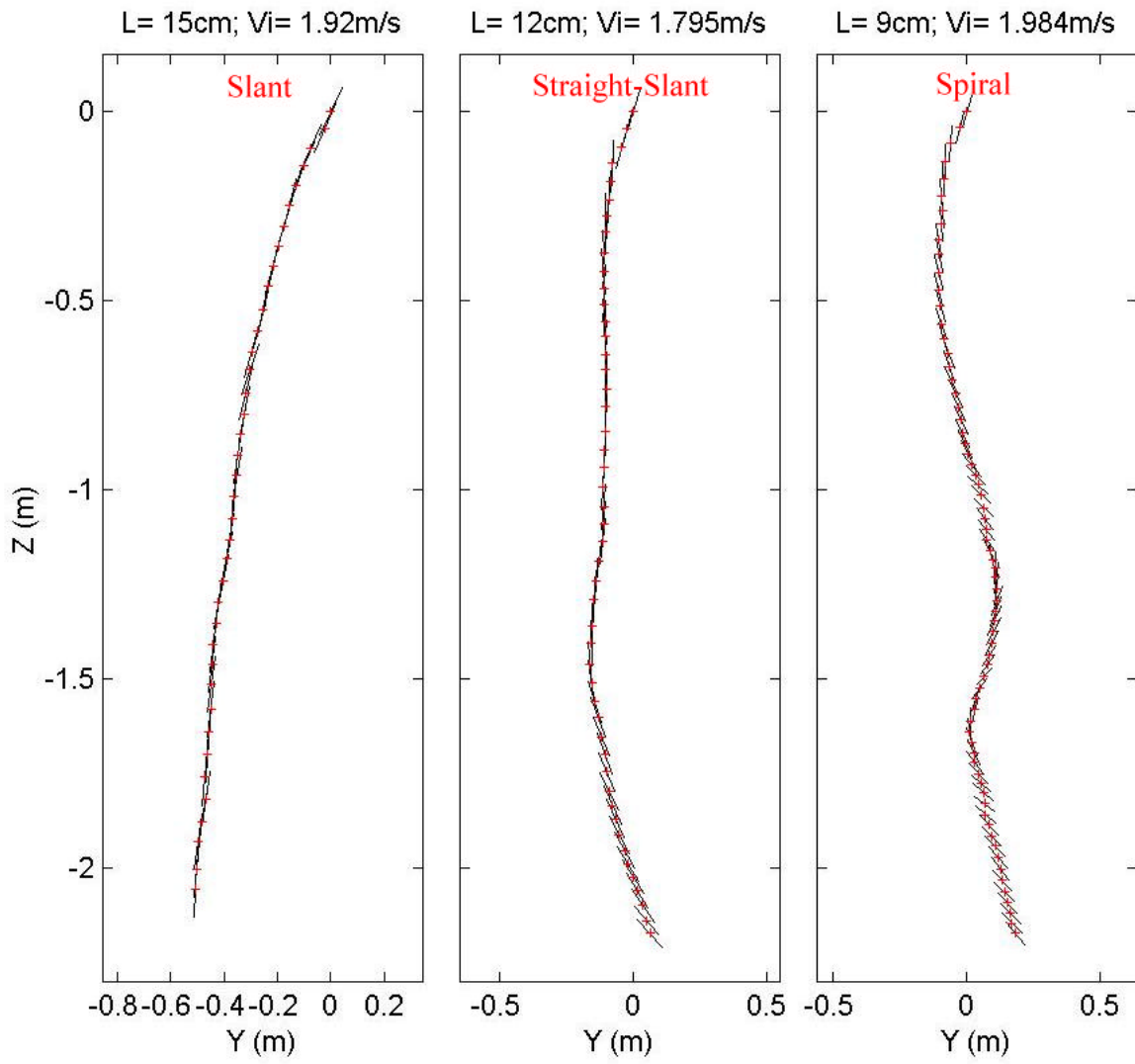
Drop Angle: 15; COM:1



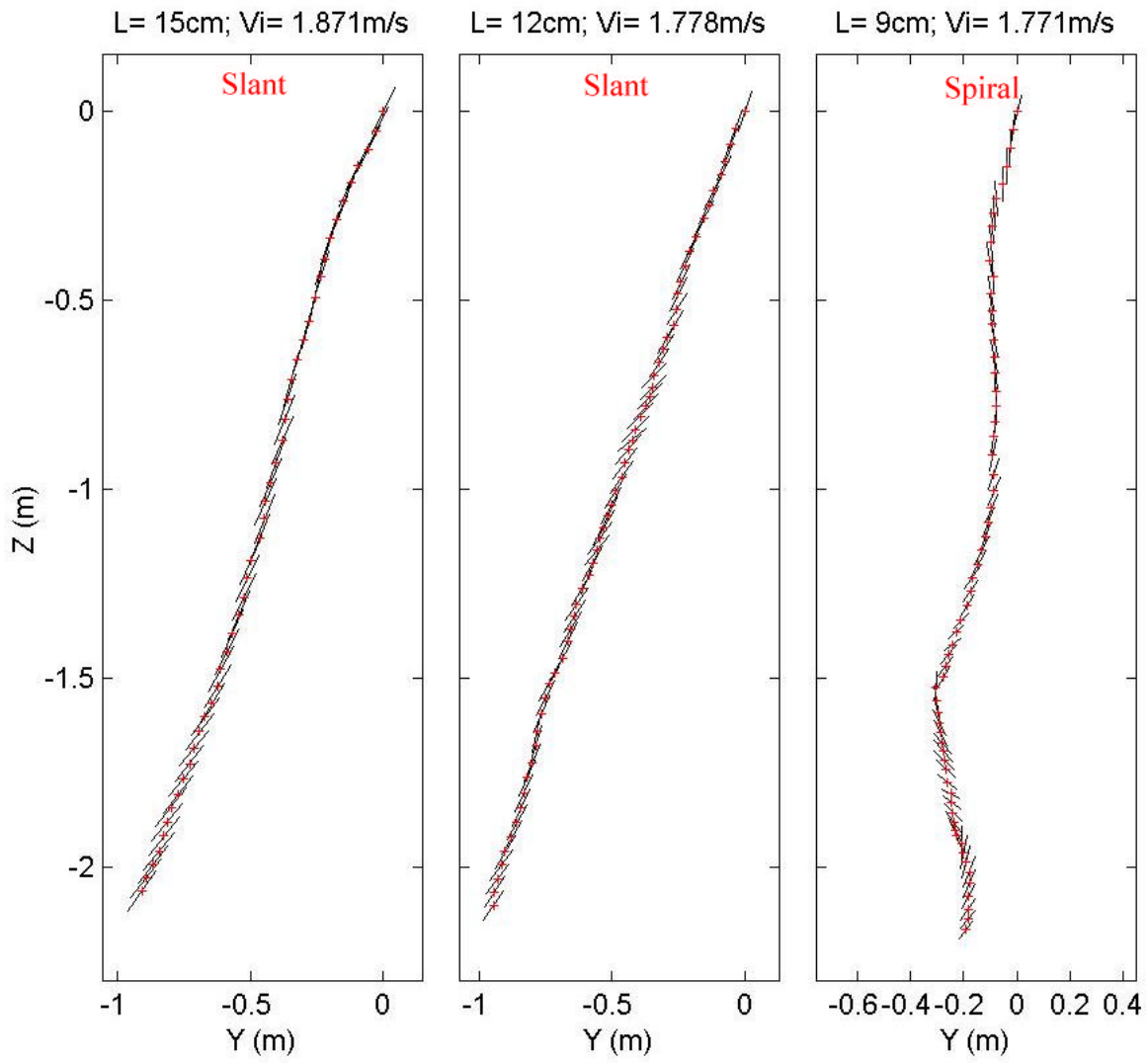
Drop Angle: 30; COM:1



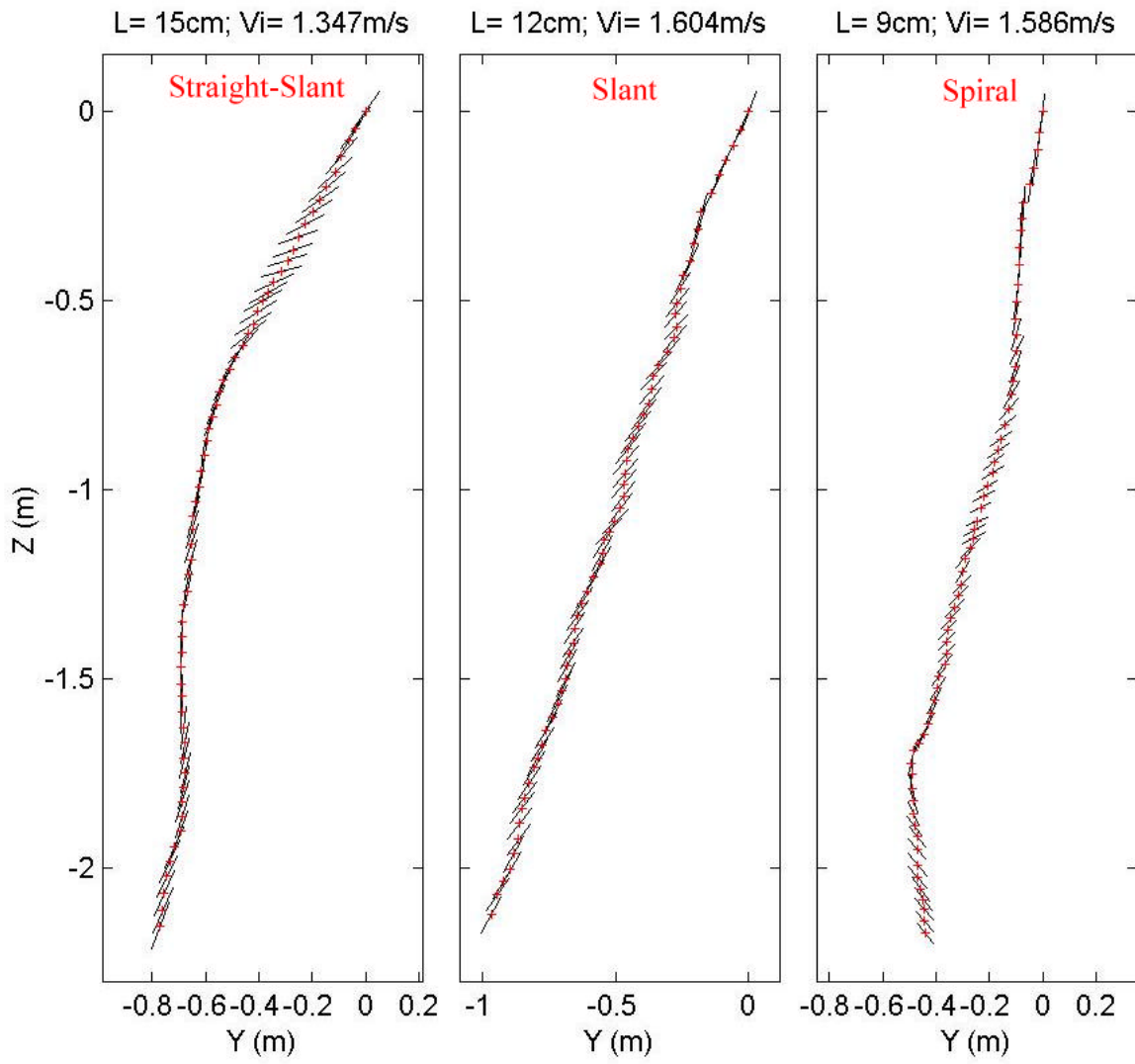
Drop Angle: 30; COM:1



Drop Angle: 30; COM:1

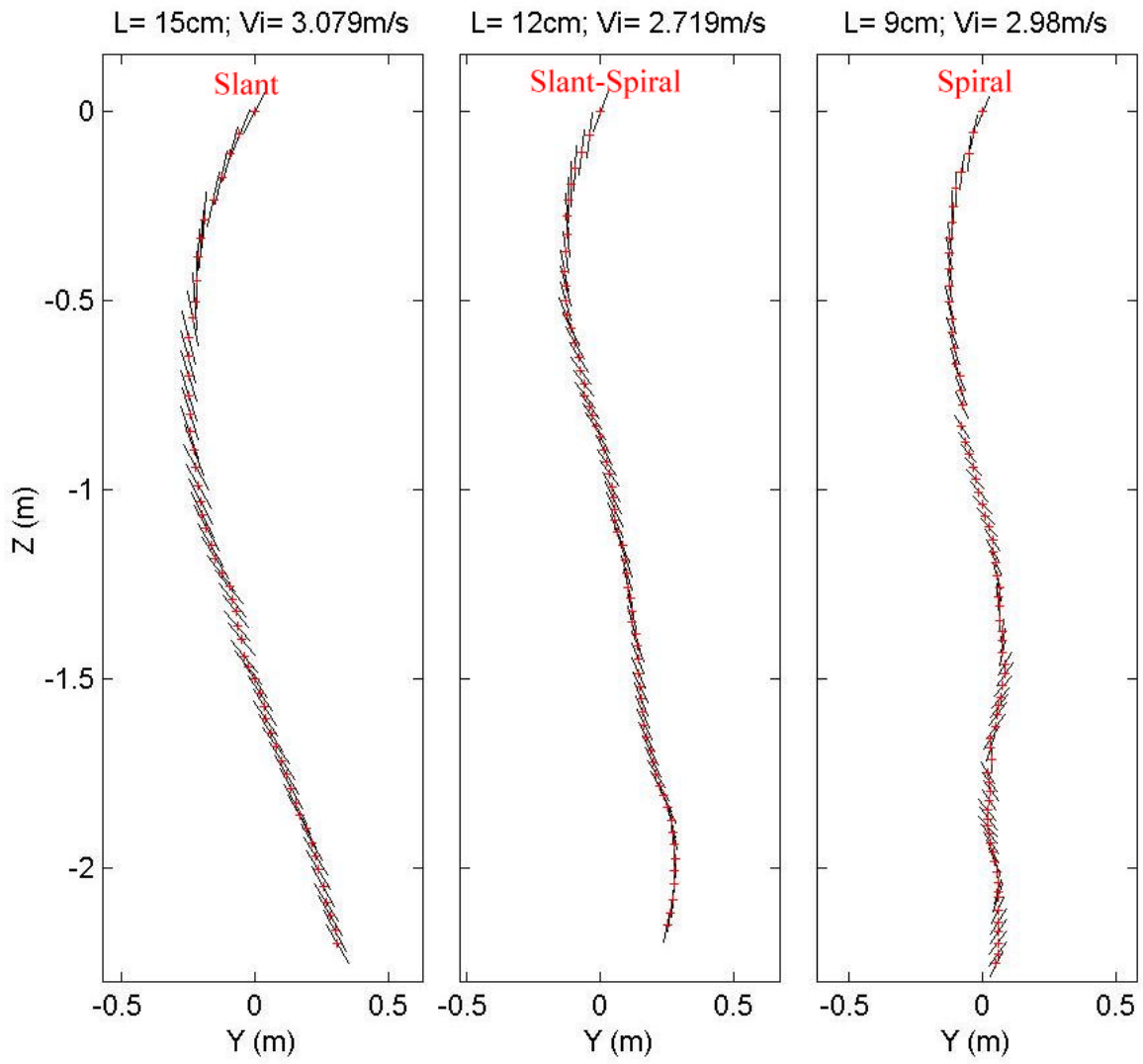


Drop Angle: 30; COM:1

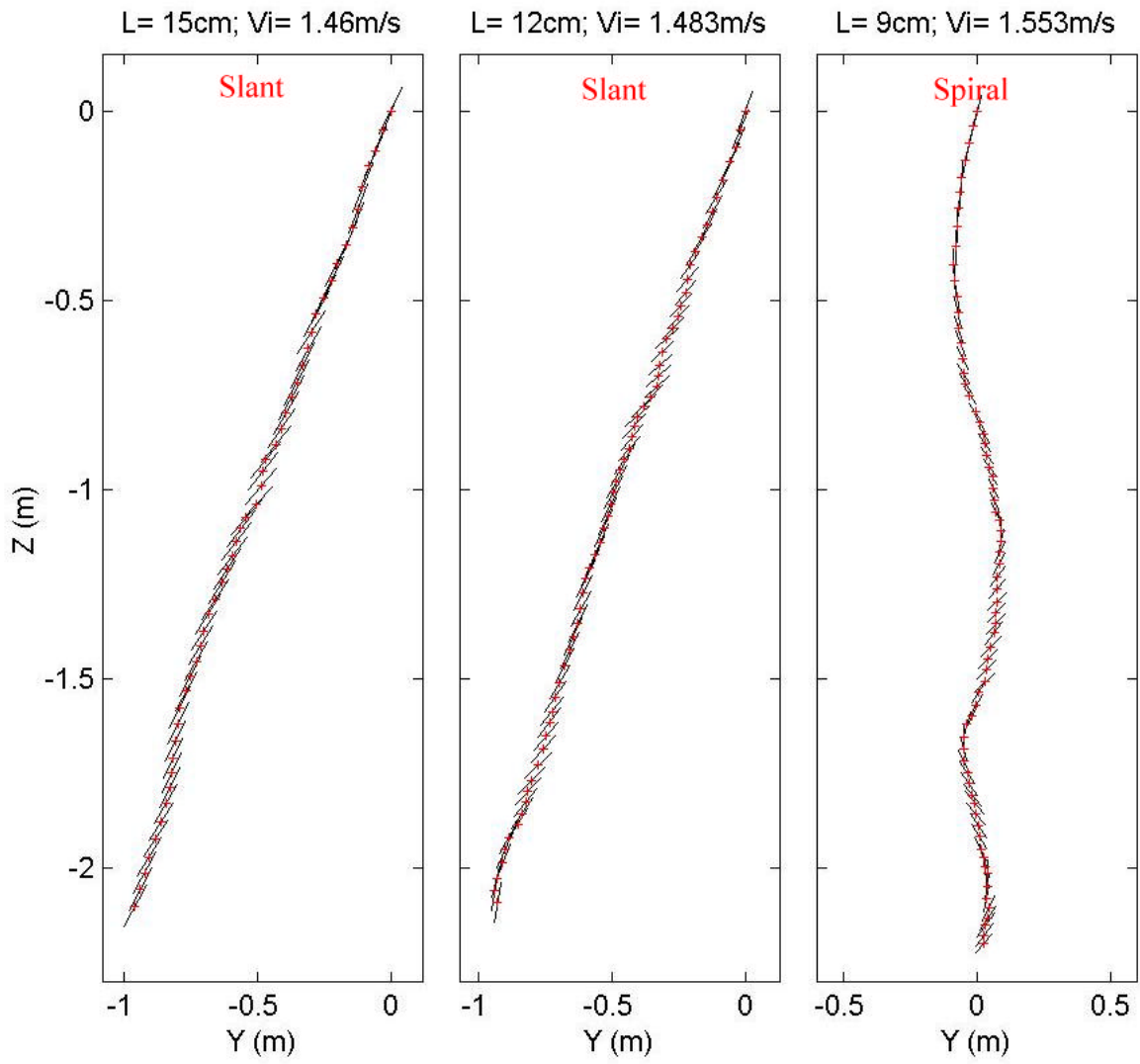




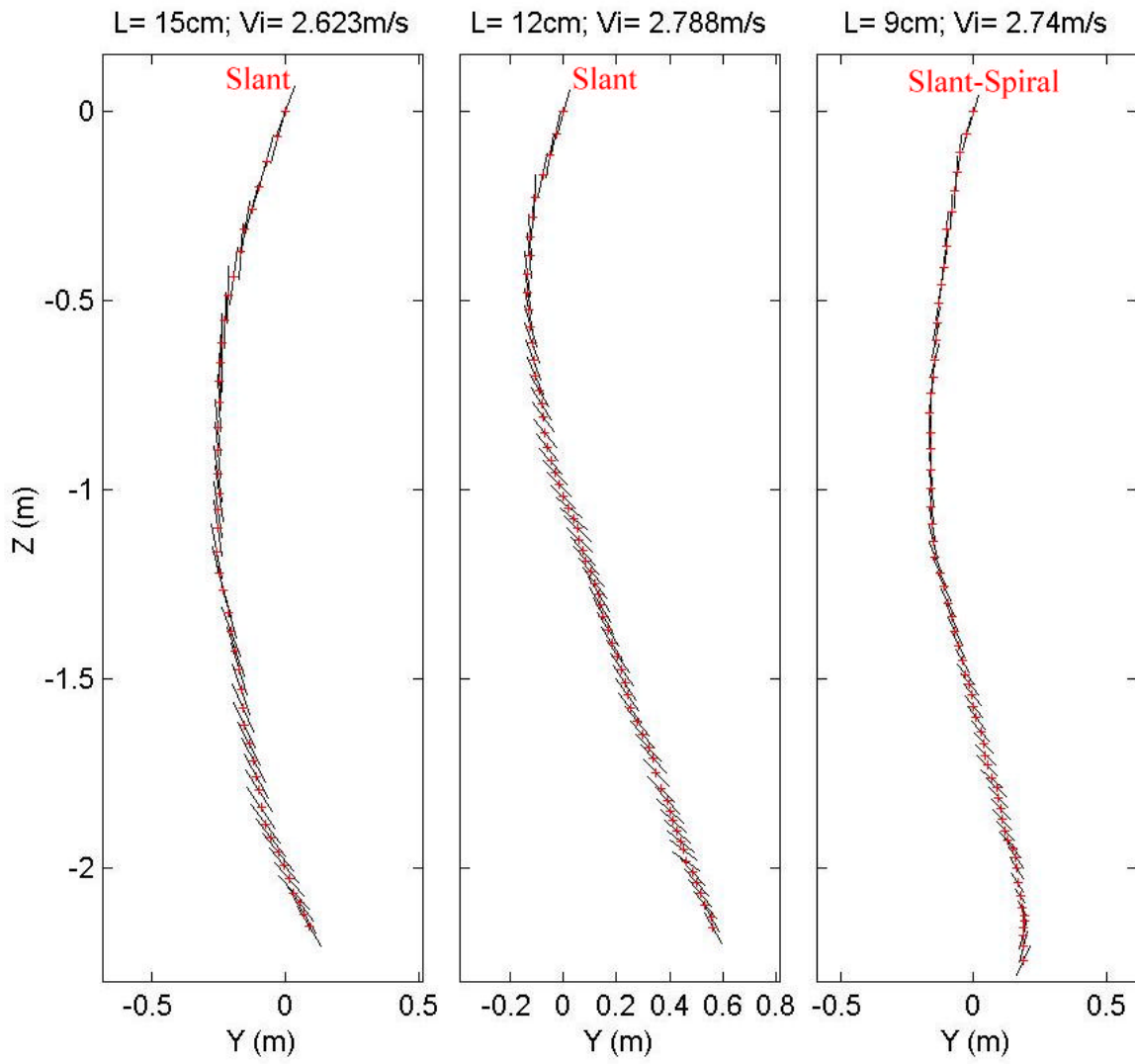
Drop Angle: 30; COM:1



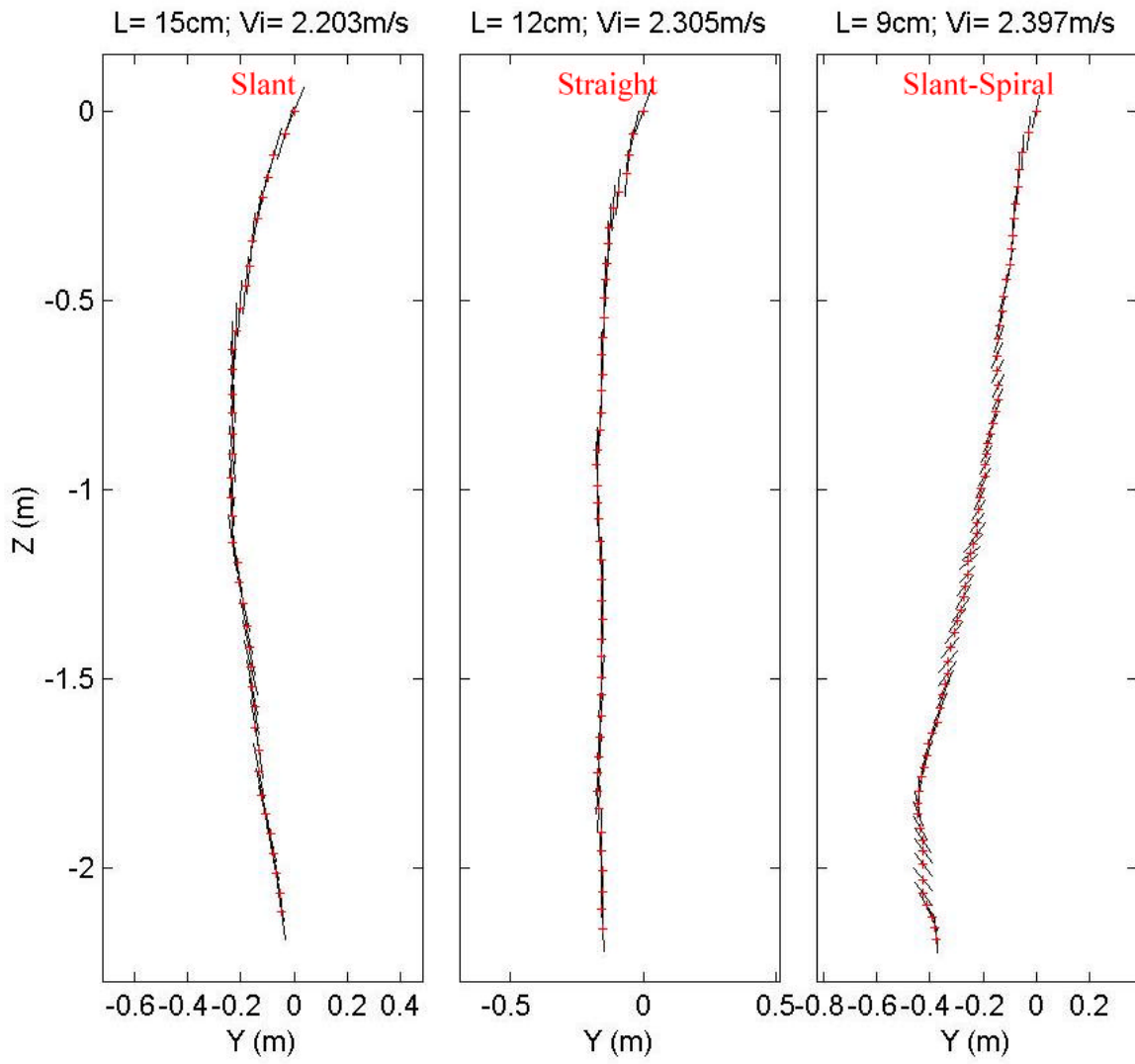
Drop Angle: 45; COM:1



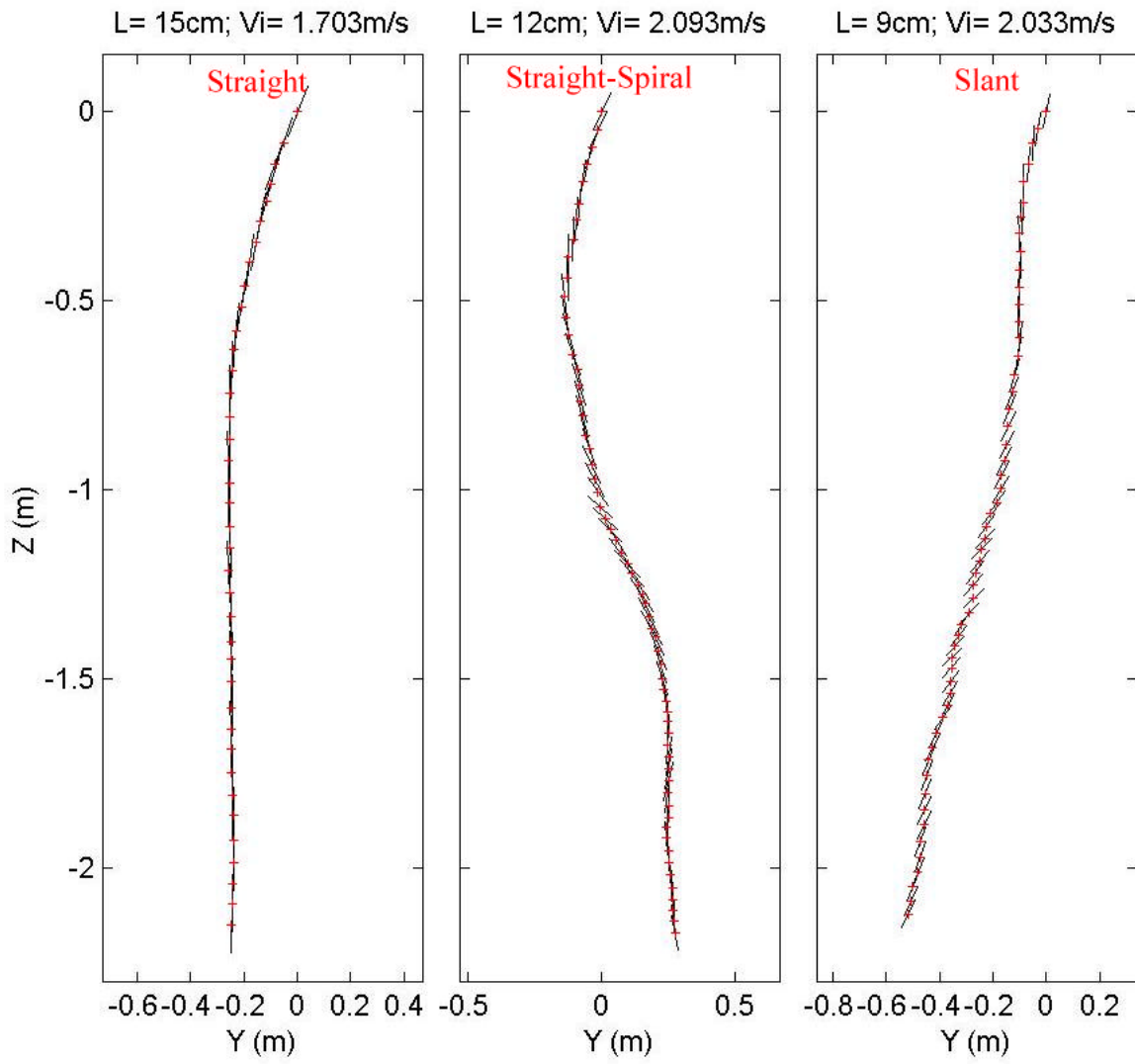
Drop Angle: 45; COM:1



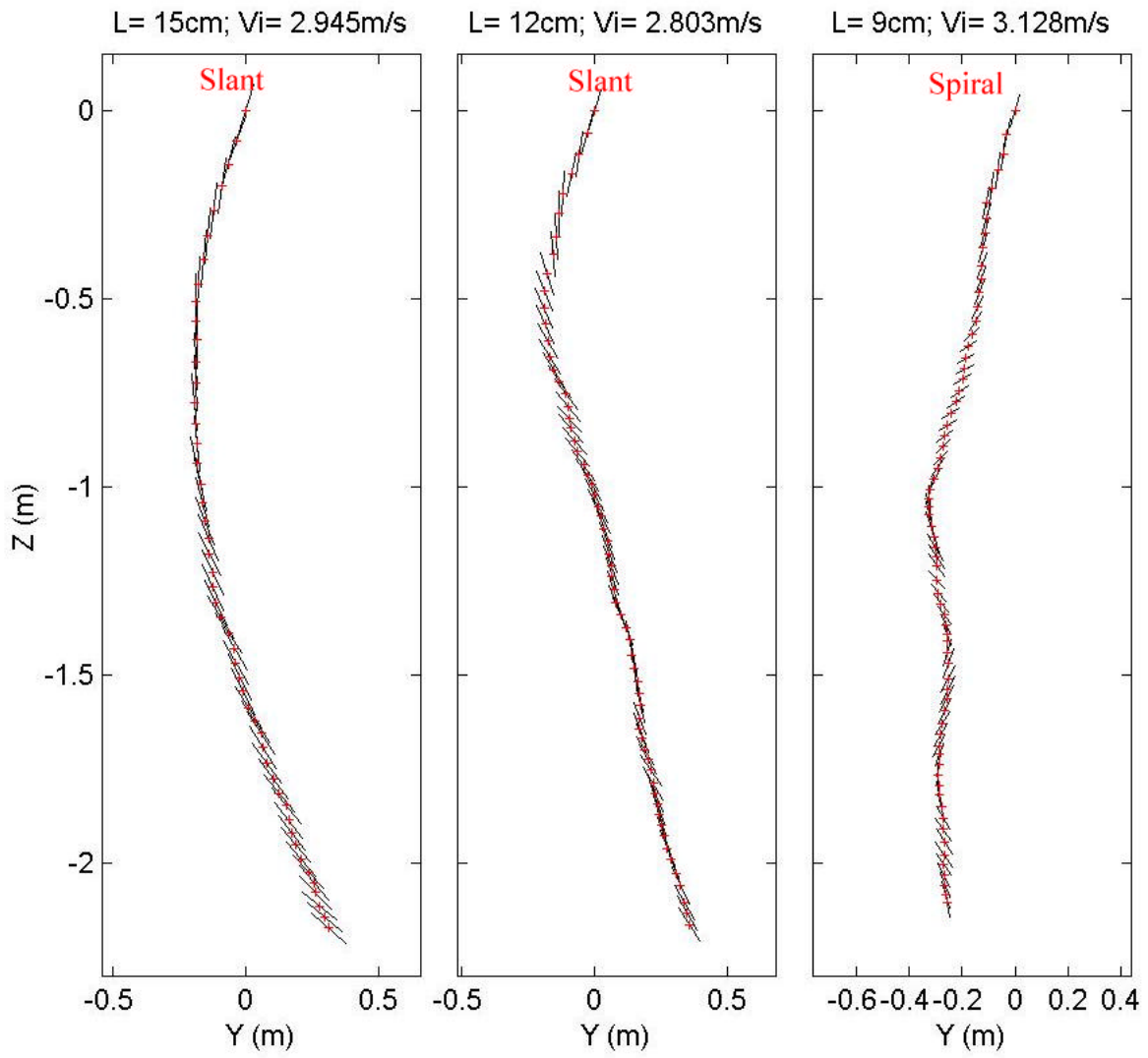
Drop Angle: 45; COM:1



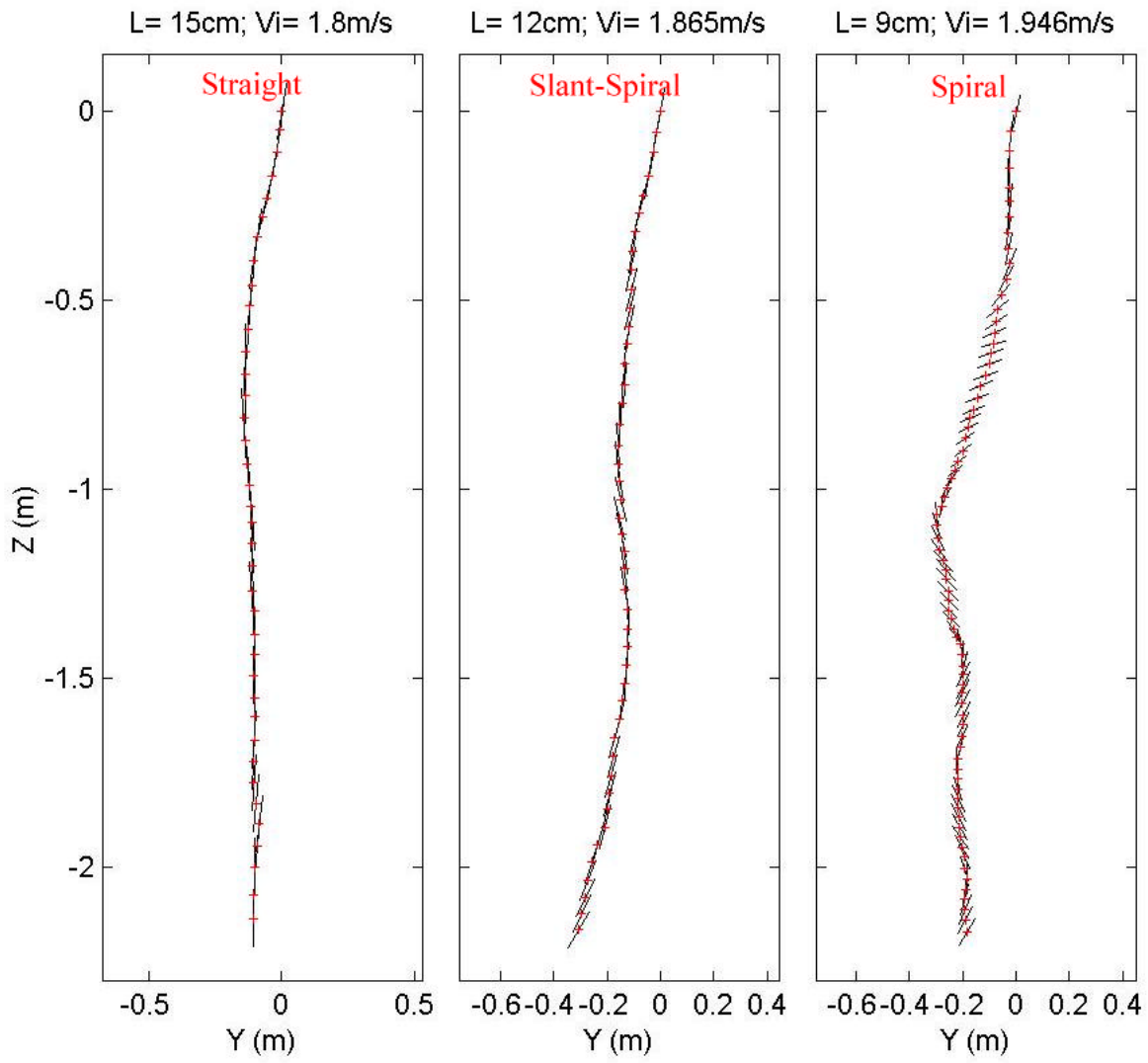
Drop Angle: 45; COM:1



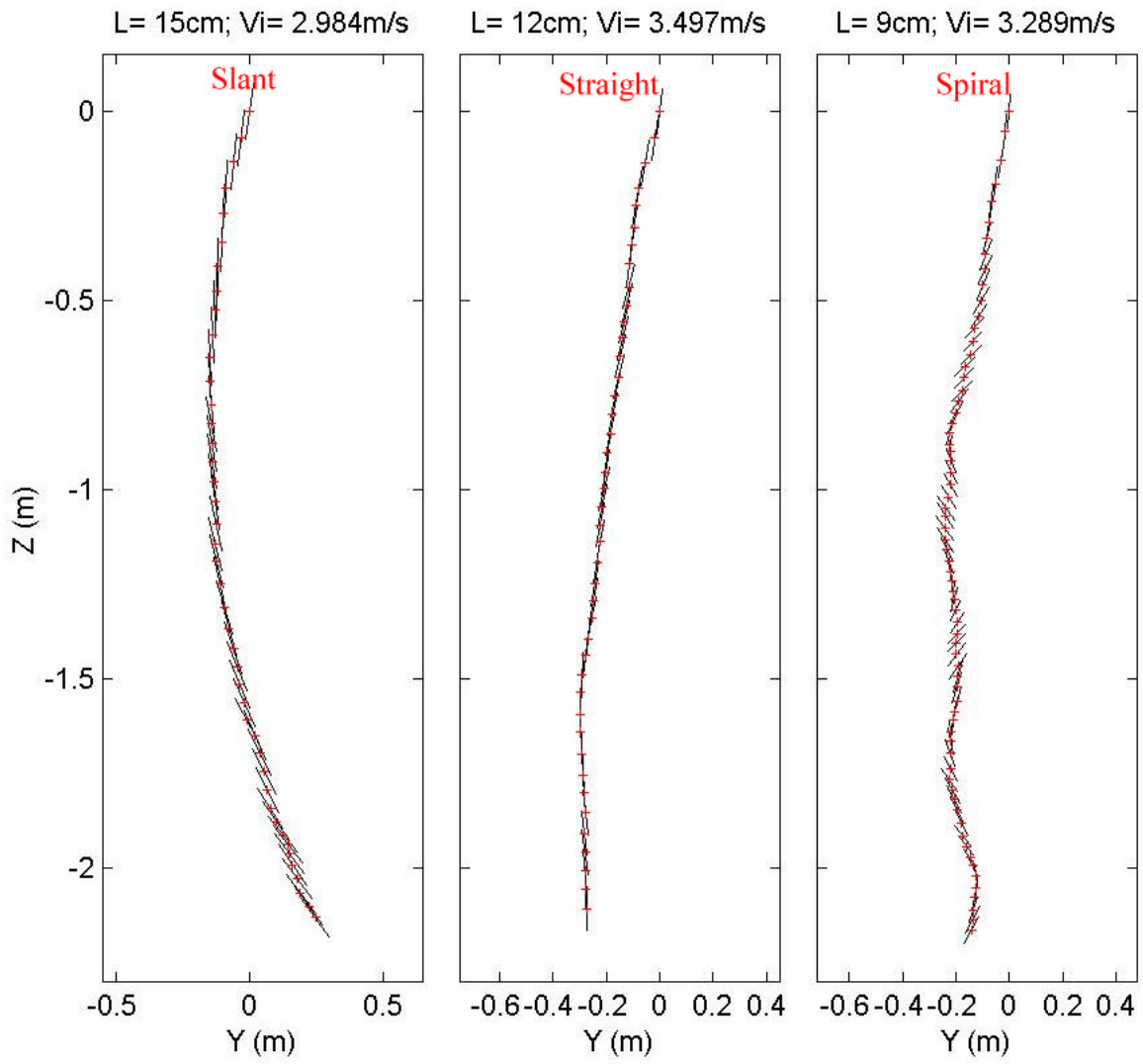
Drop Angle: 45; COM:1



Drop Angle: 60; COM:1

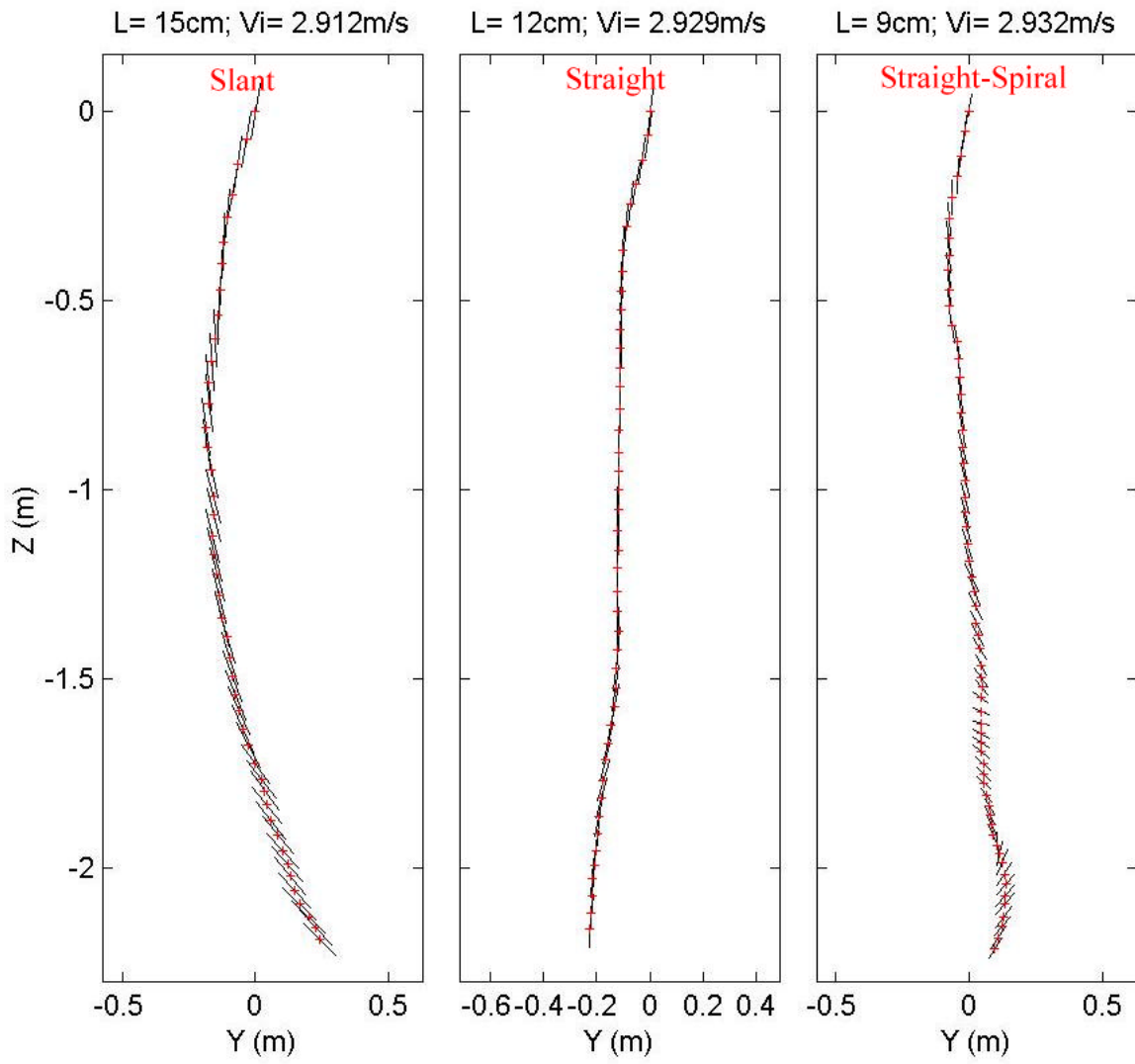


Drop Angle: 60; COM:1

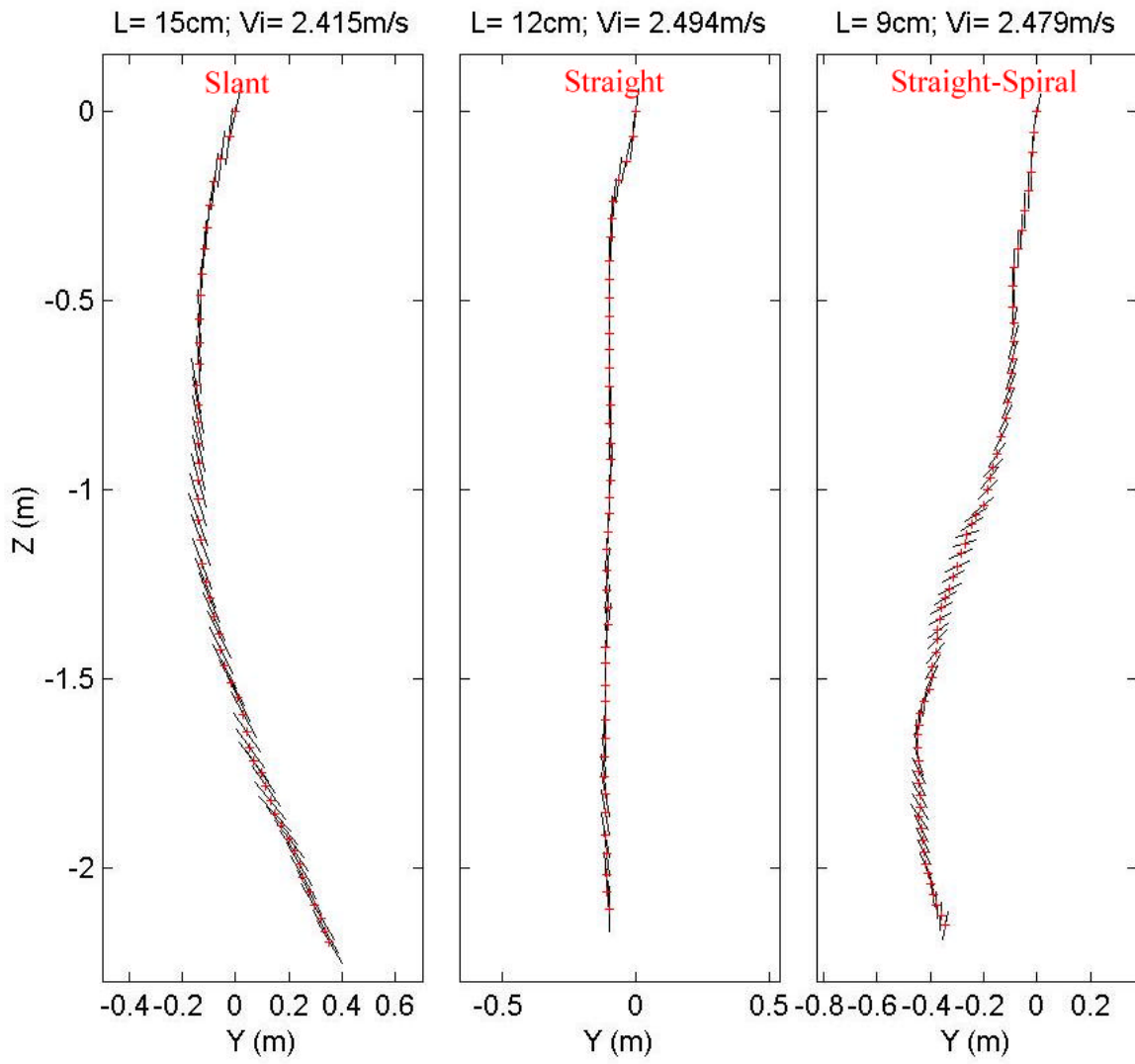




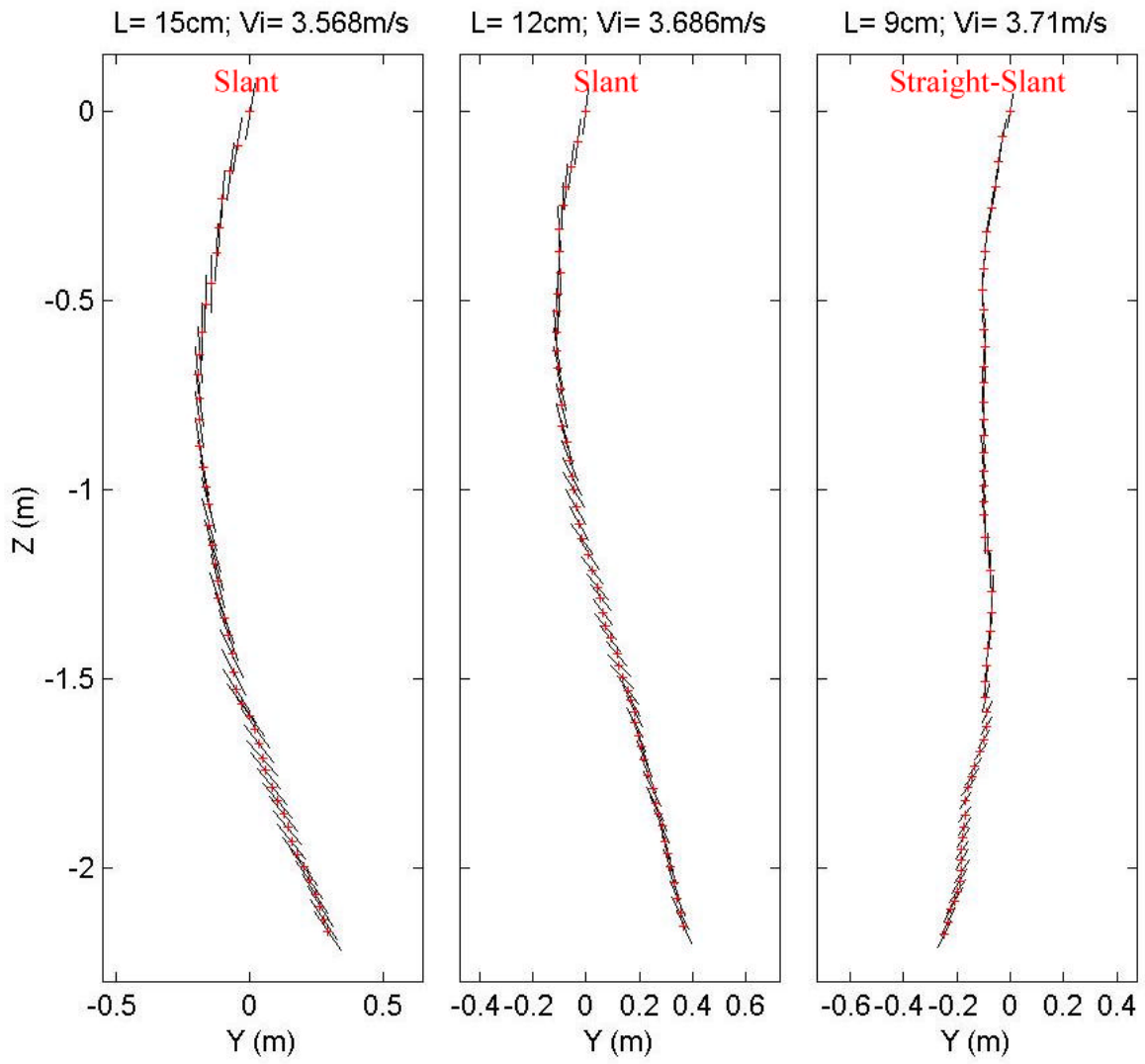
Drop Angle: 60; COM:1



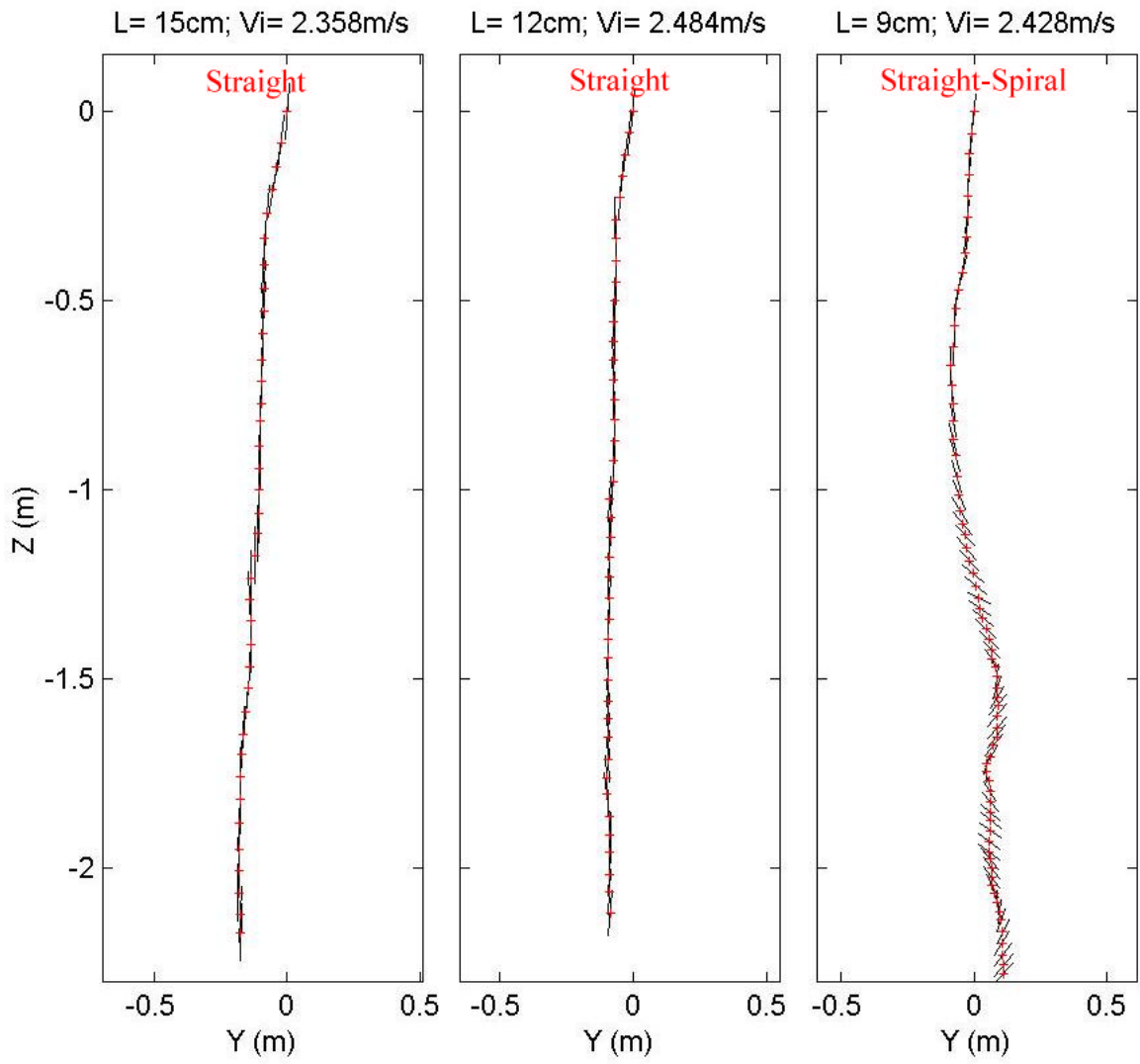
Drop Angle: 60; COM:1



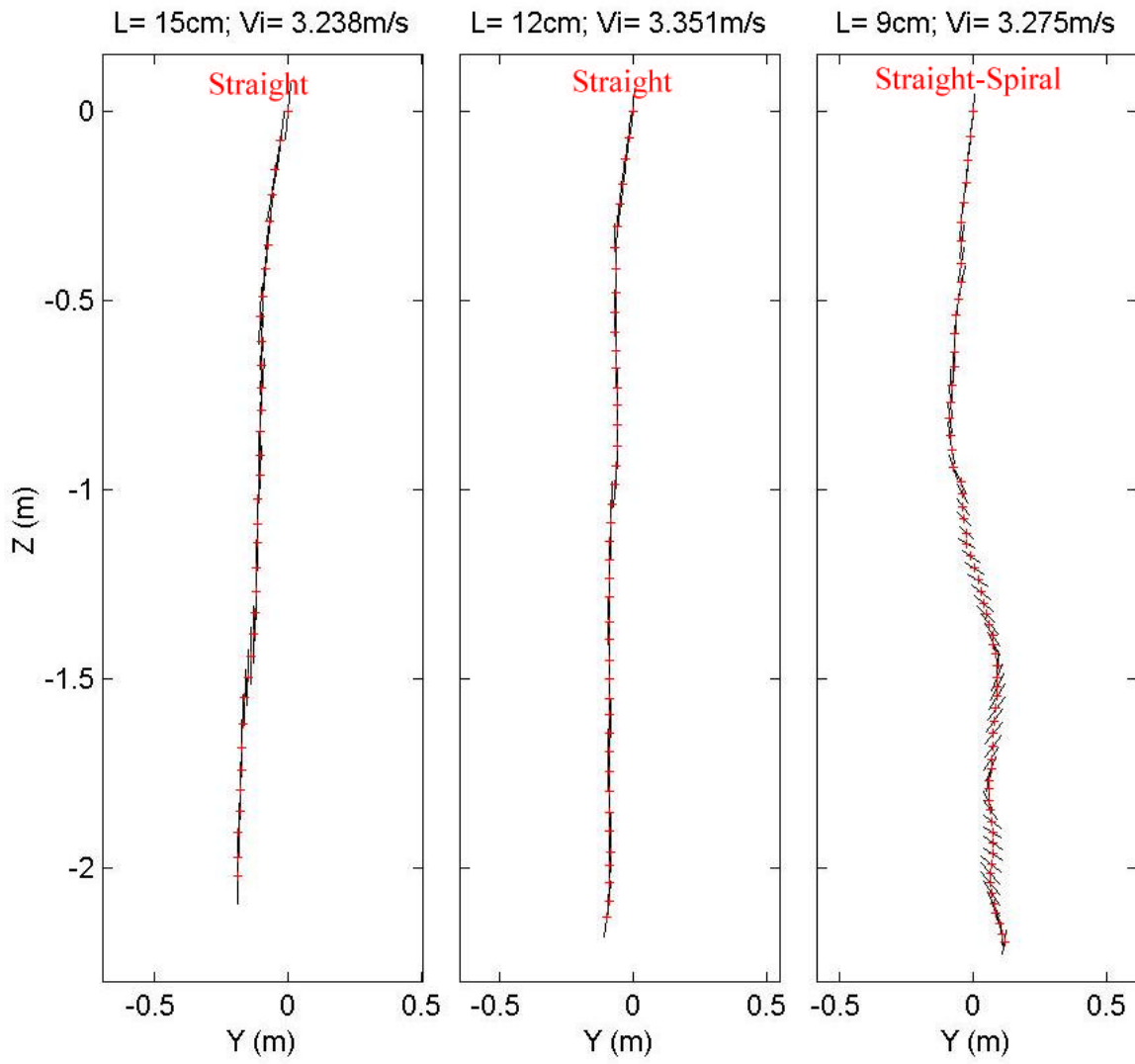
Drop Angle: 60; COM:1



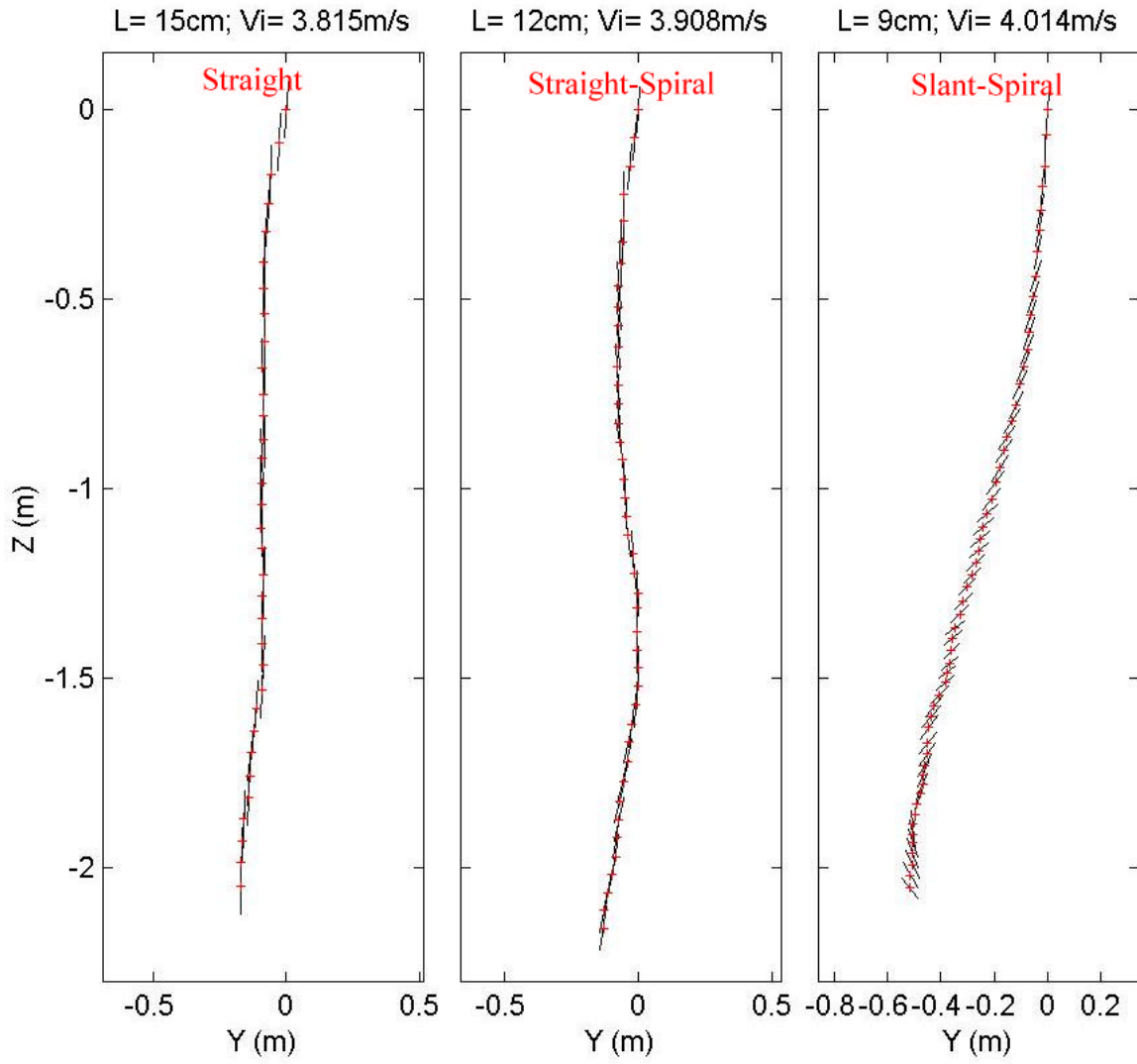
Drop Angle: 75; COM:1



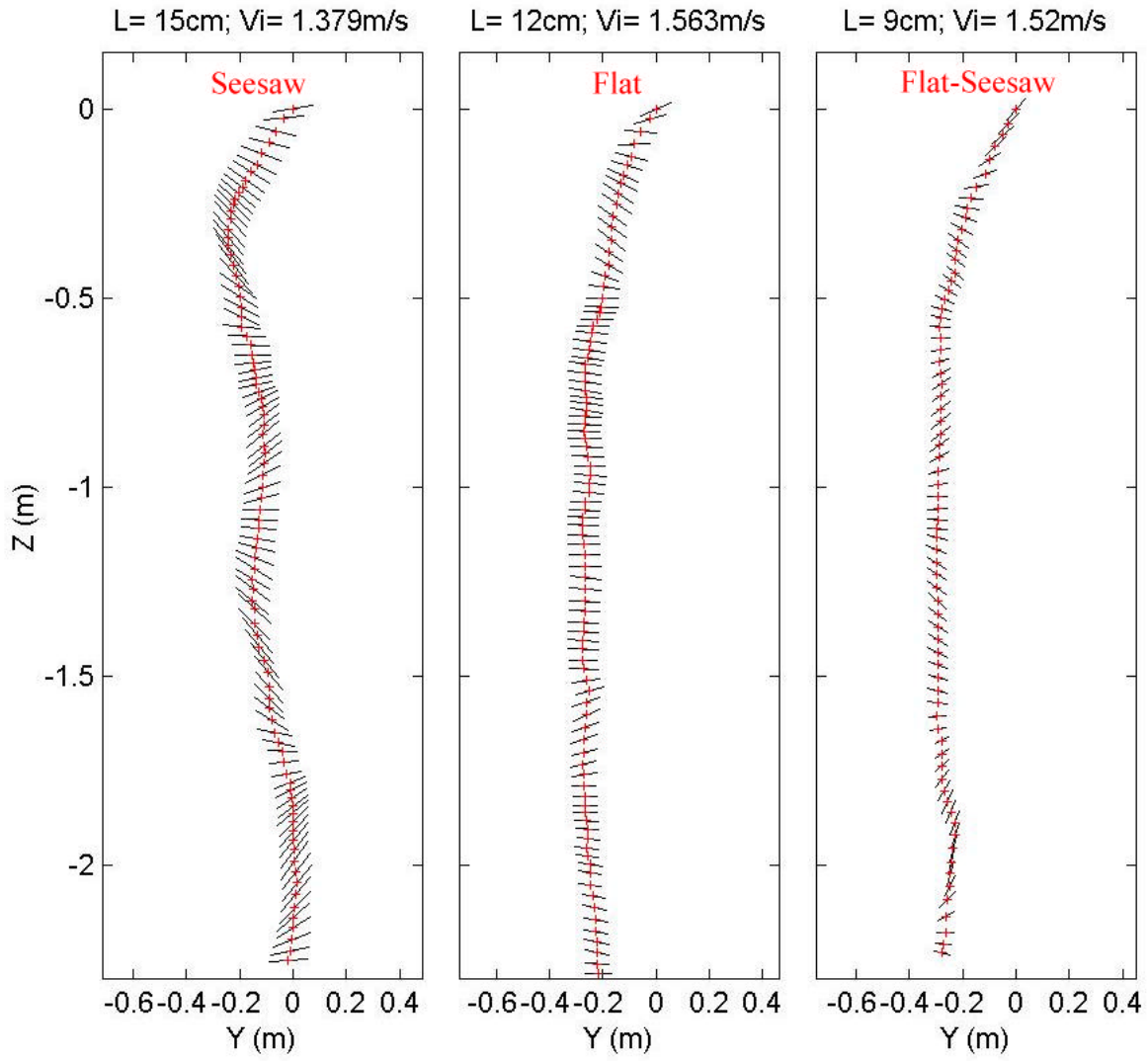
Drop Angle: 75; COM:1



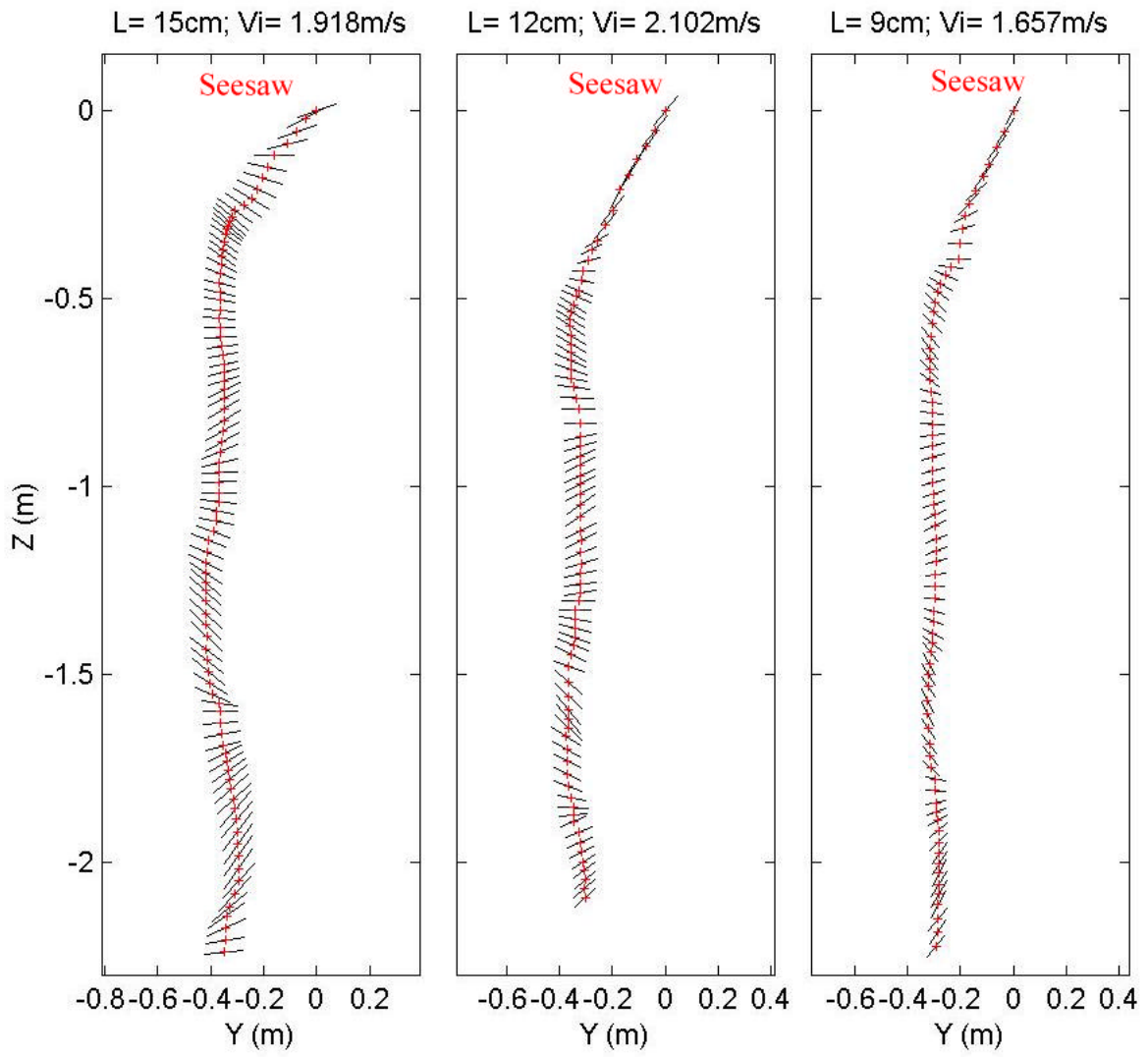
Drop Angle: 75; COM:1



Drop Angle: 15; COM:0

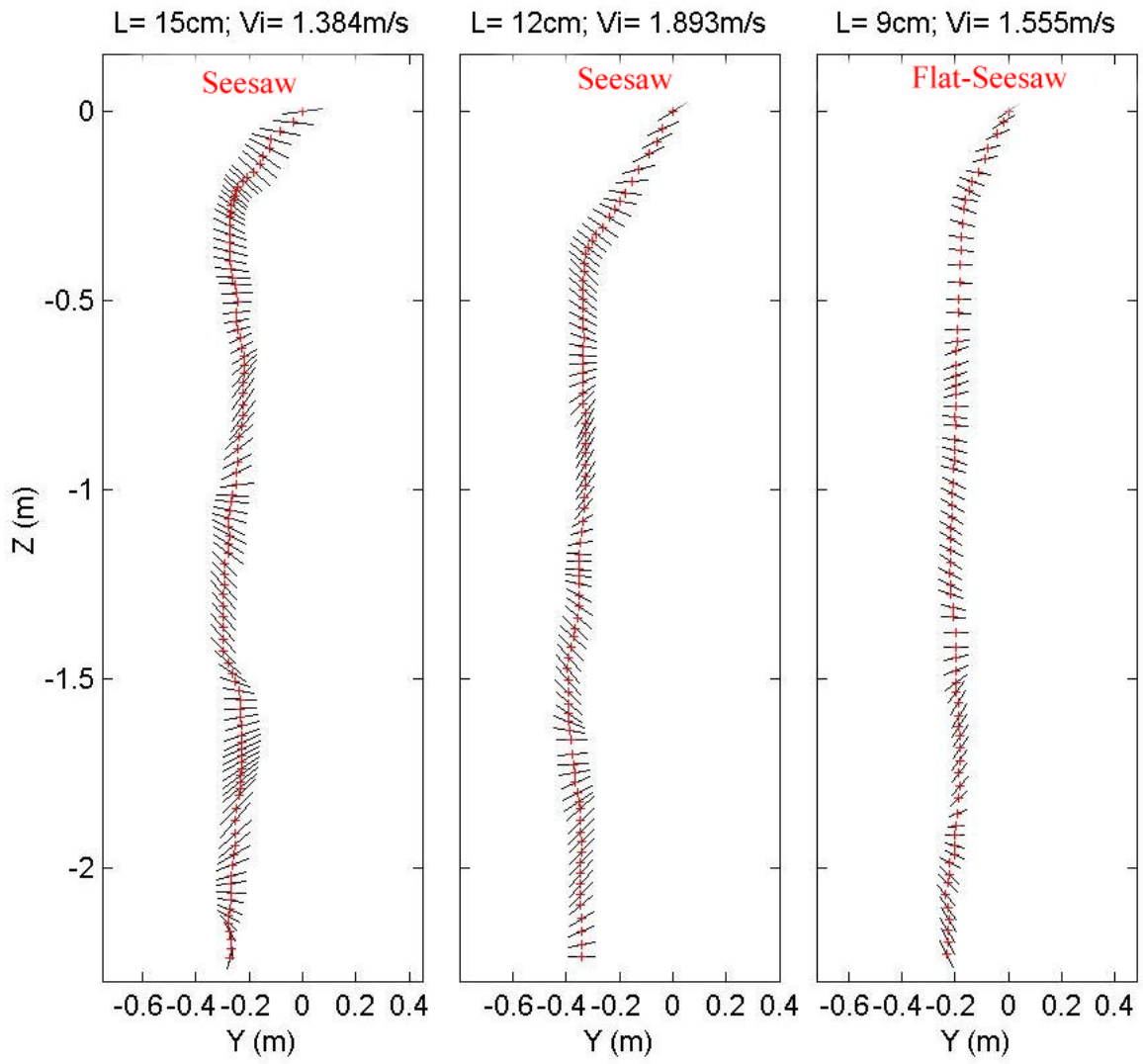


Drop Angle: 15; COM:0

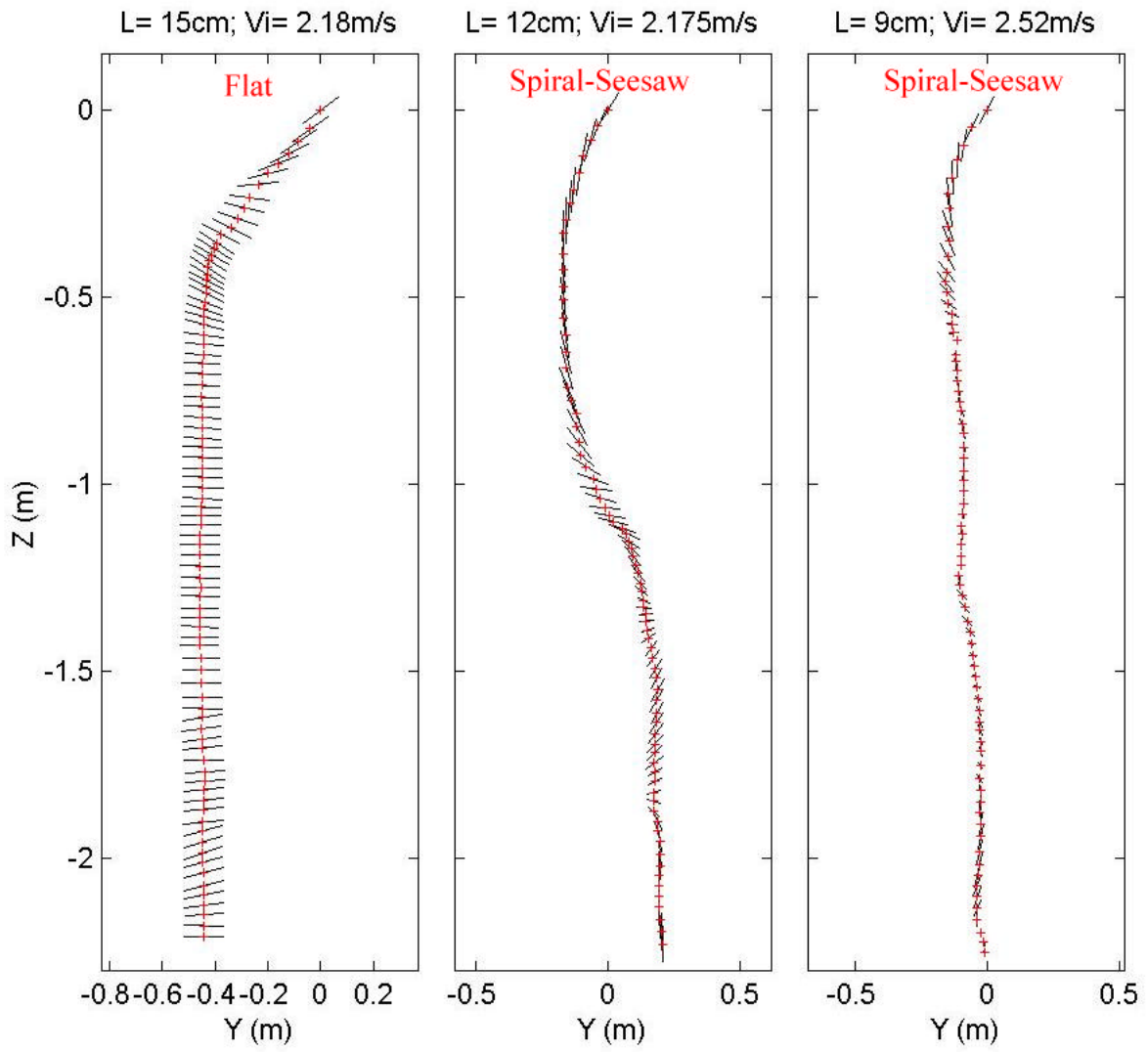




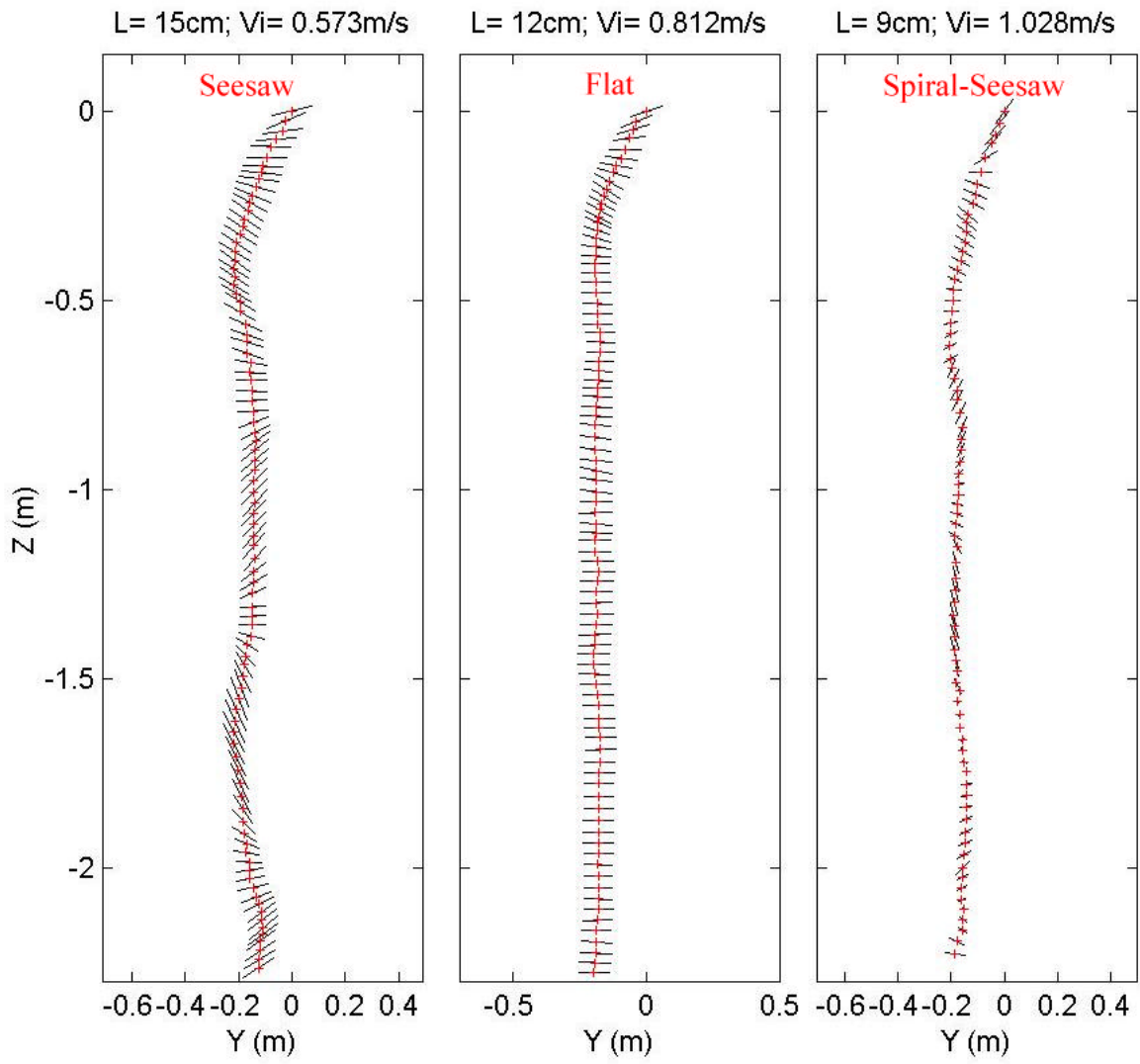
Drop Angle: 15; COM:0



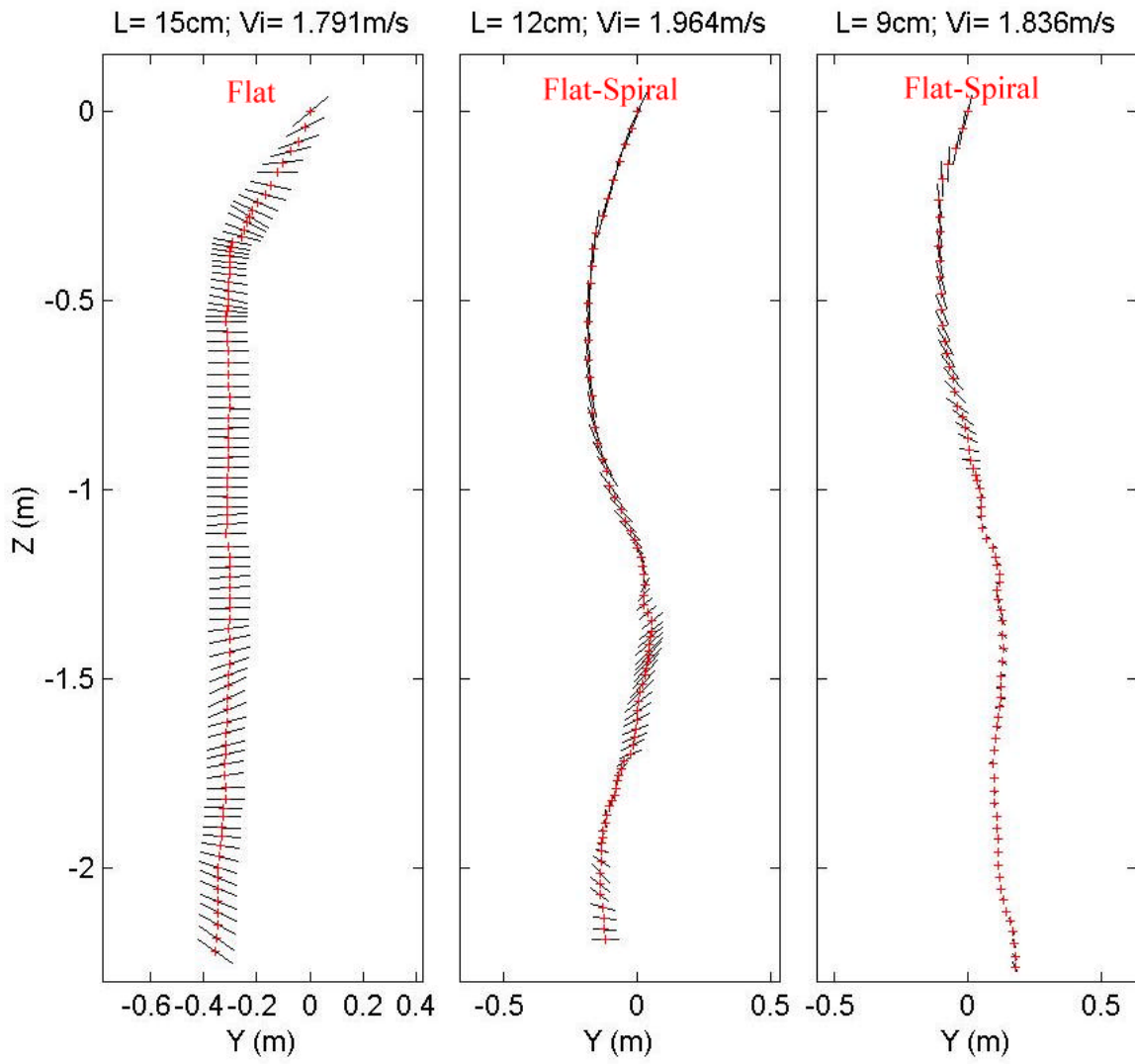
Drop Angle: 15; COM:0



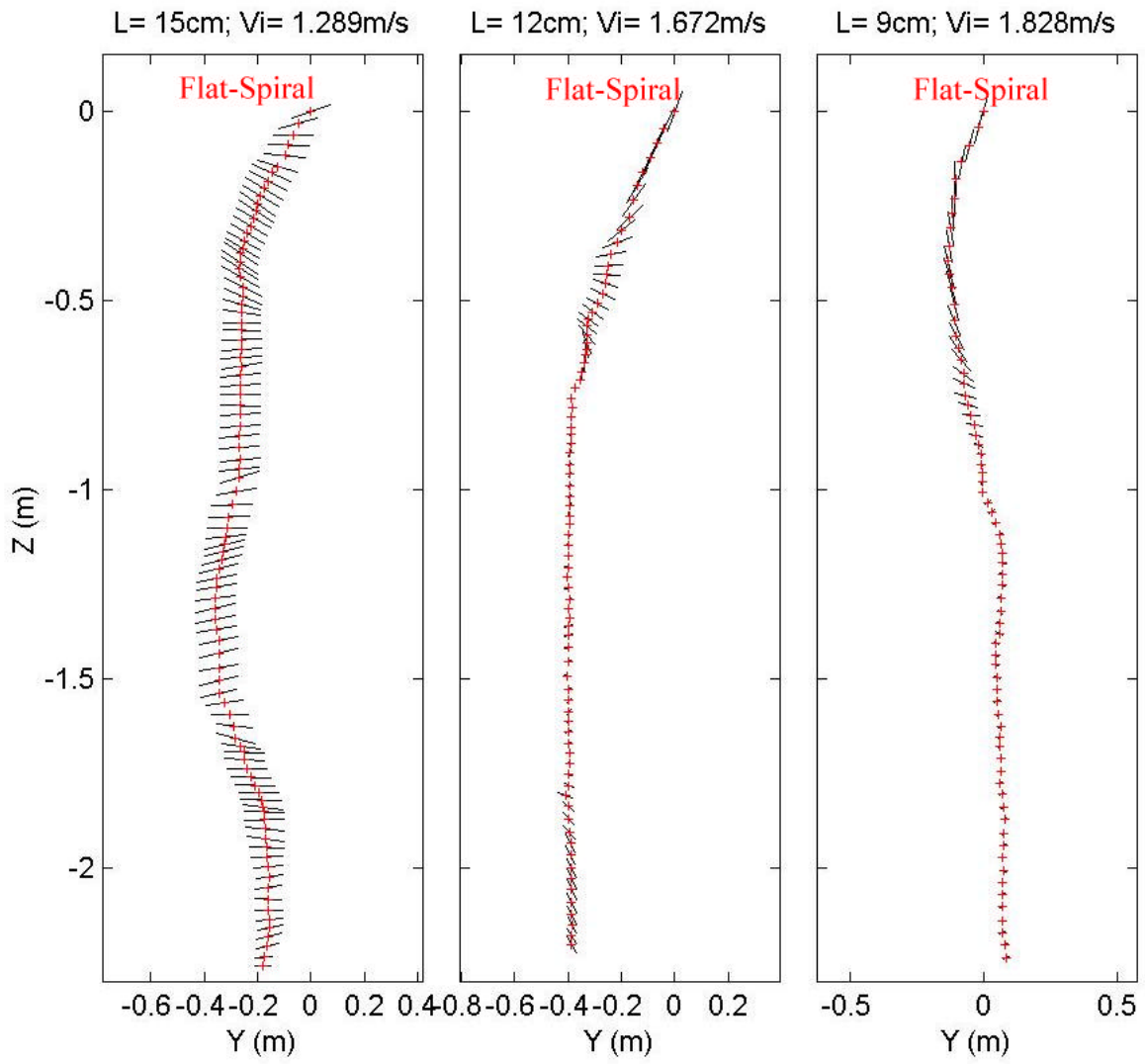
Drop Angle: 30; COM:0



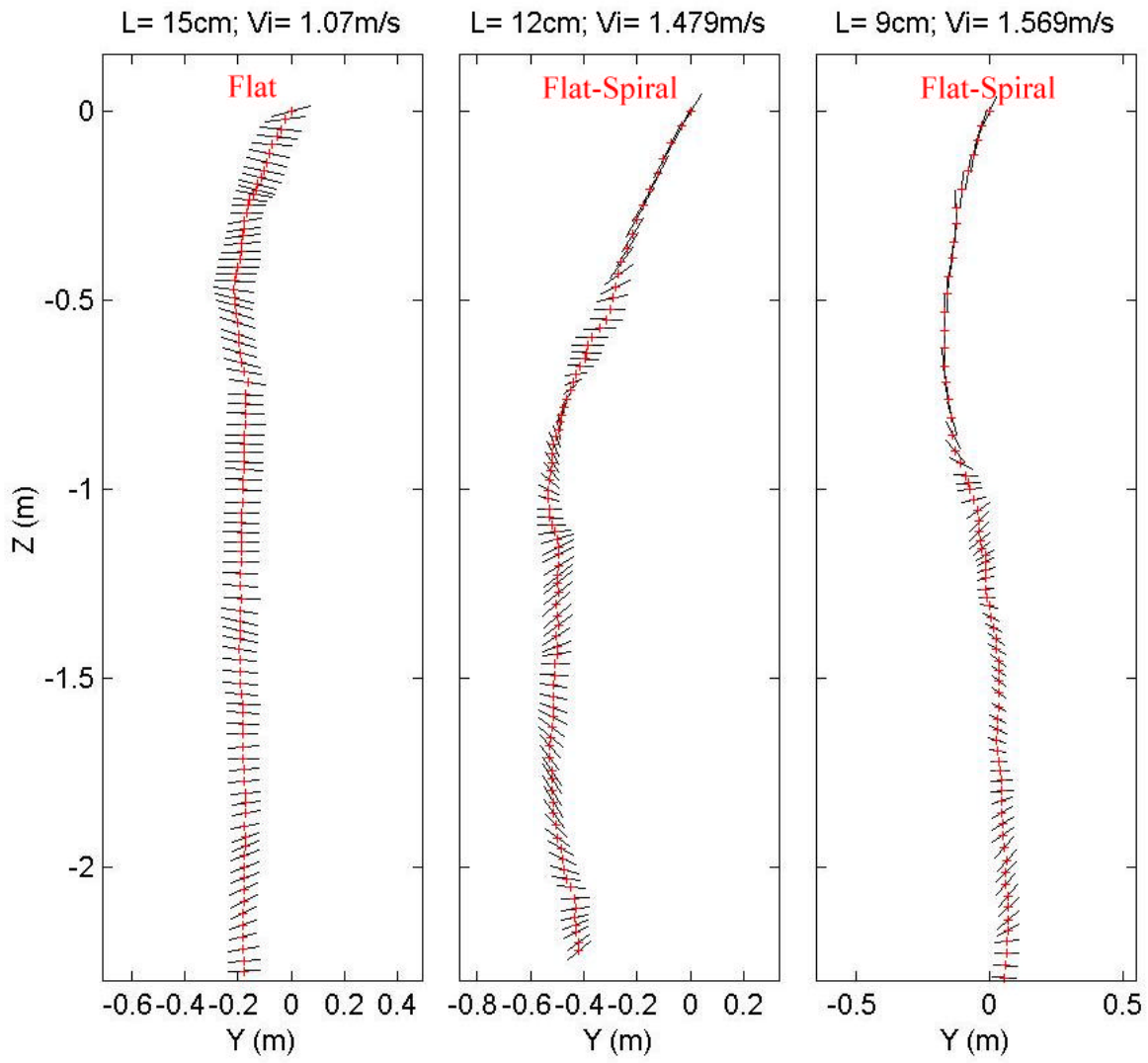
Drop Angle: 30; COM:0



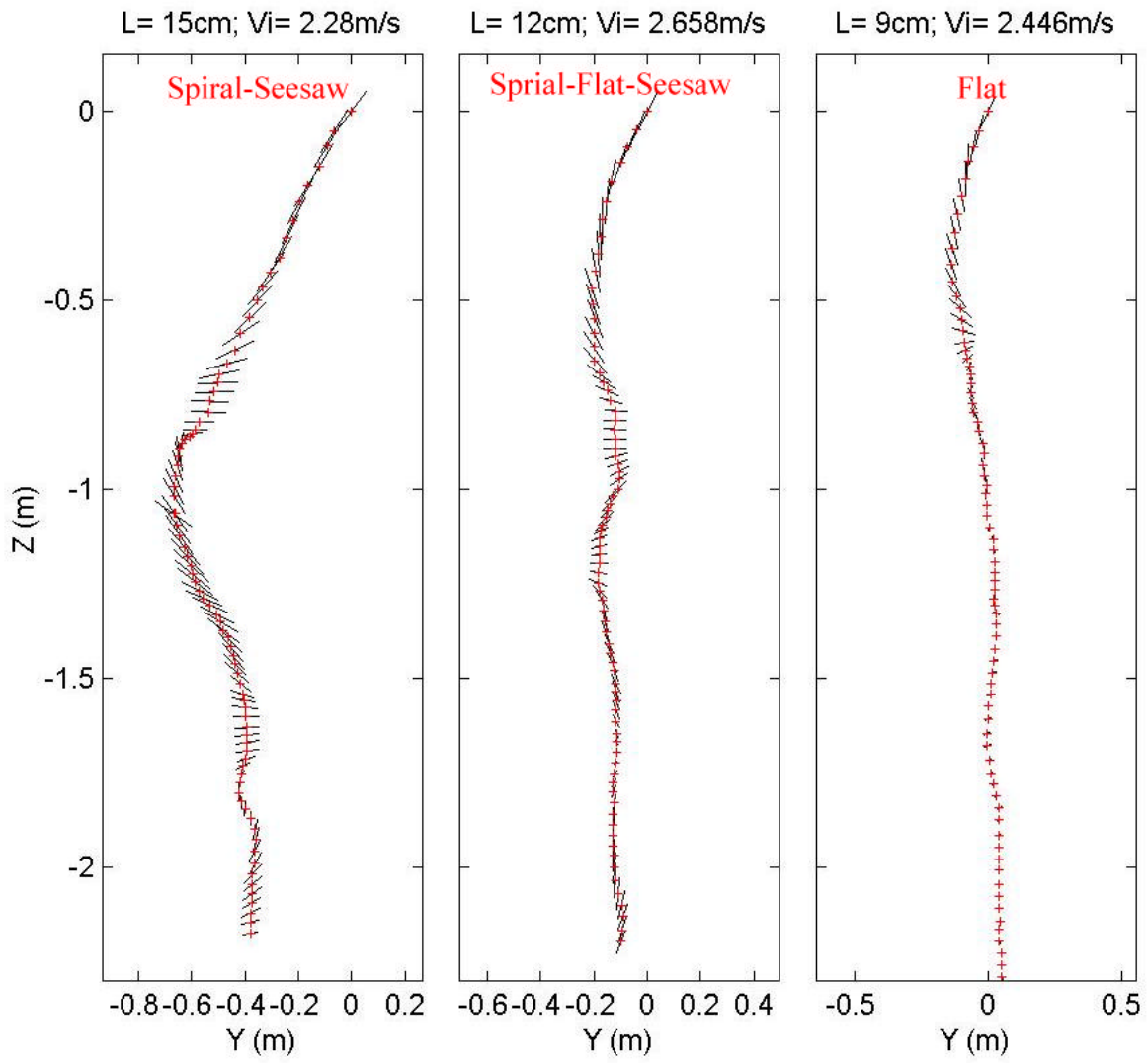
Drop Angle: 30; COM:0



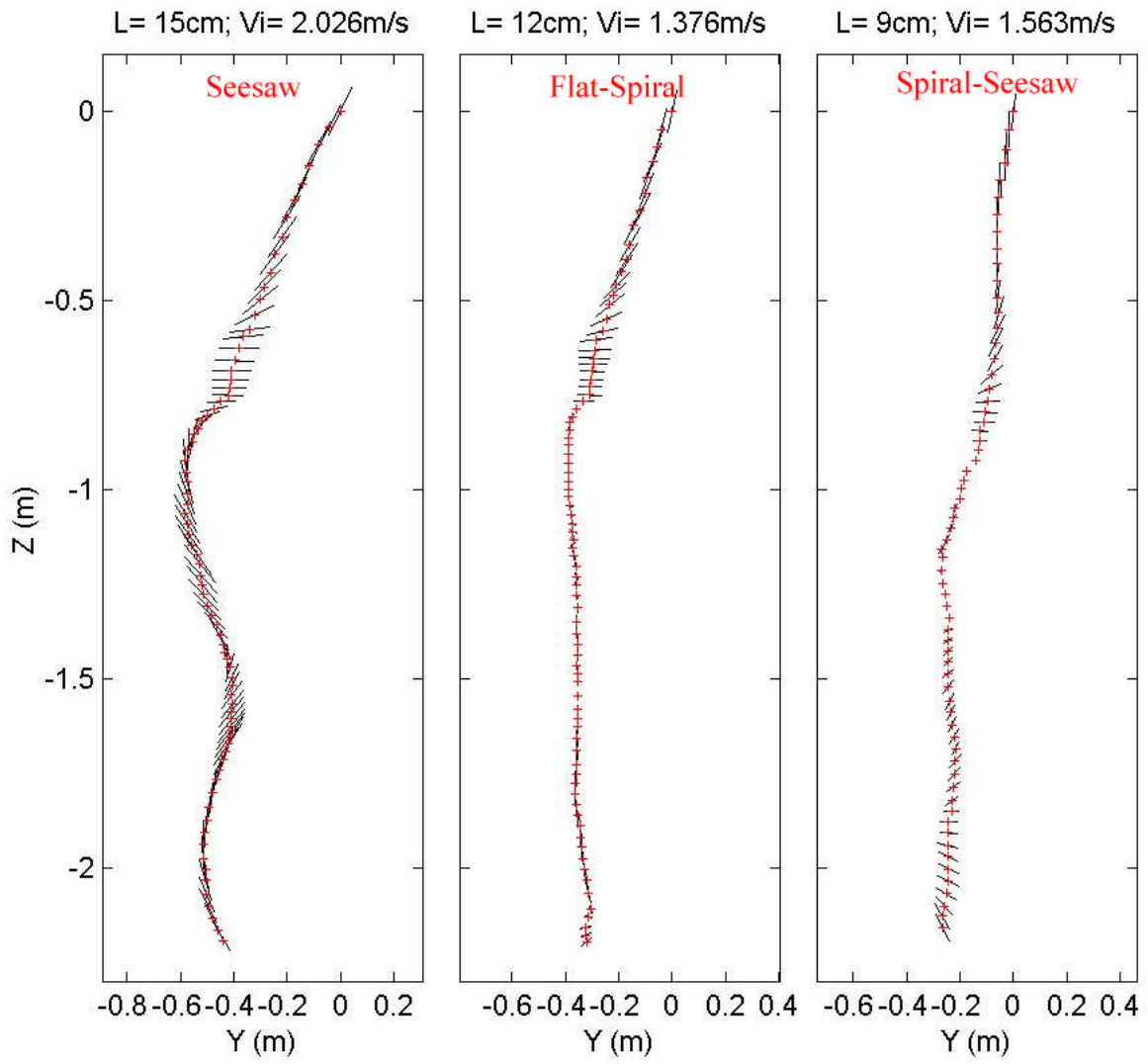
Drop Angle: 30; COM:0



Drop Angle: 30; COM:0

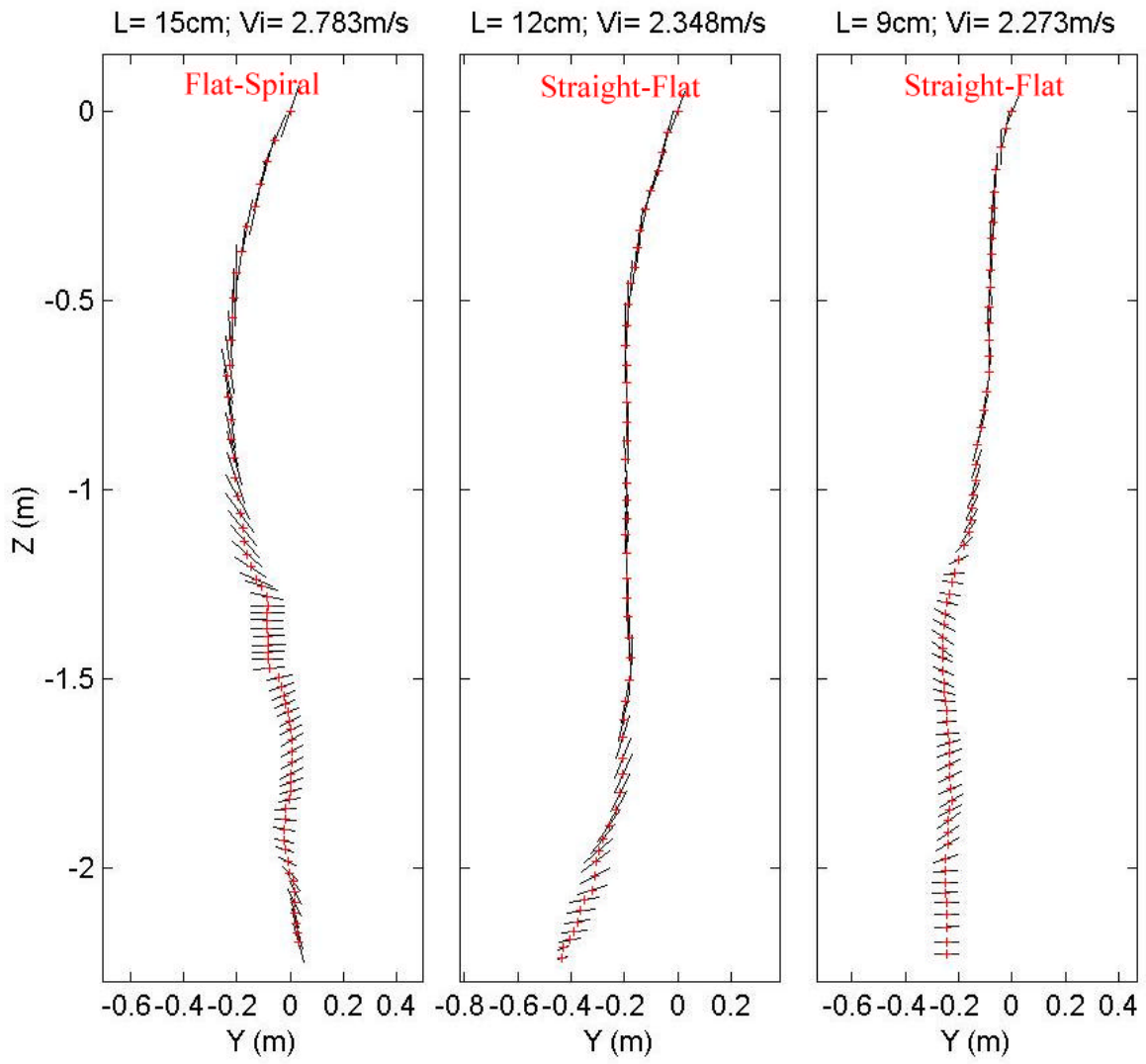


Drop Angle: 45; COM:0

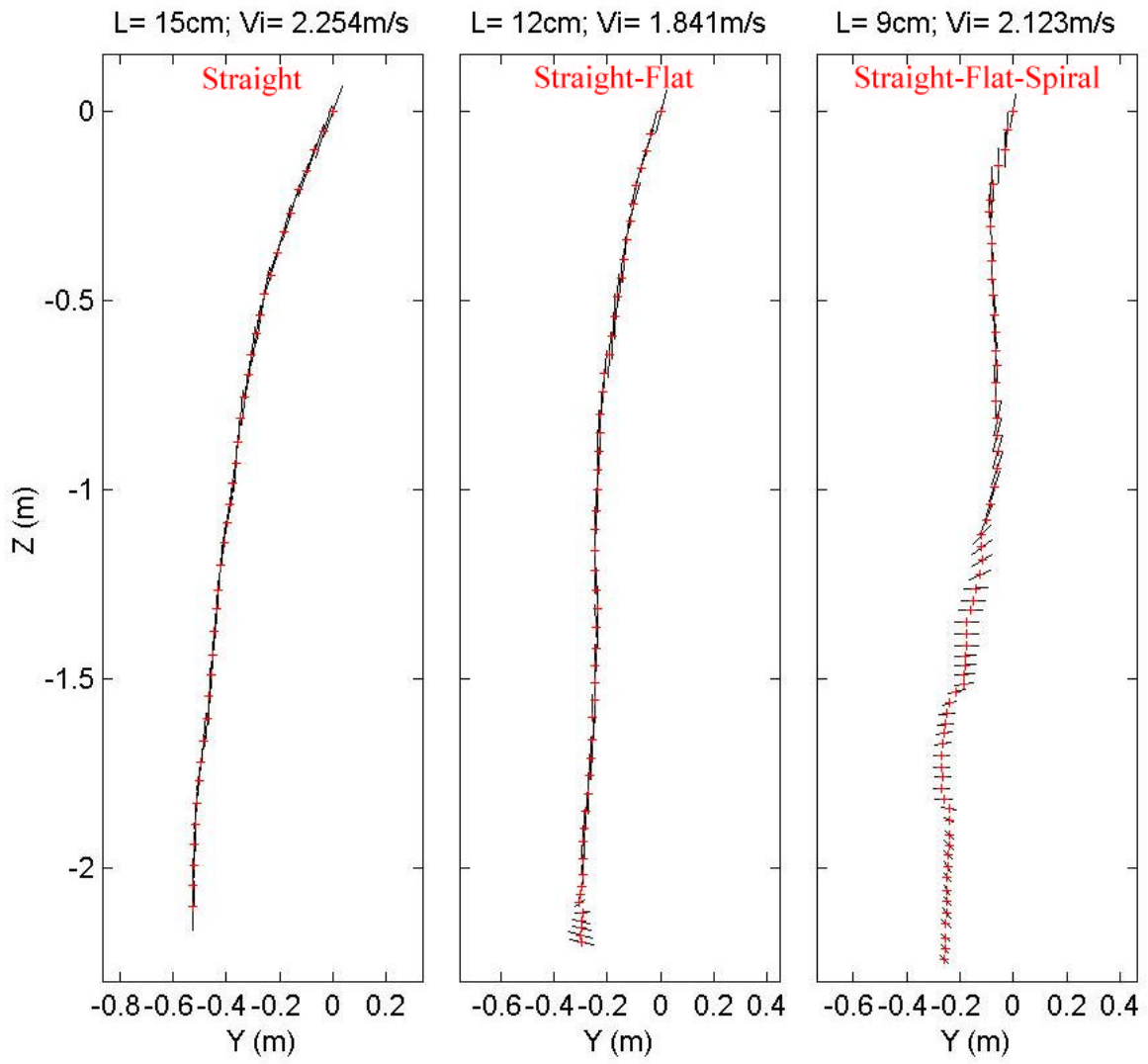




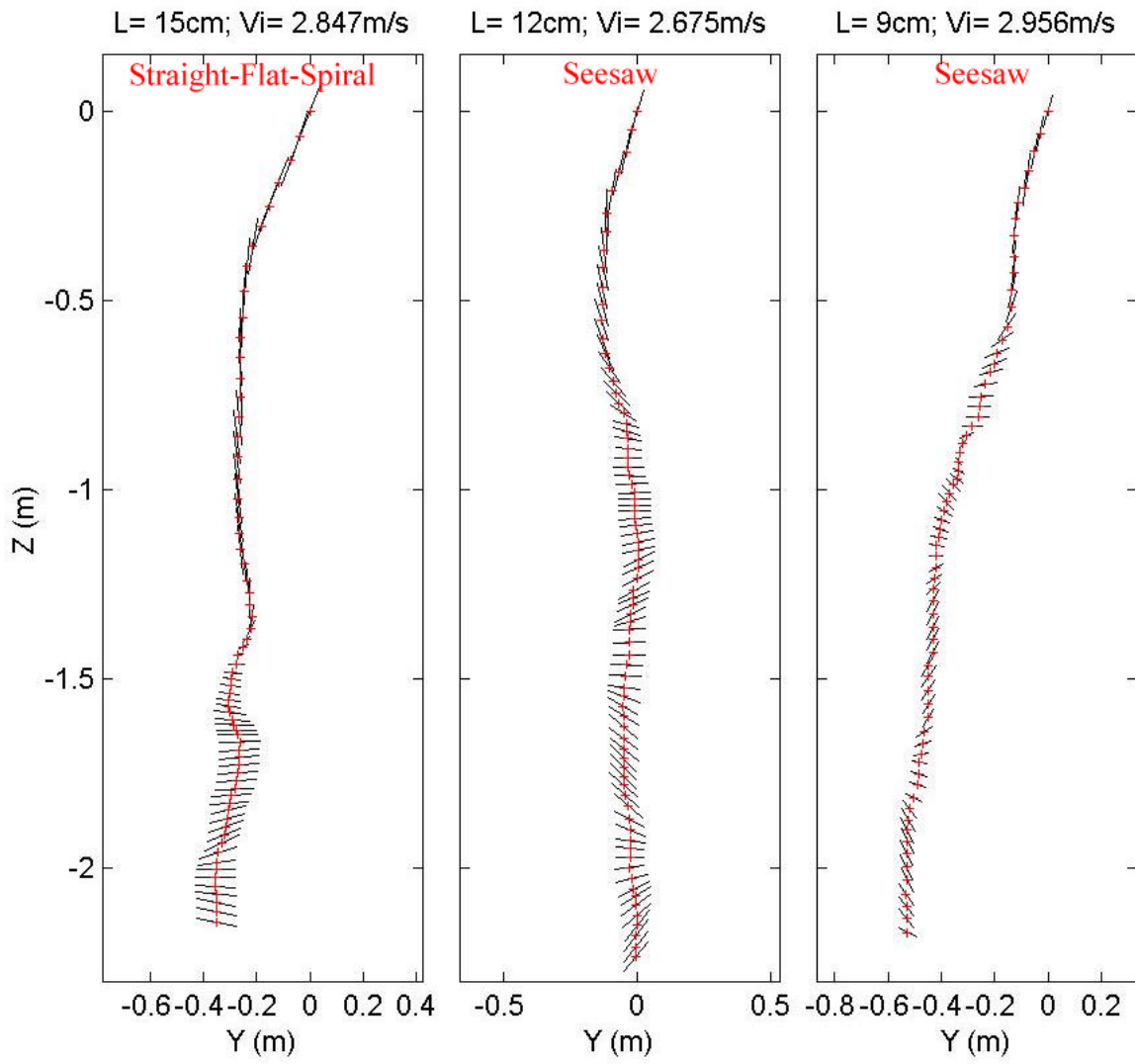
Drop Angle: 45; COM:0



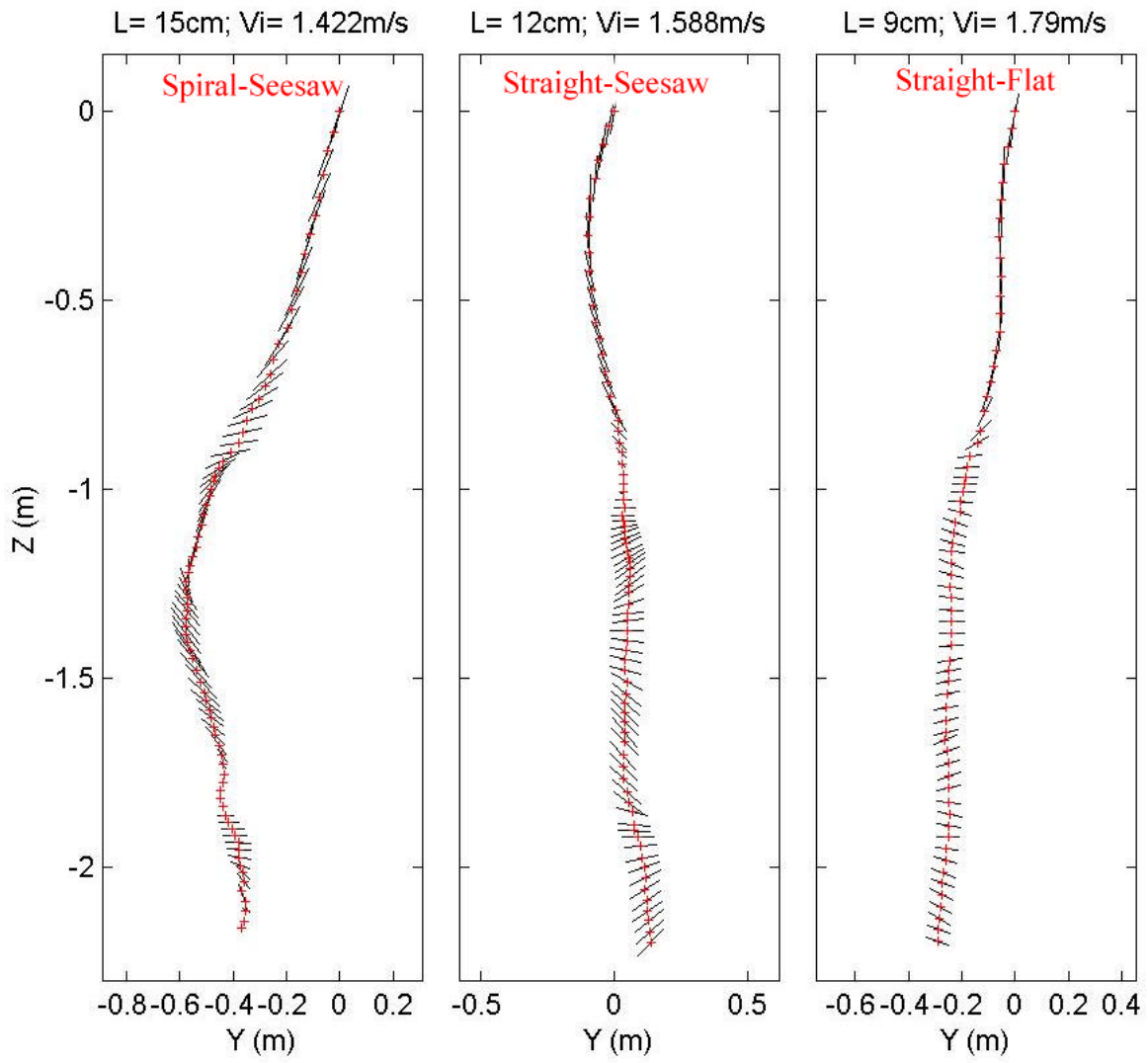
Drop Angle: 45; COM:0



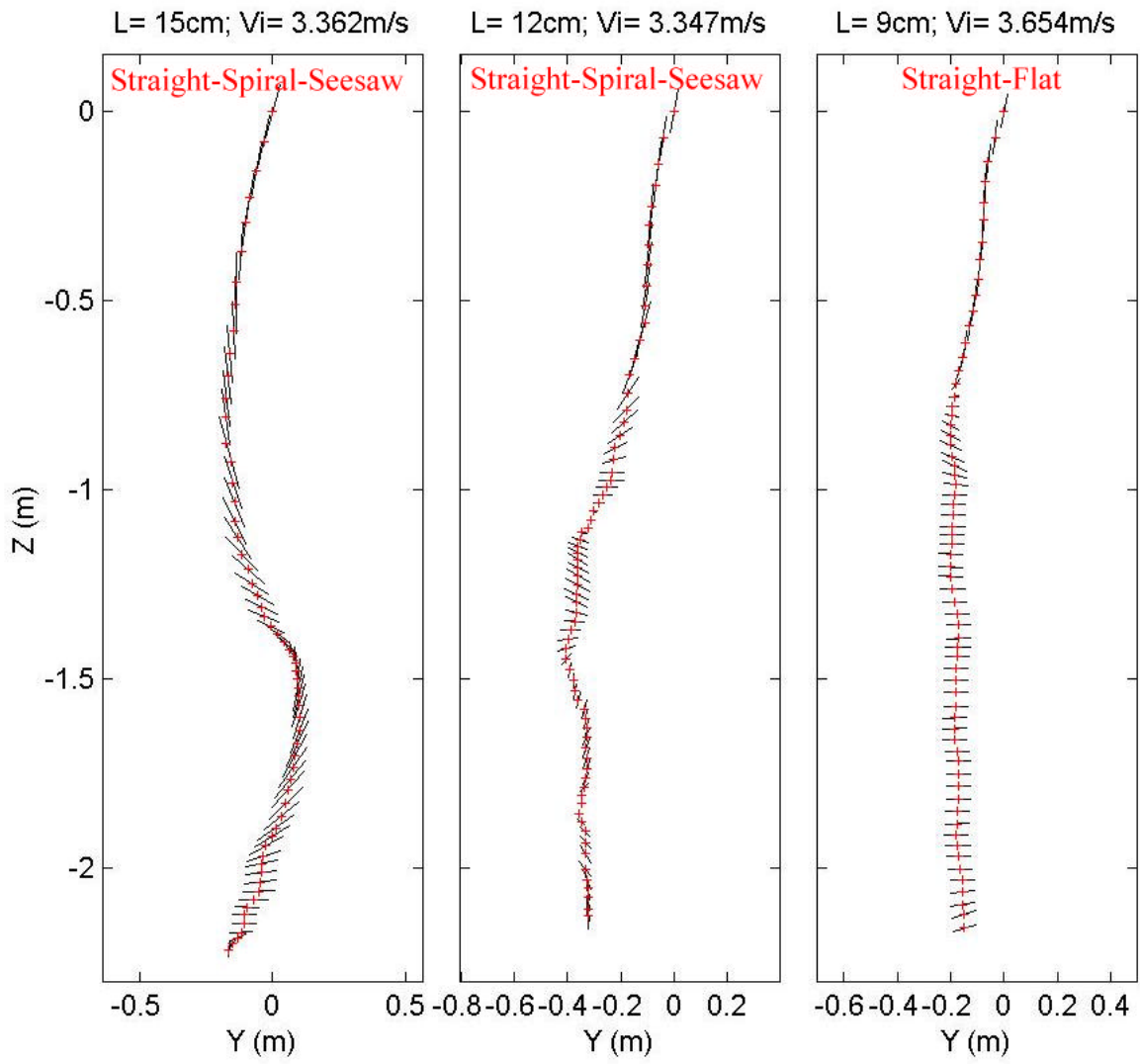
Drop Angle: 45; COM:0



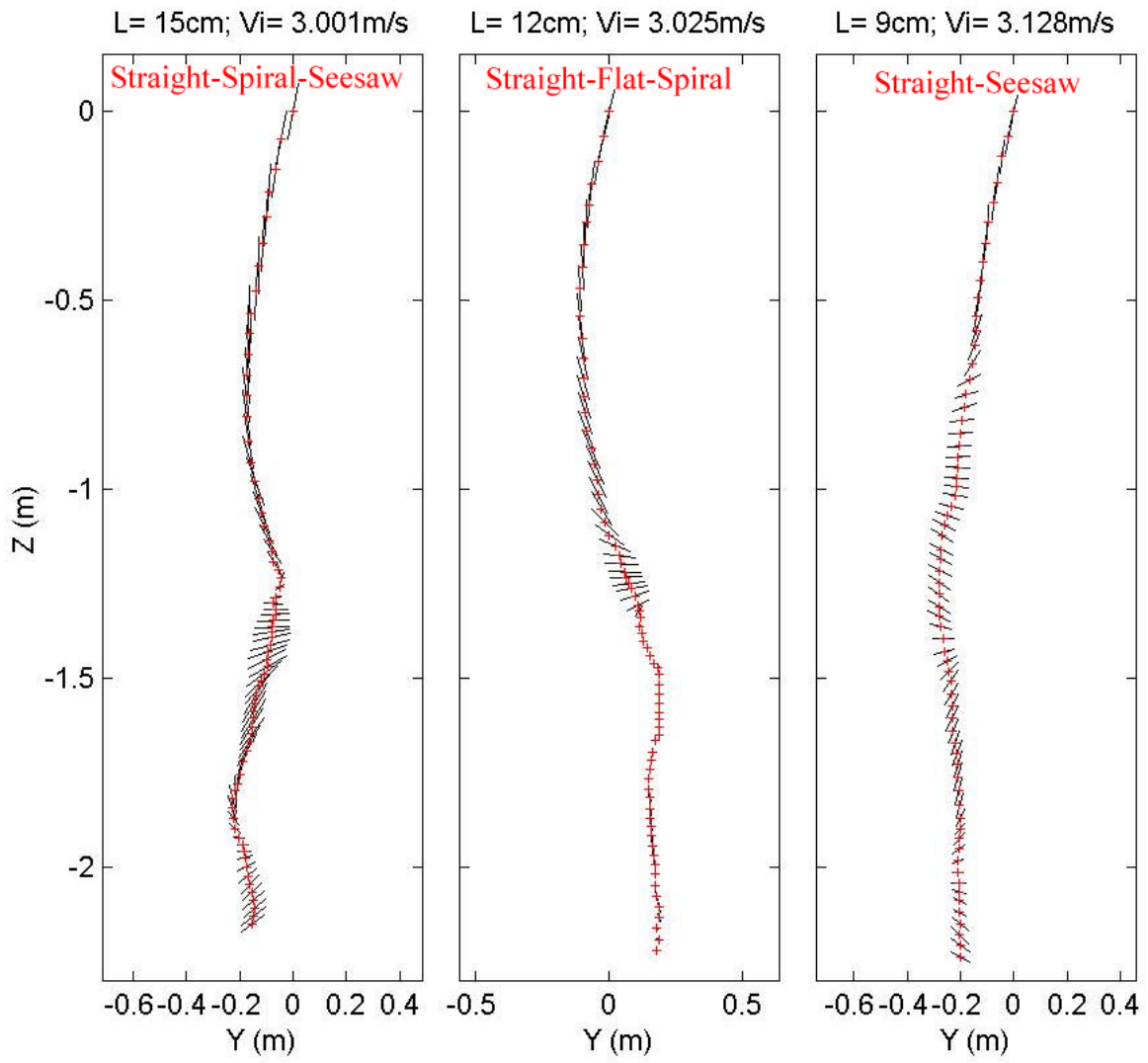
Drop Angle: 60; COM:0



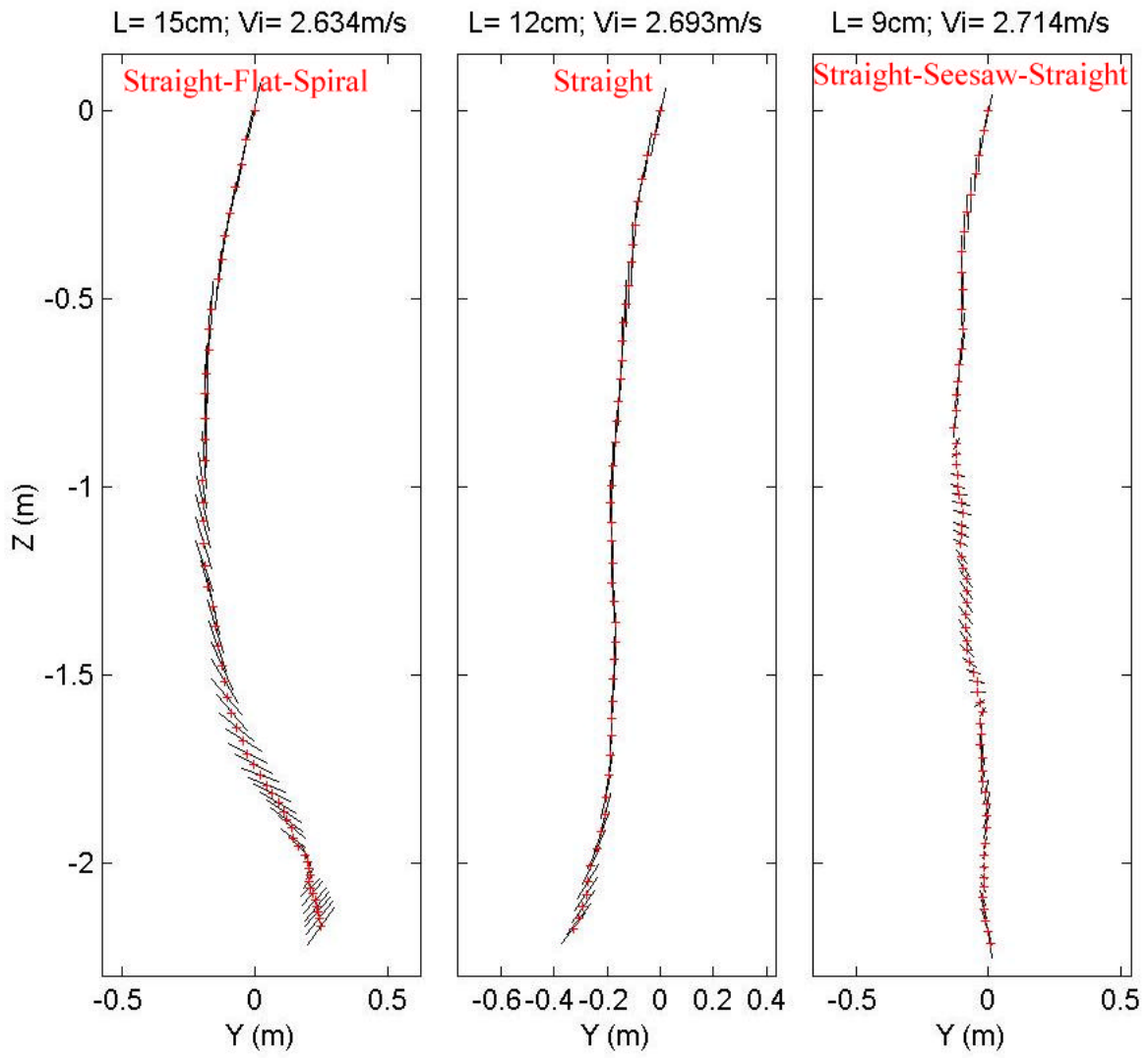
Drop Angle: 60; COM:0



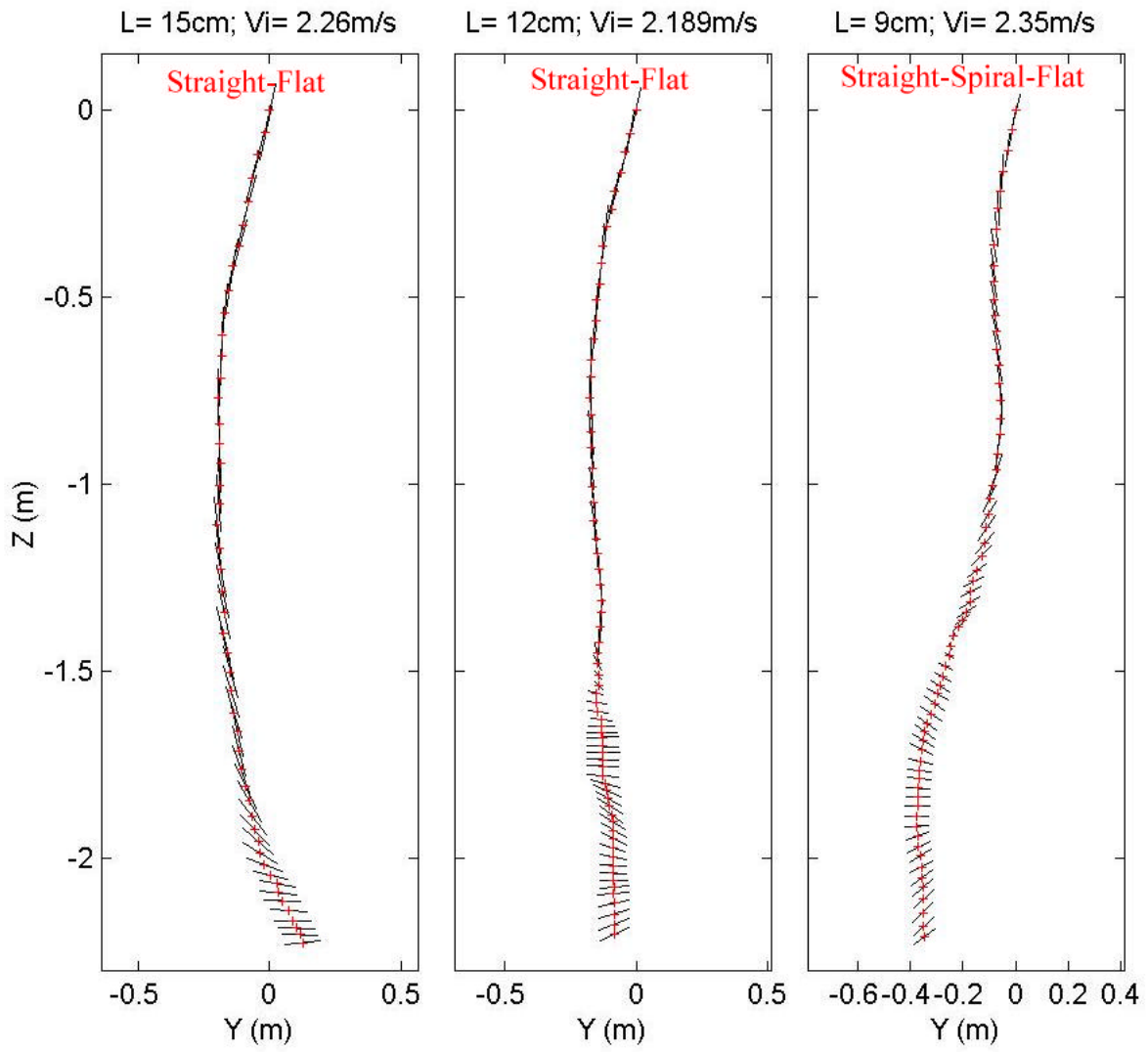
Drop Angle: 60; COM:0



Drop Angle: 60; COM:0

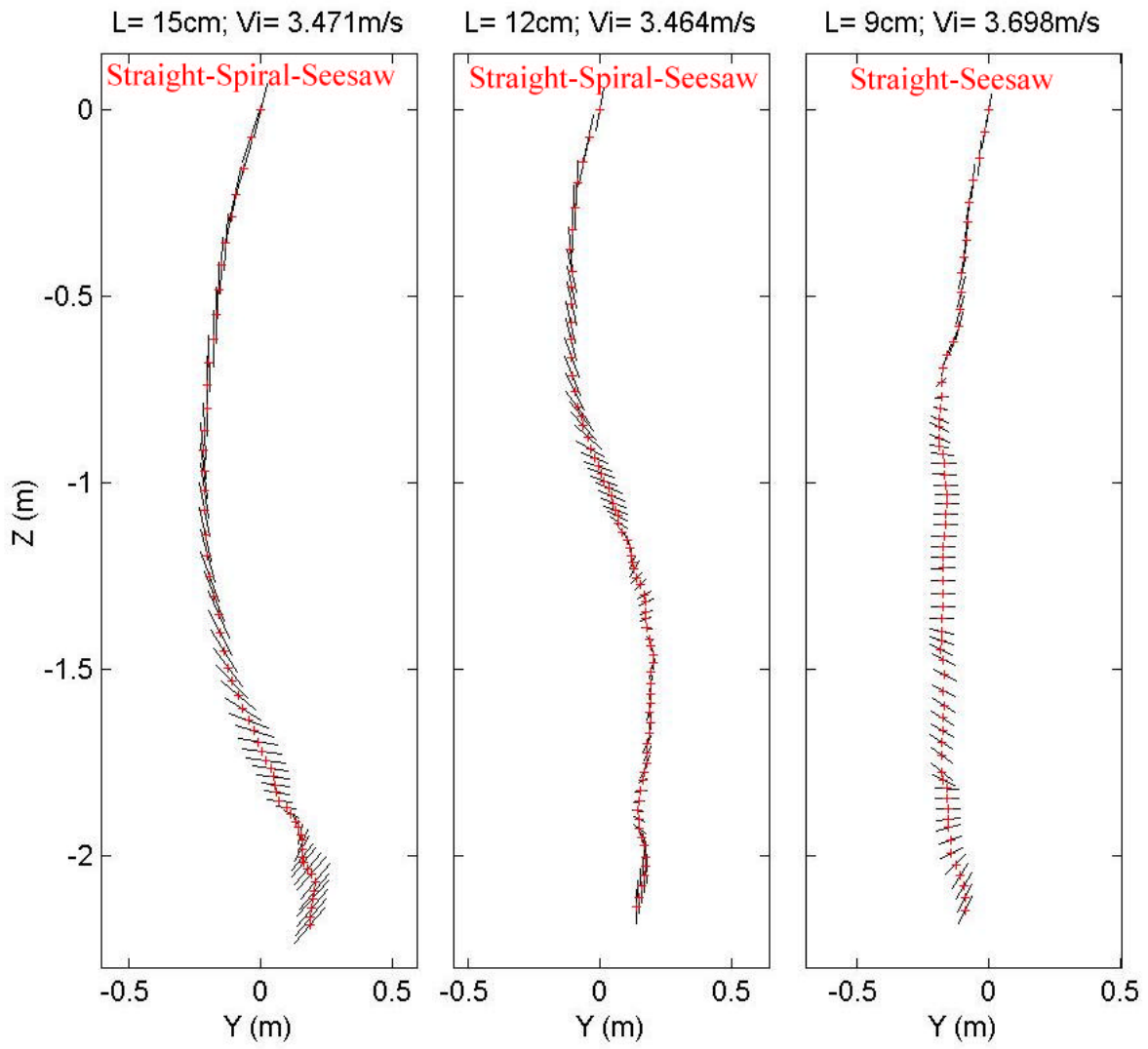


Drop Angle: 60; COM:0

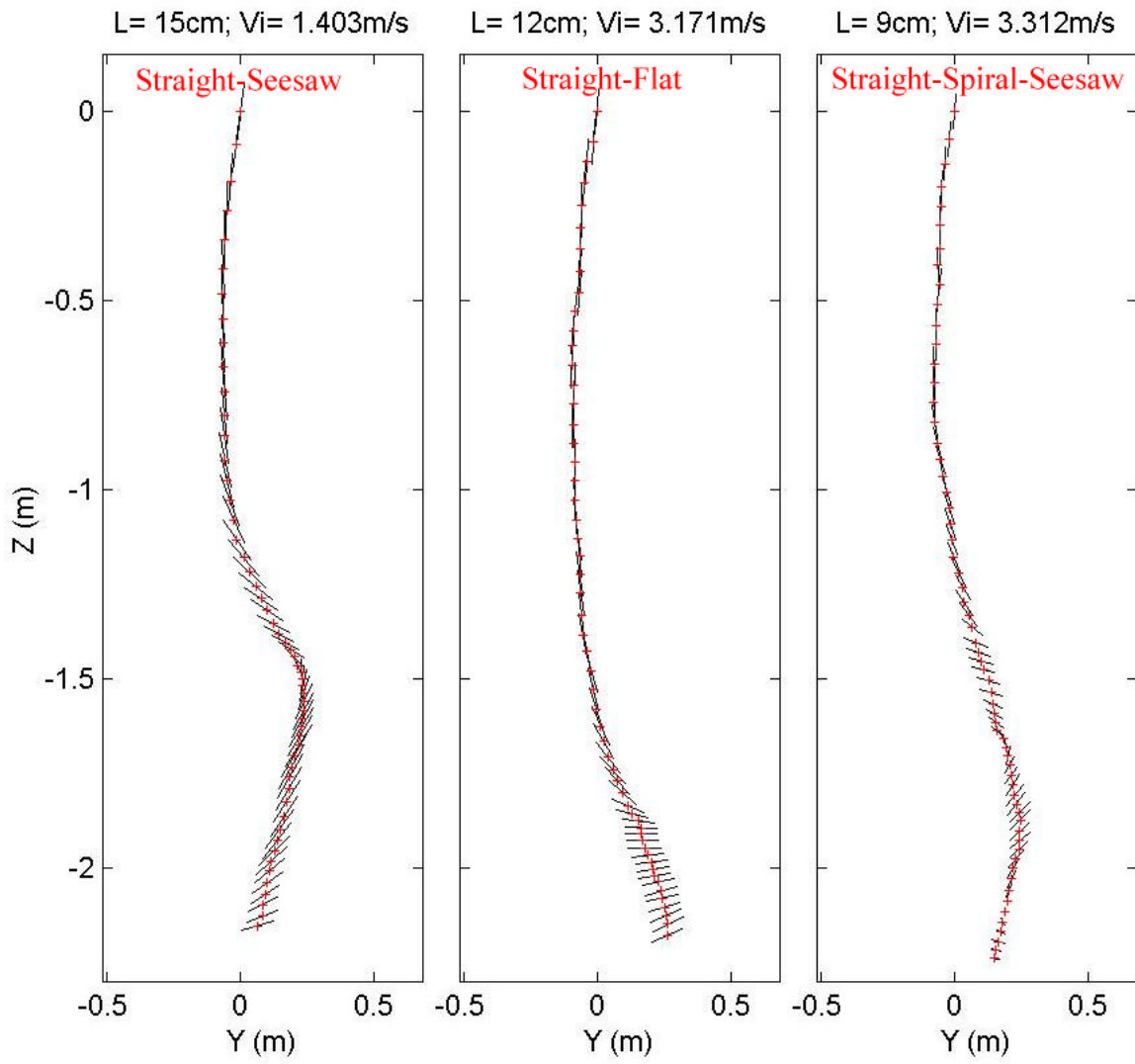




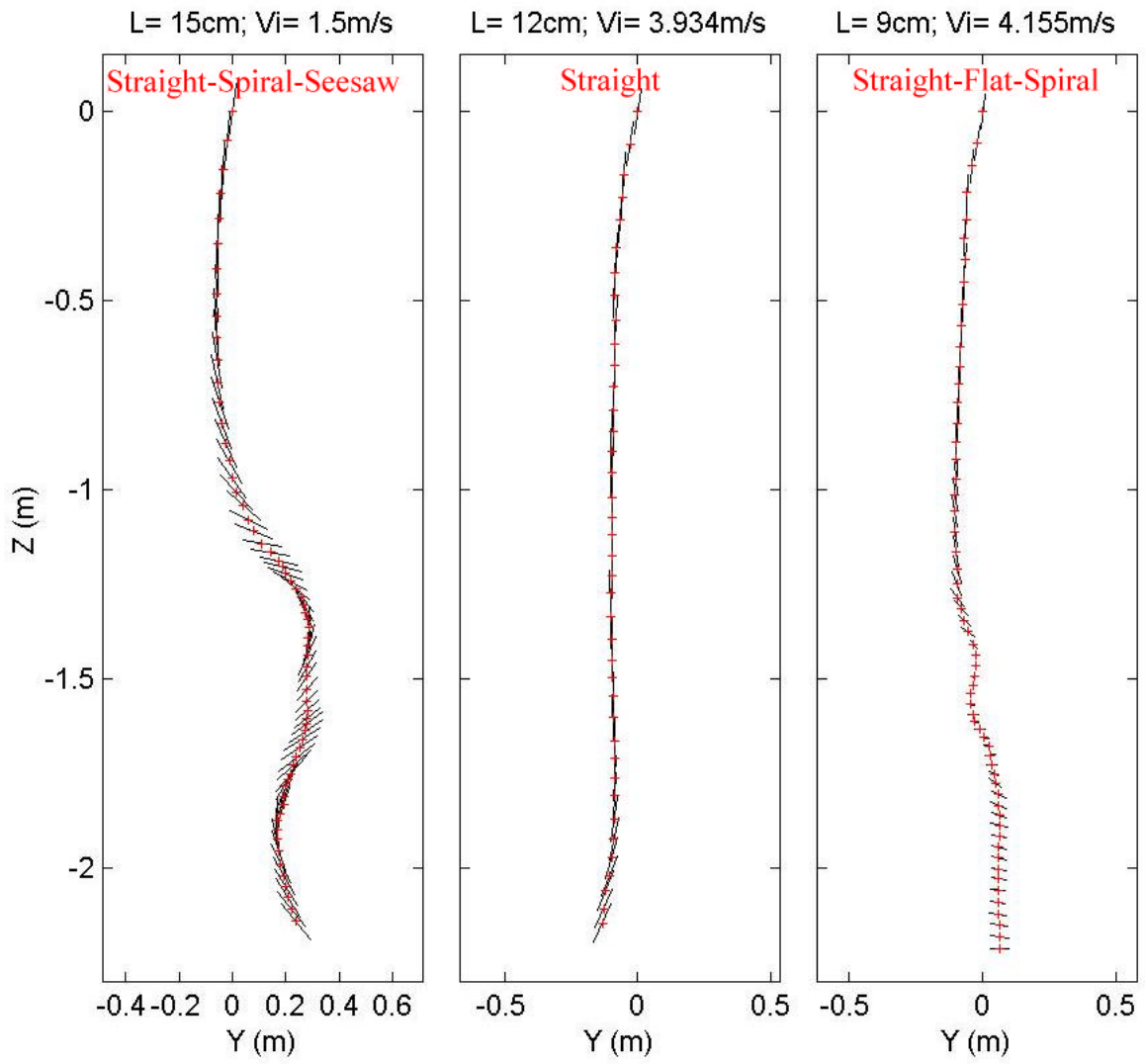
Drop Angle: 60; COM:0



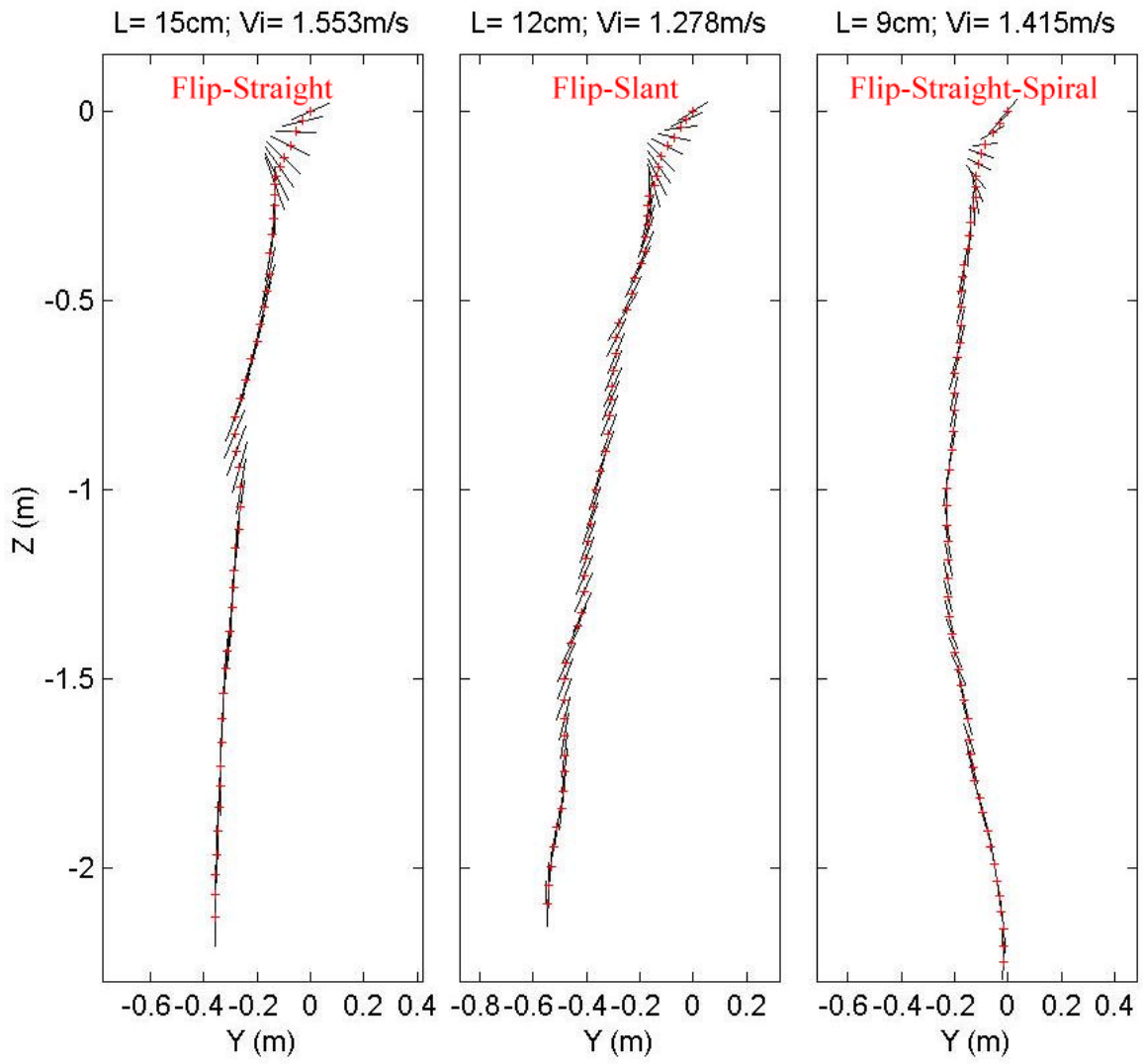
Drop Angle: 75; COM:0



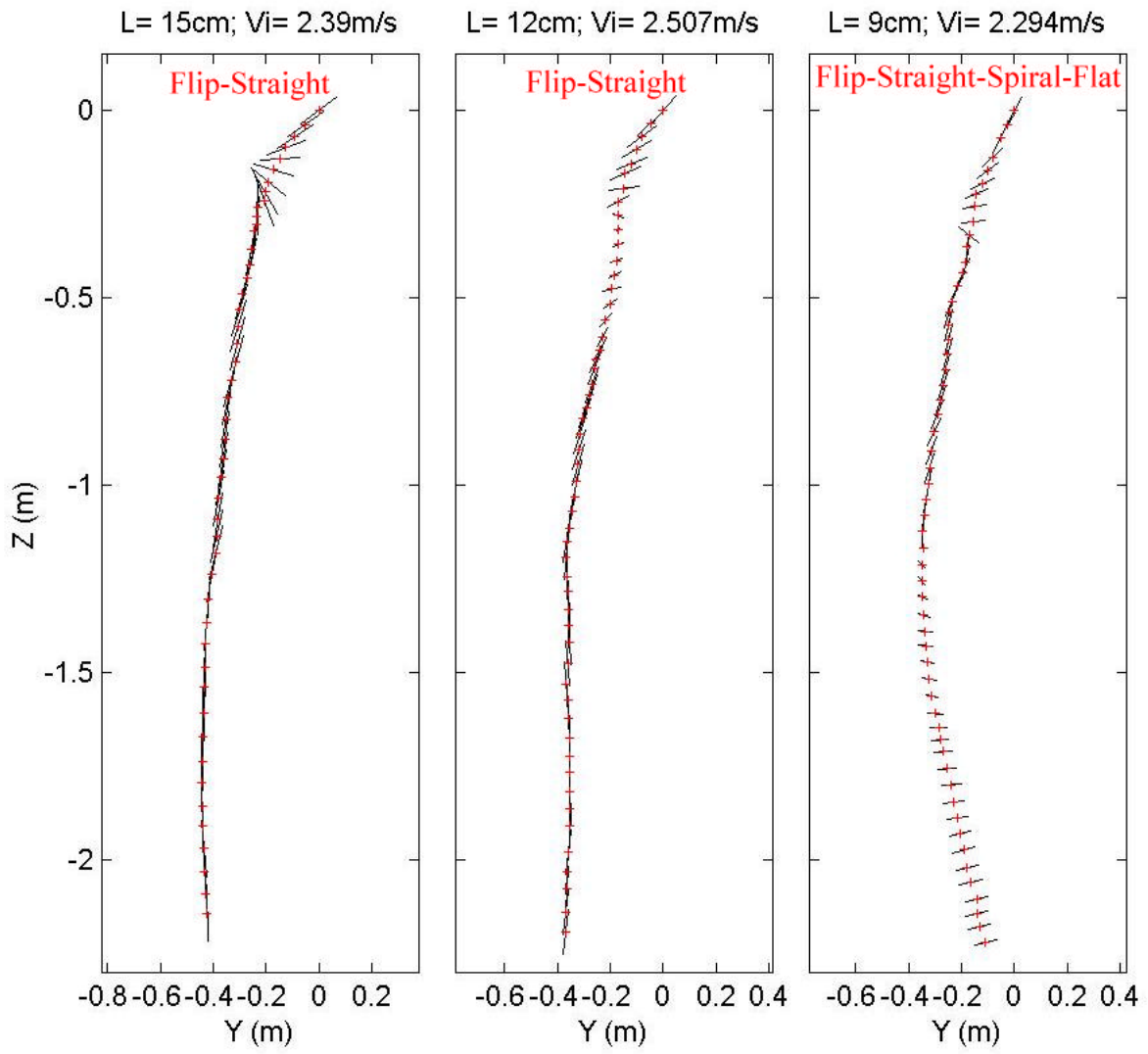
Drop Angle: 75; COM:0



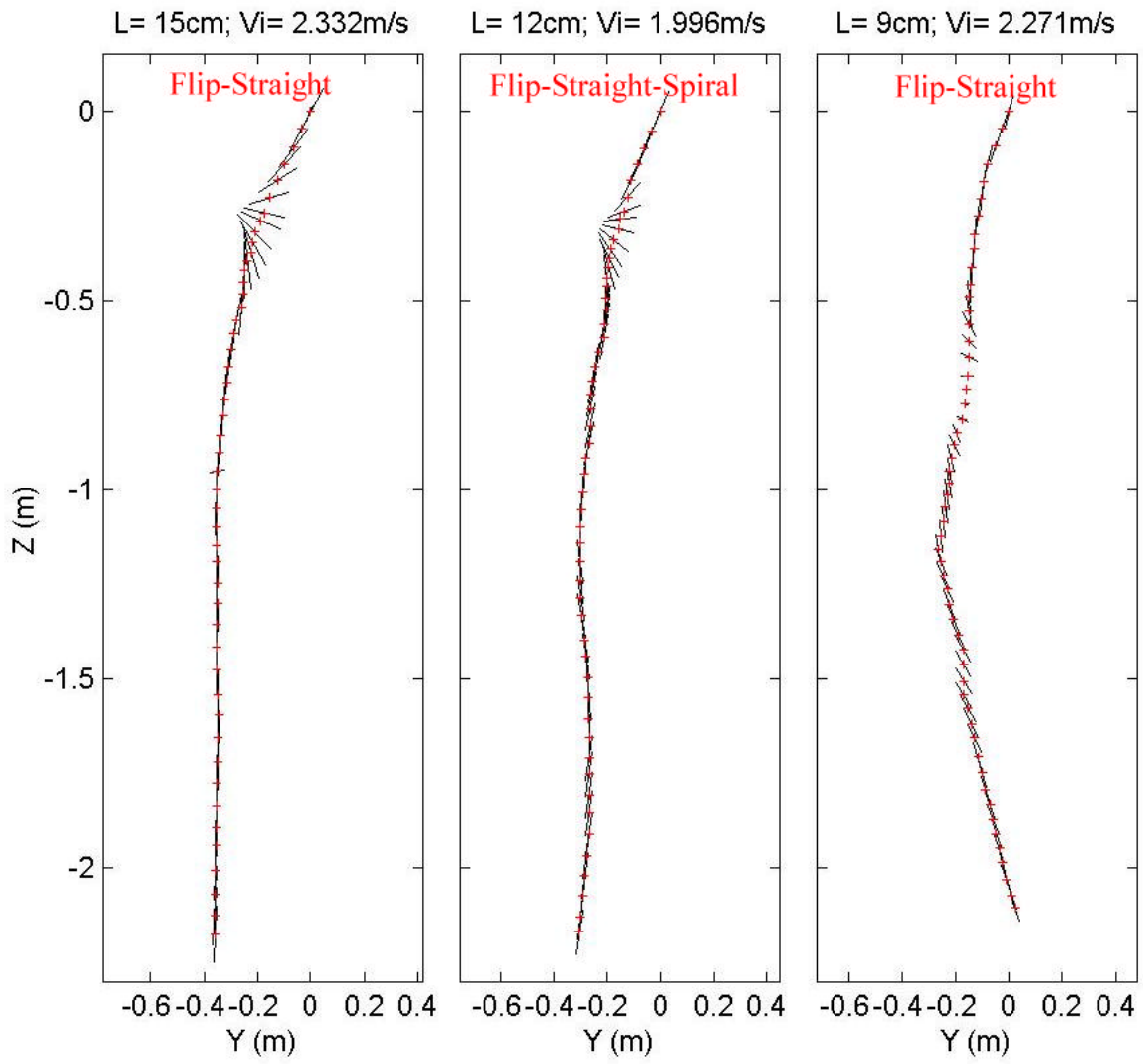
Drop Angle: 30; COM:-2



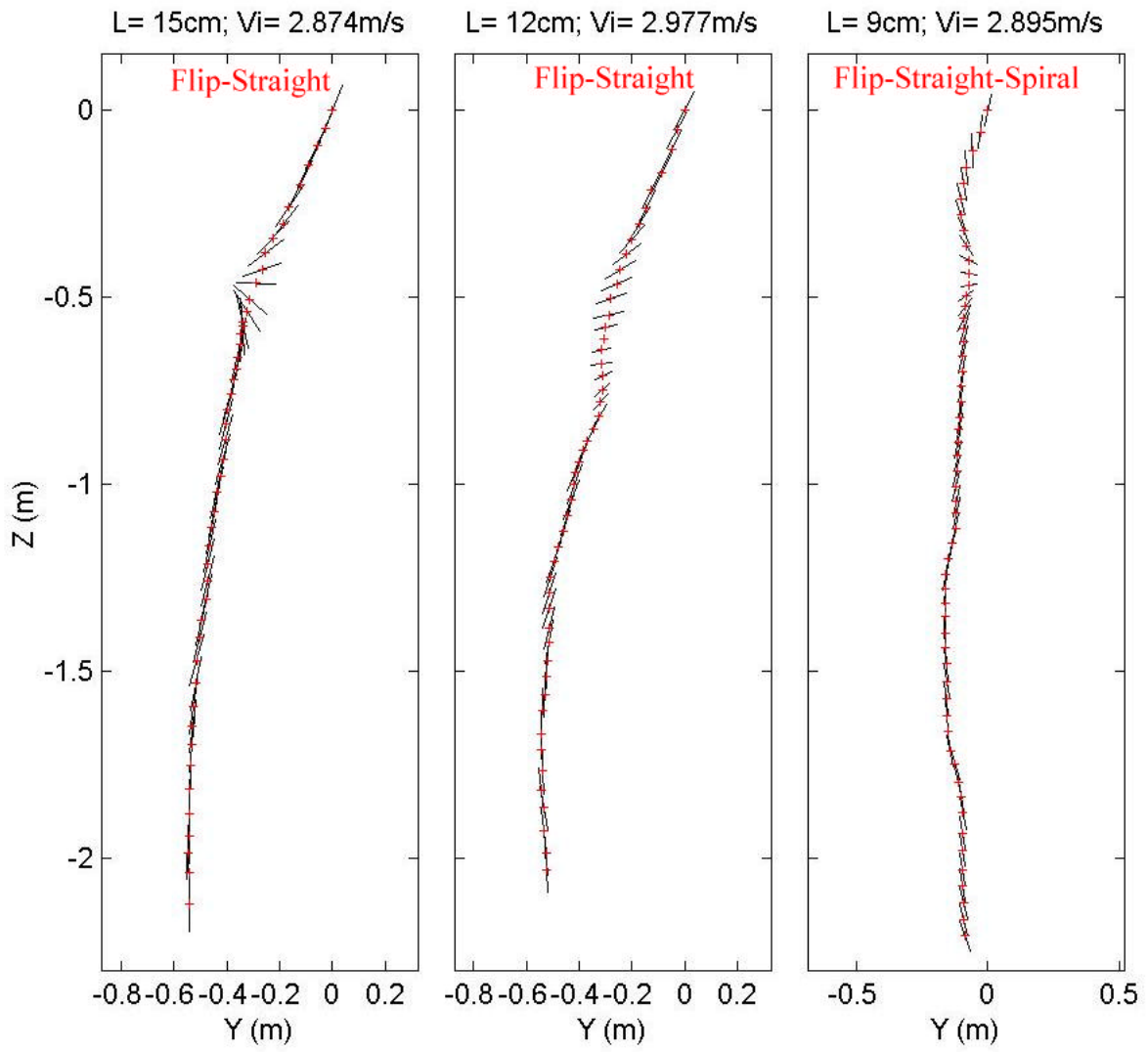
Drop Angle: 30; COM:-2



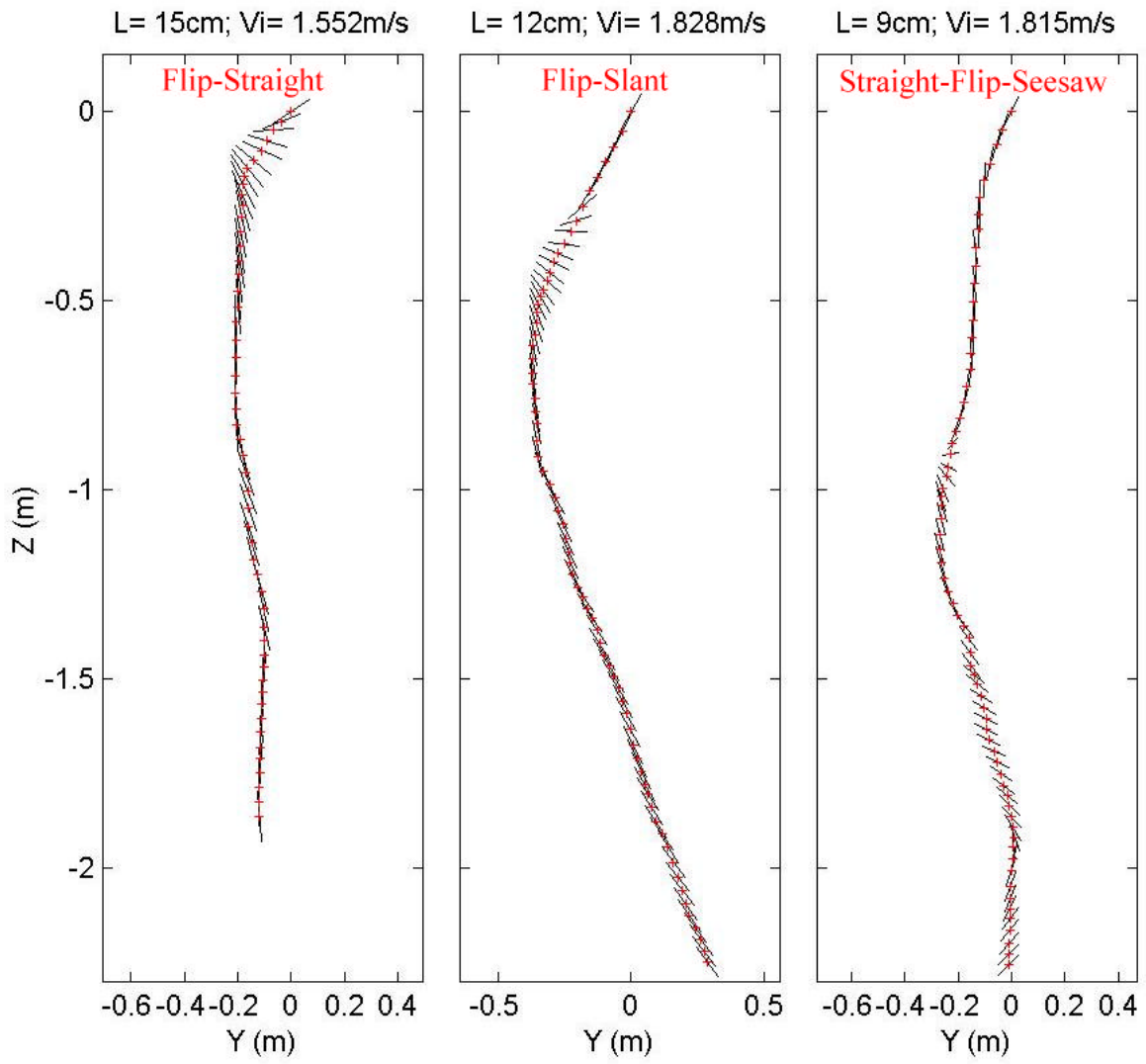
Drop Angle: 45; COM:-2



Drop Angle: 45; COM:-2

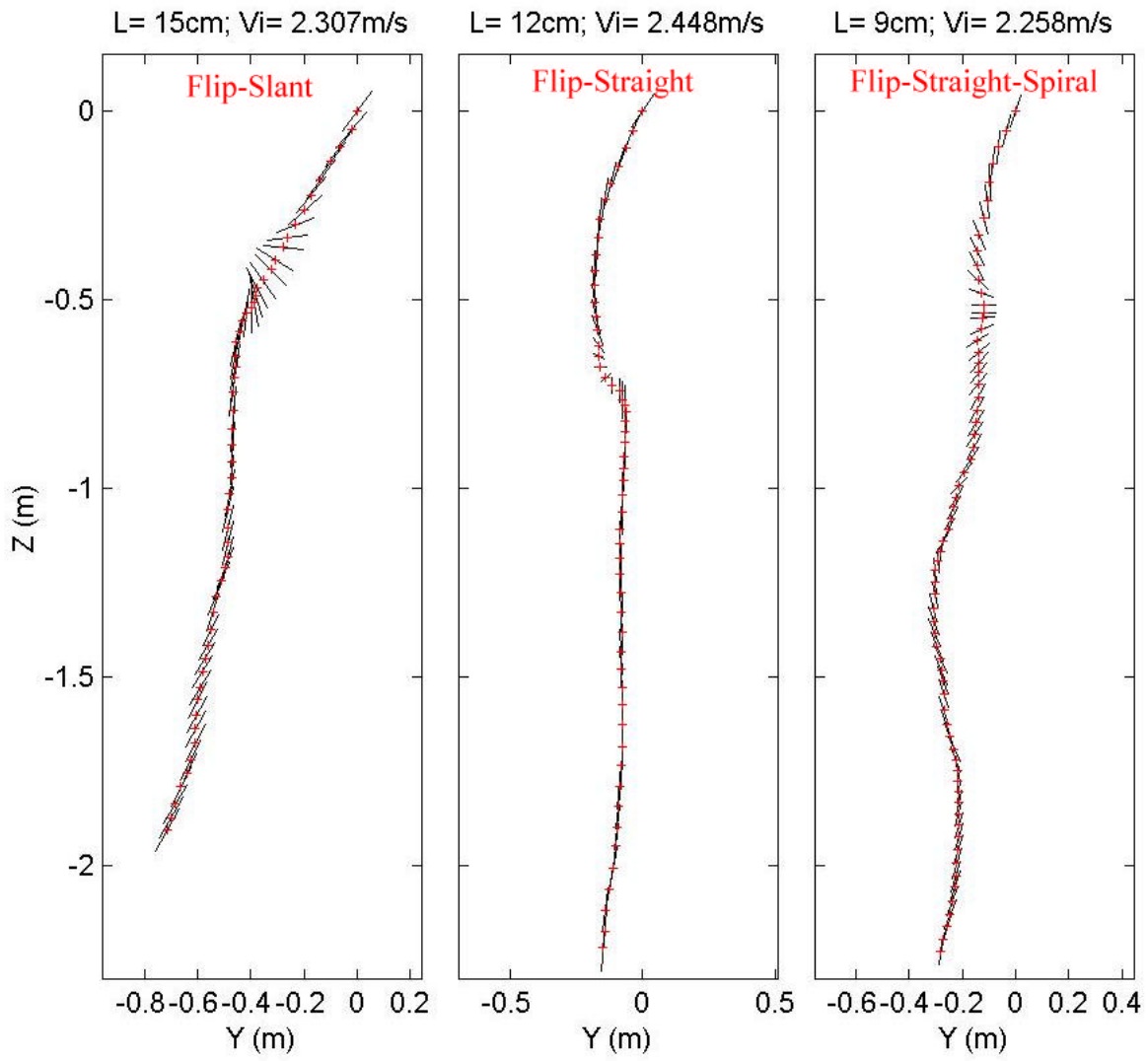


Drop Angle: 30; COM:-1

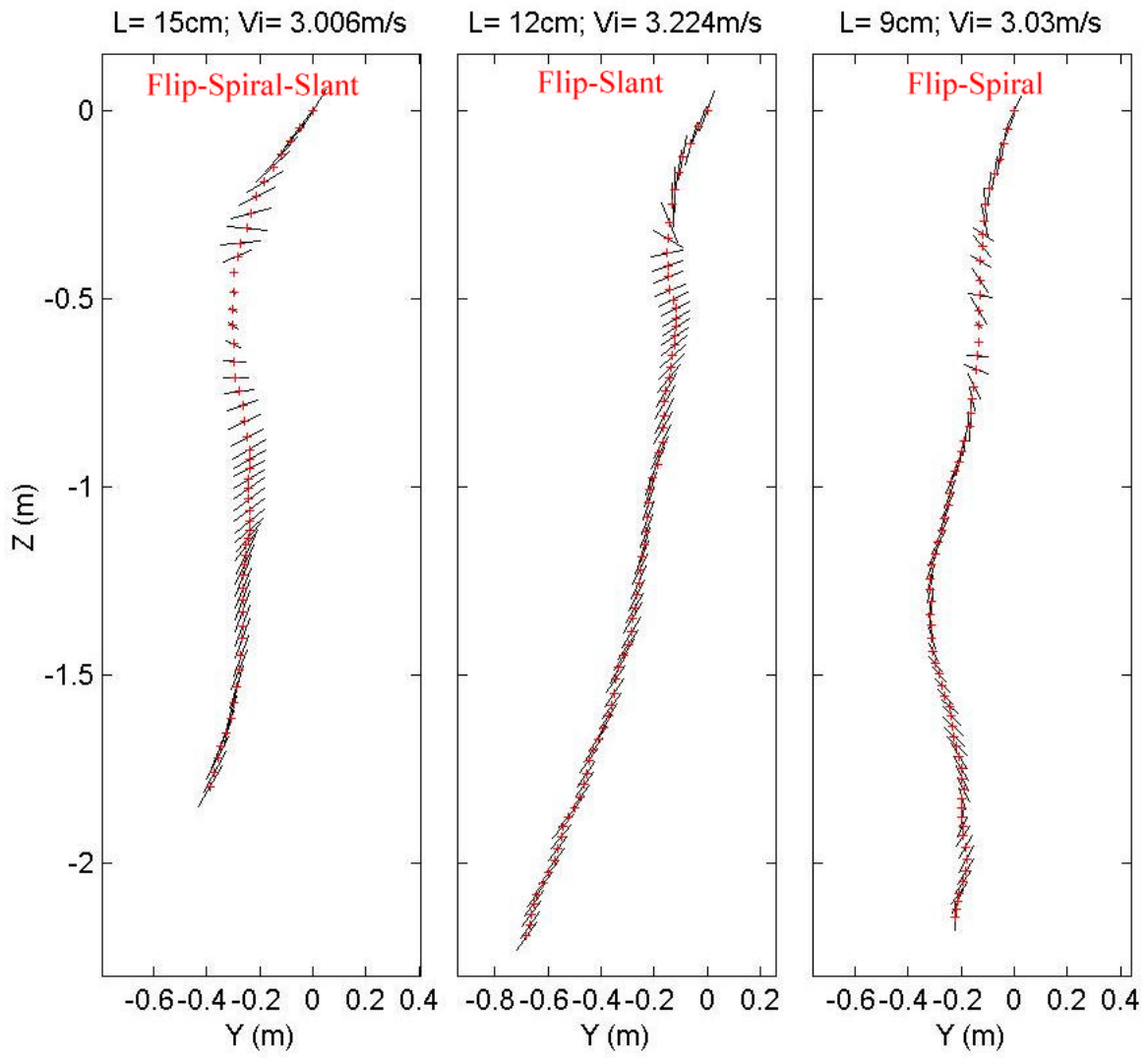




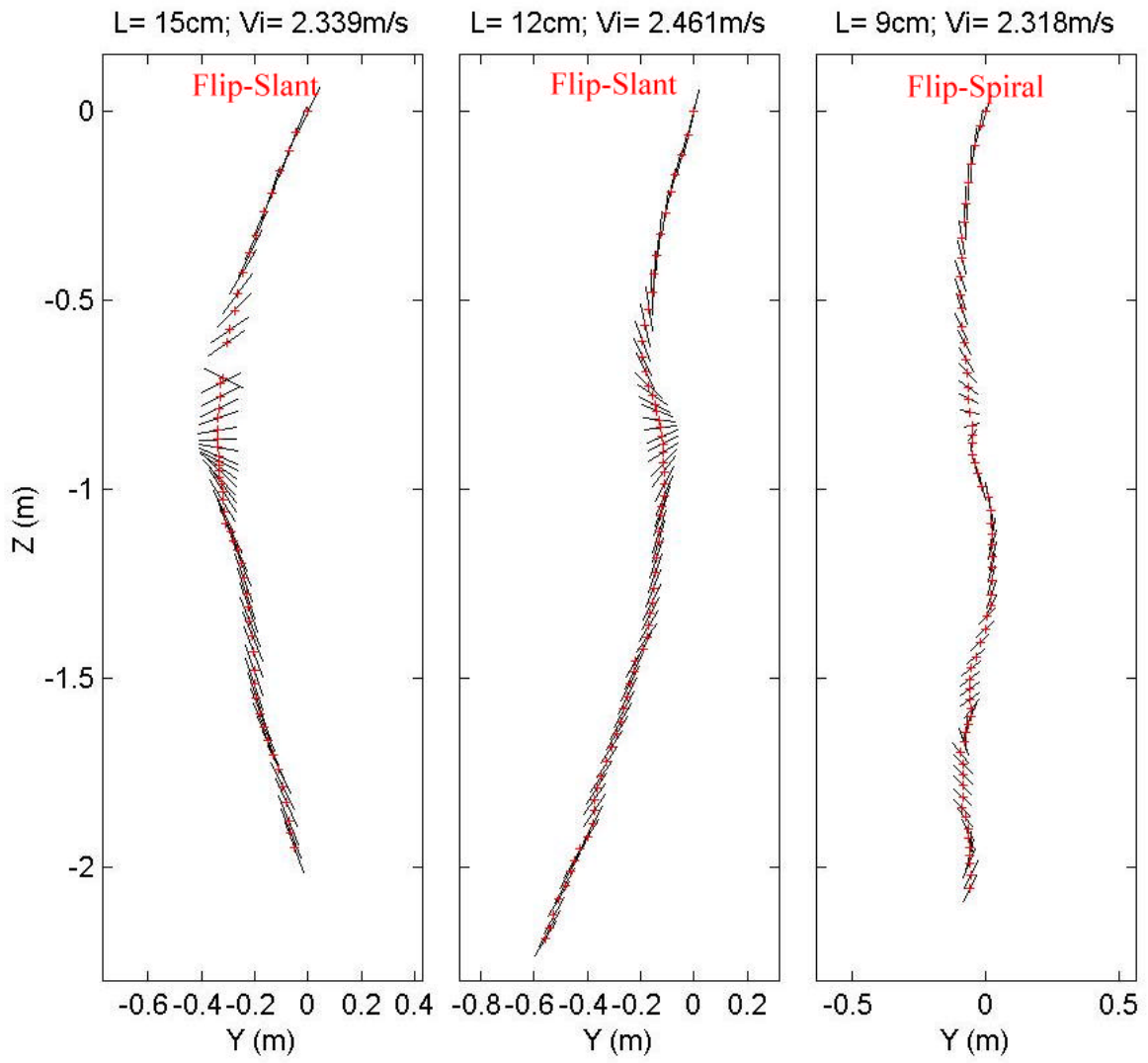
Drop Angle: 30; COM:-1



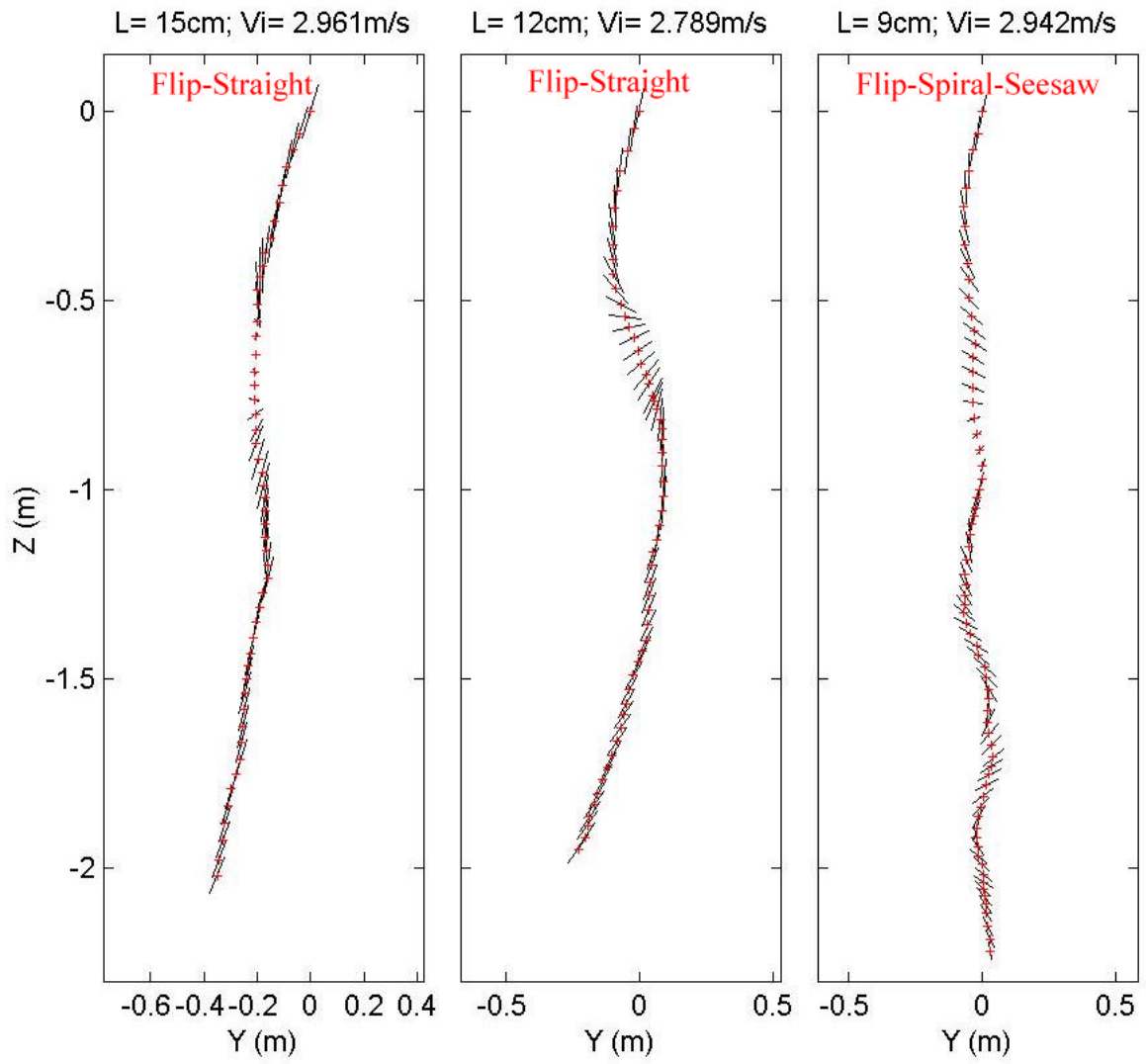
Drop Angle: 45; COM:-1



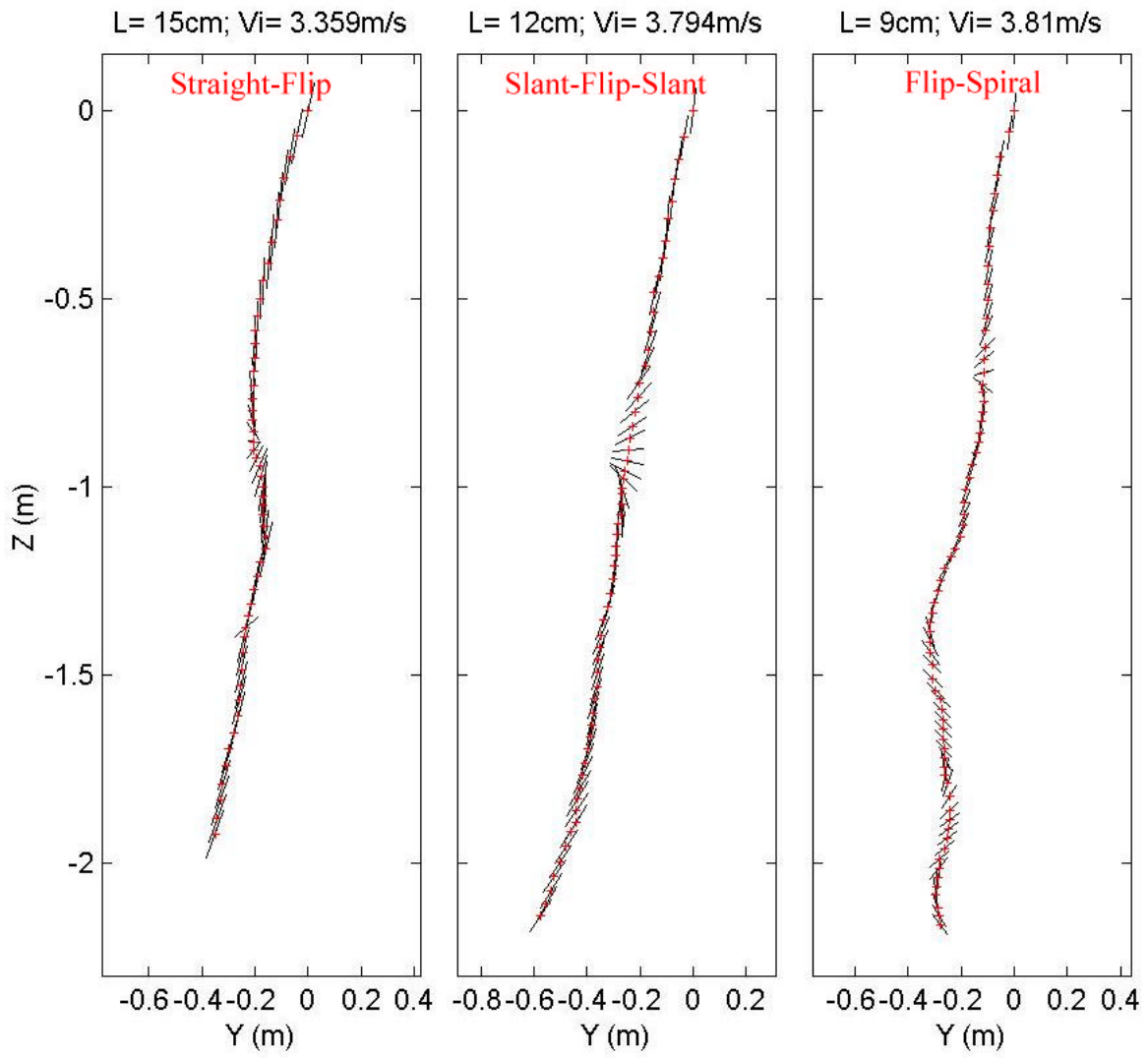
Drop Angle: 45; COM:-1



Drop Angle: 60; COM:-1



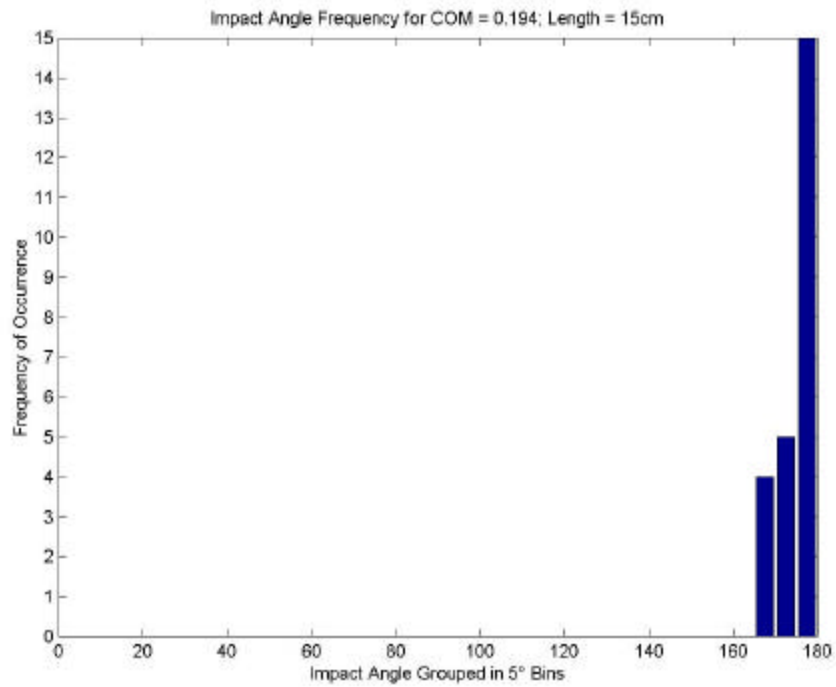
Drop Angle: 60; COM:-1

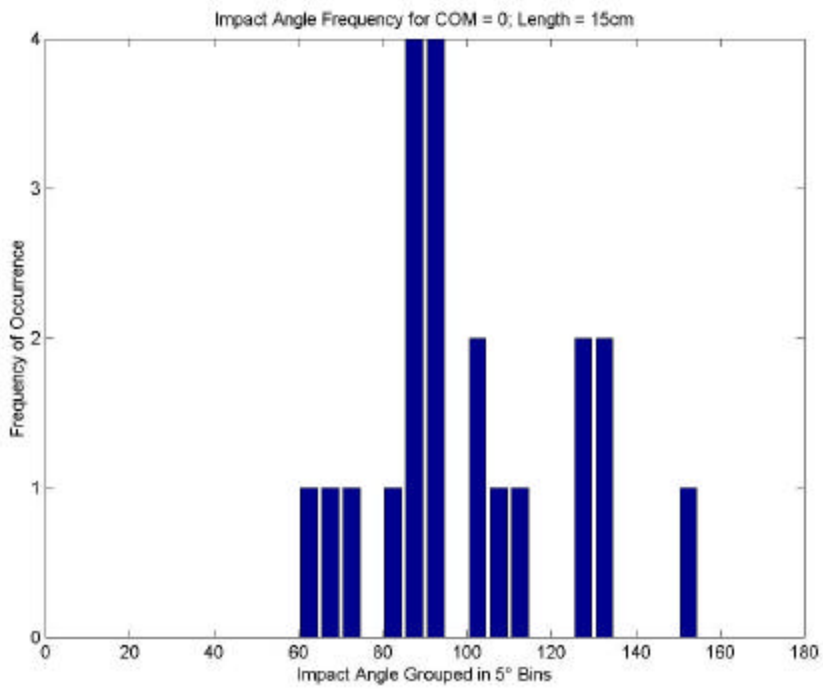
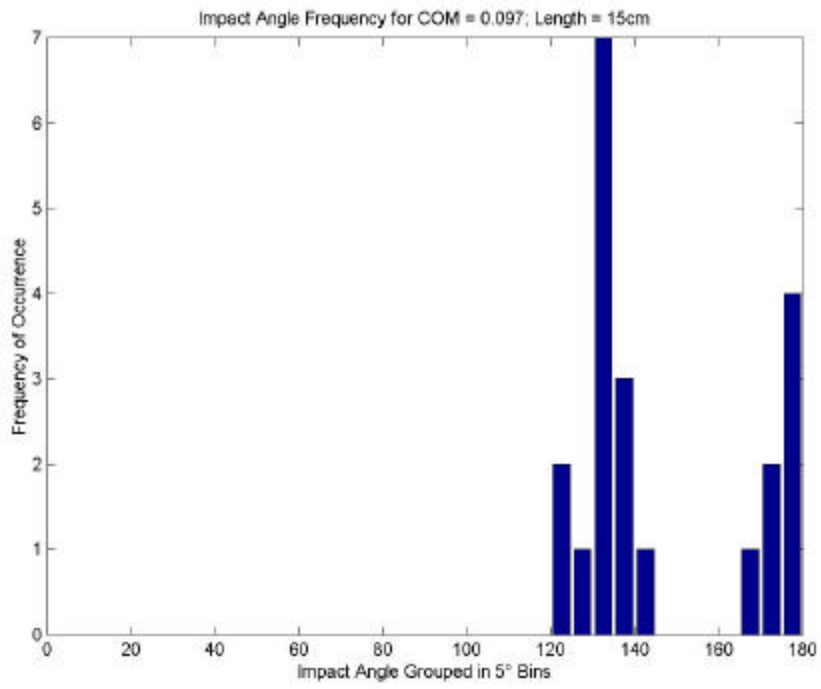


THIS PAGE INTENTIONALLY LEFT BLANK

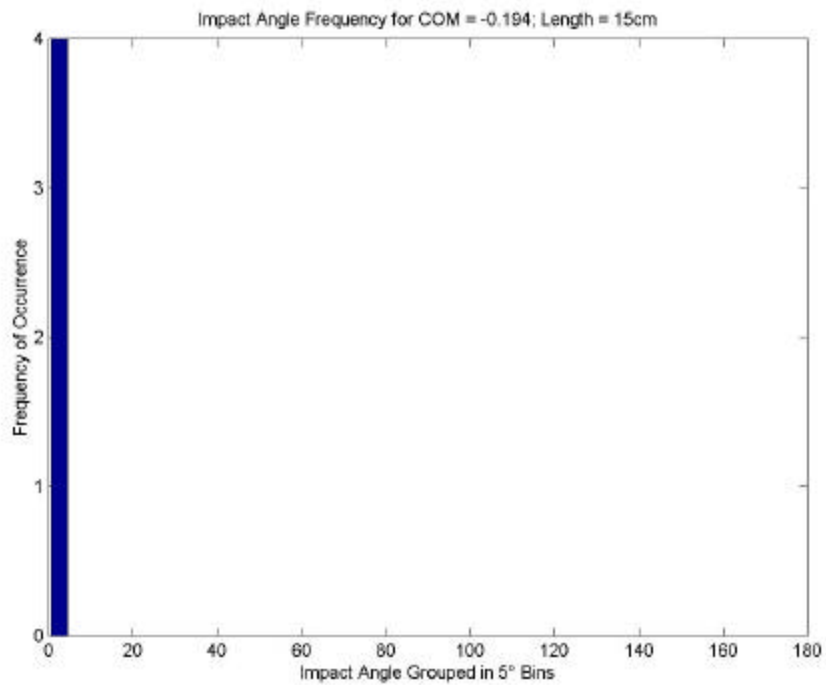
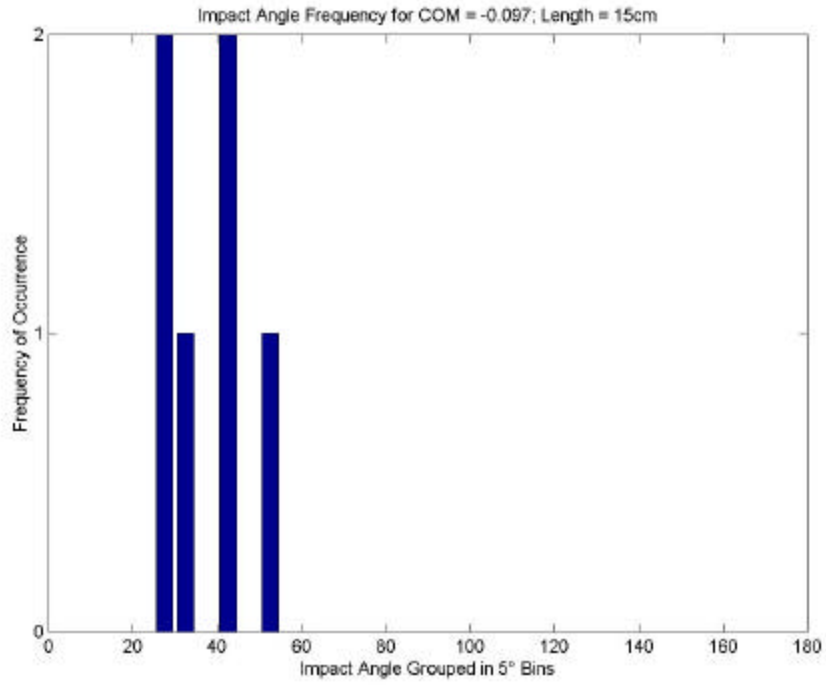
## APPENDIX B. HISTOGRAM PLOTS

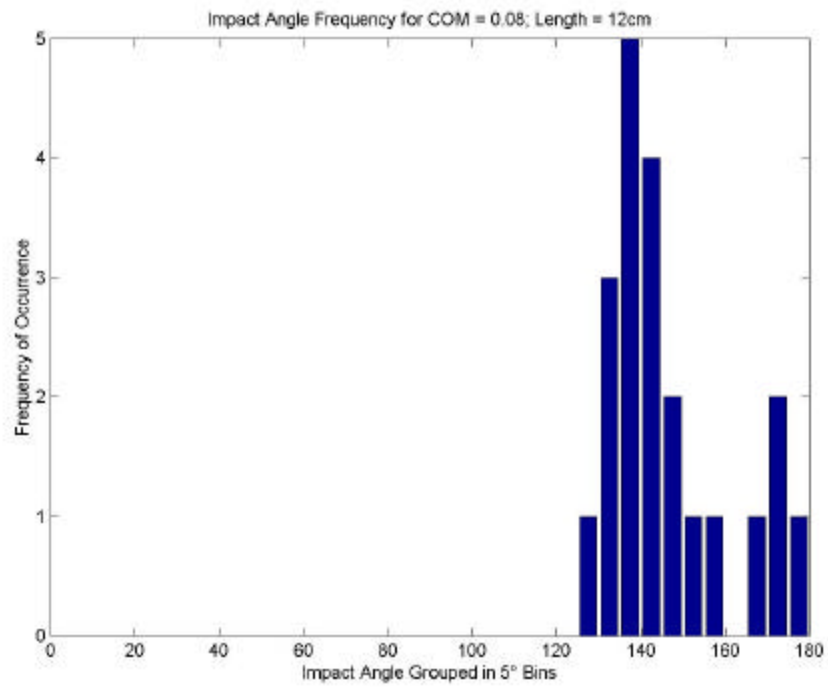
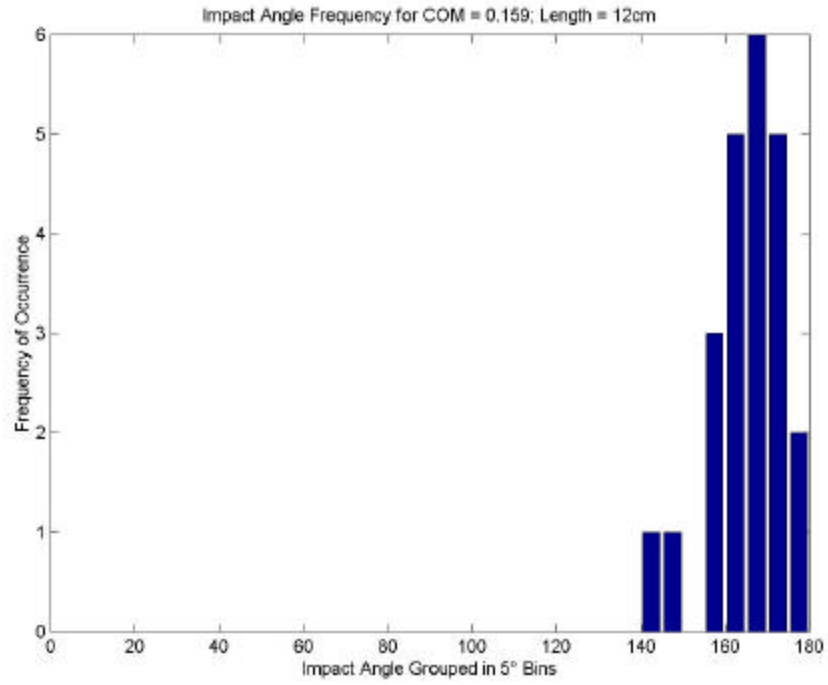
Appendix B contains all of the histogram plots that were derived from the last recorded data point. The data tables used for histogram production are found in Appendix D. The histograms are broken down by mine length and non-dimensional COM position.

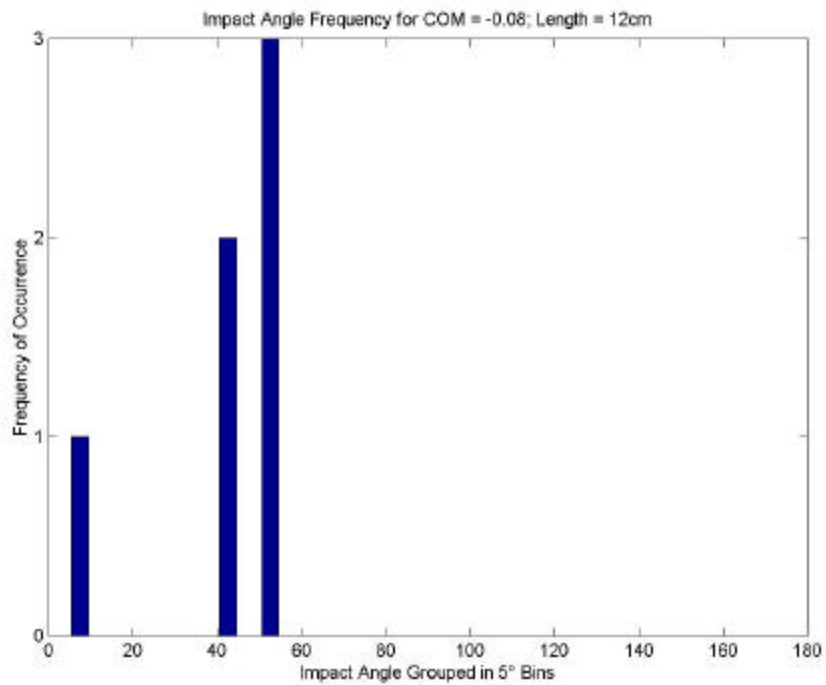
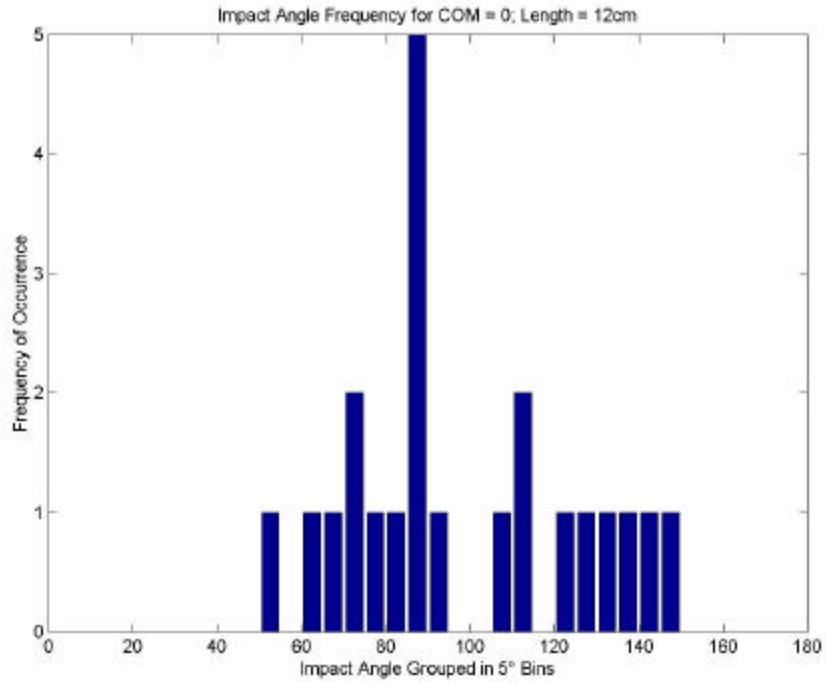


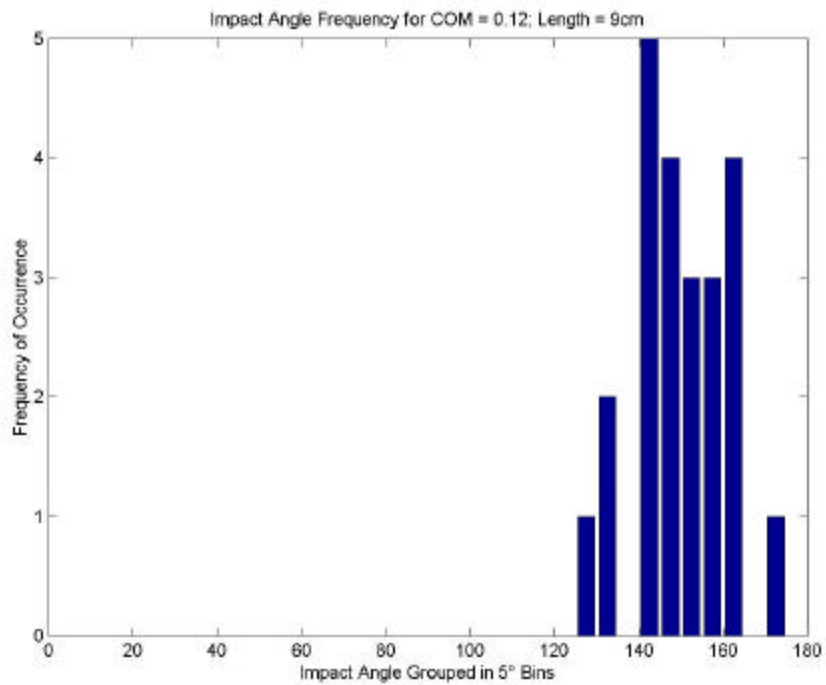
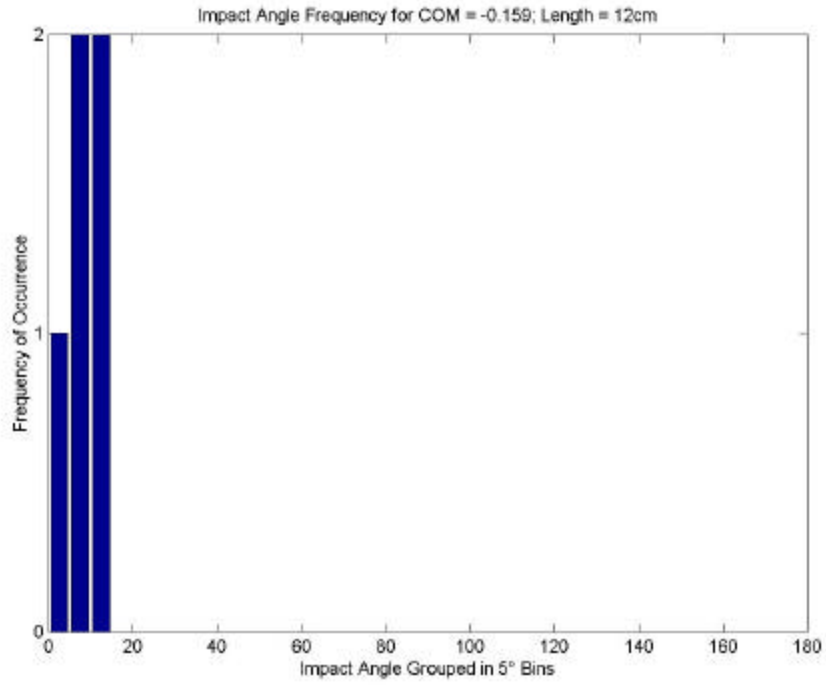


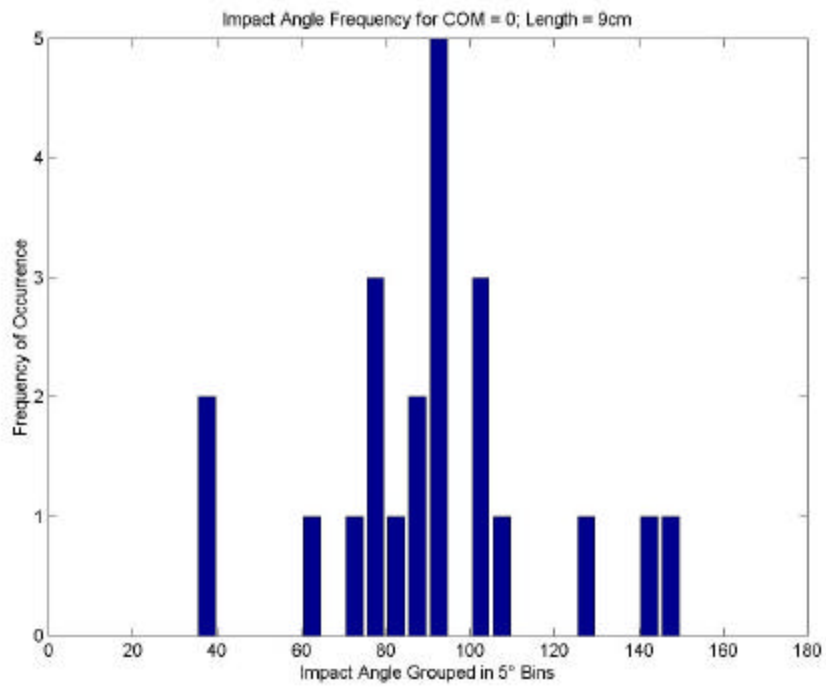
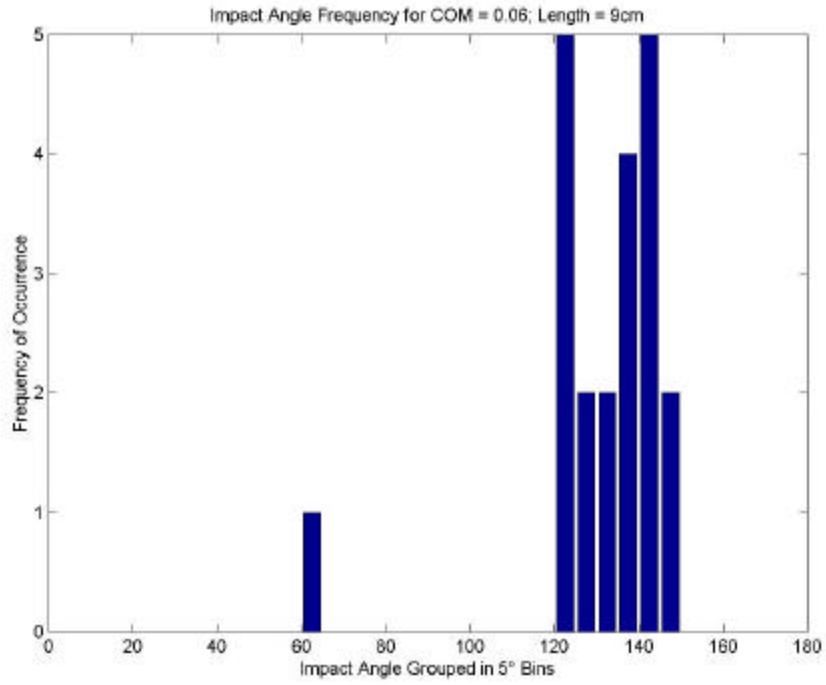


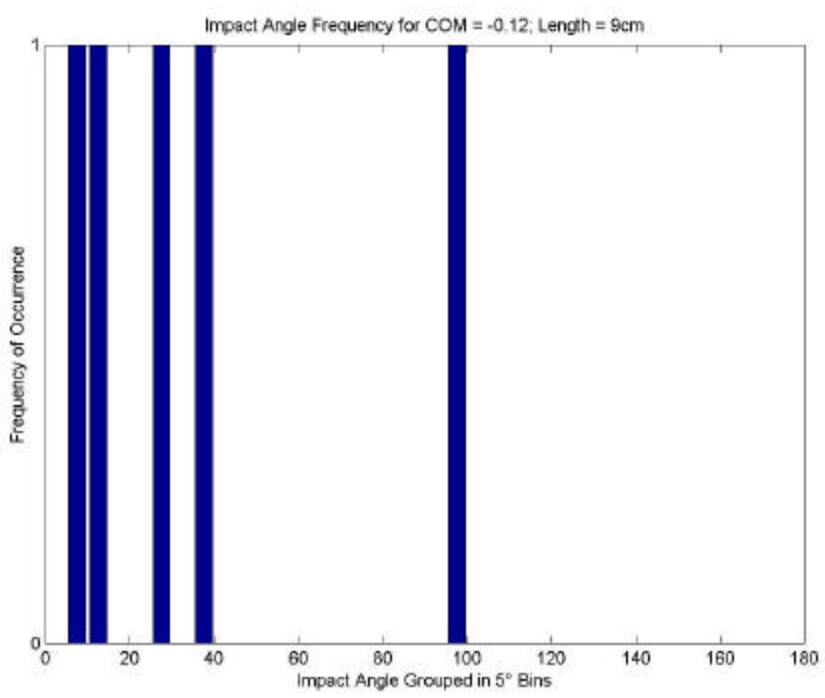
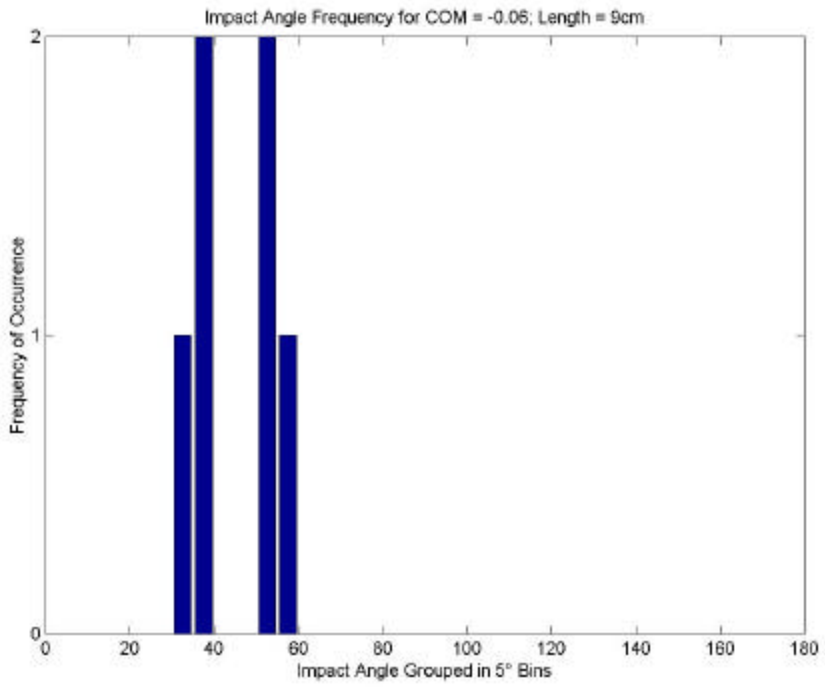








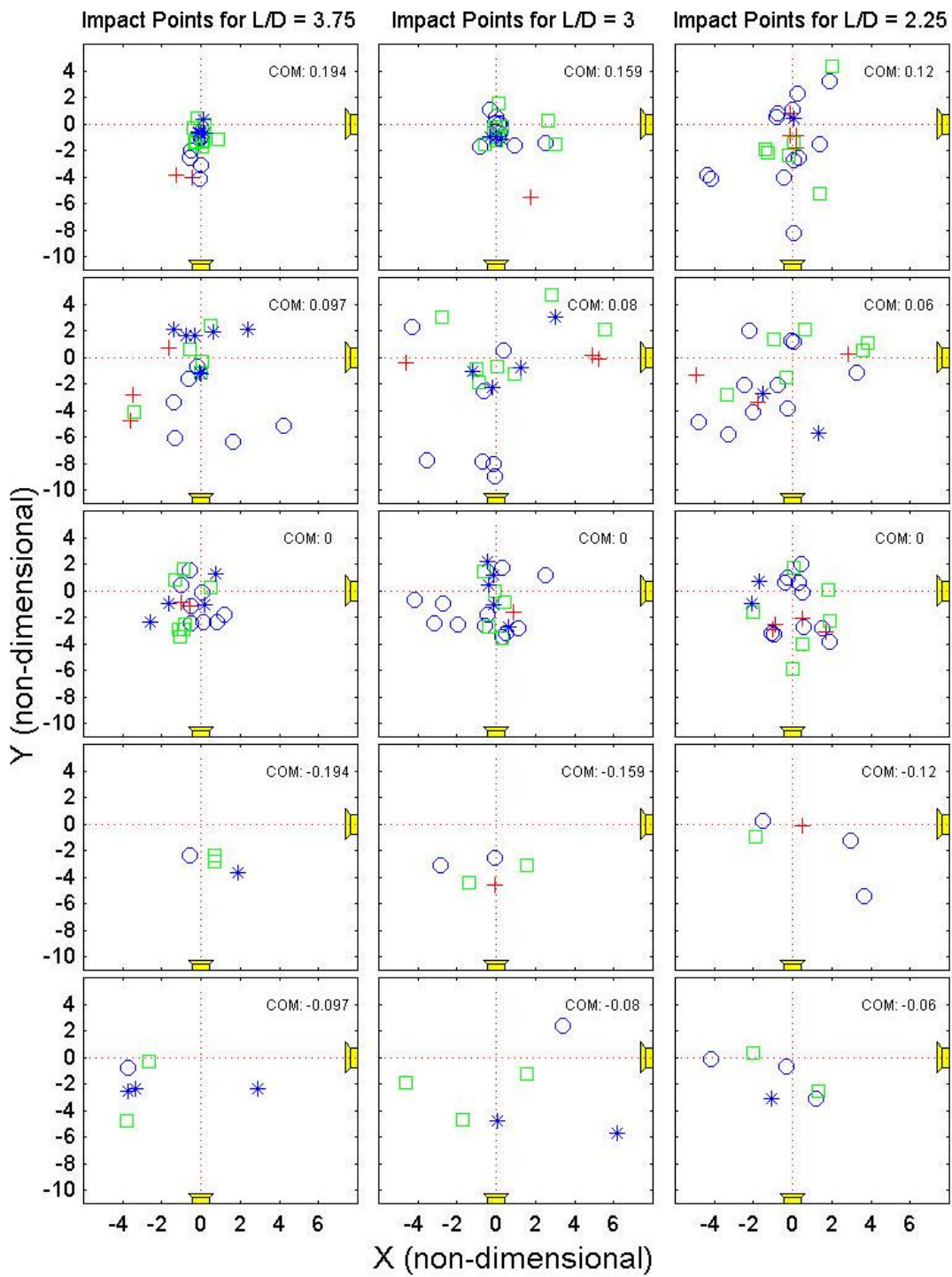




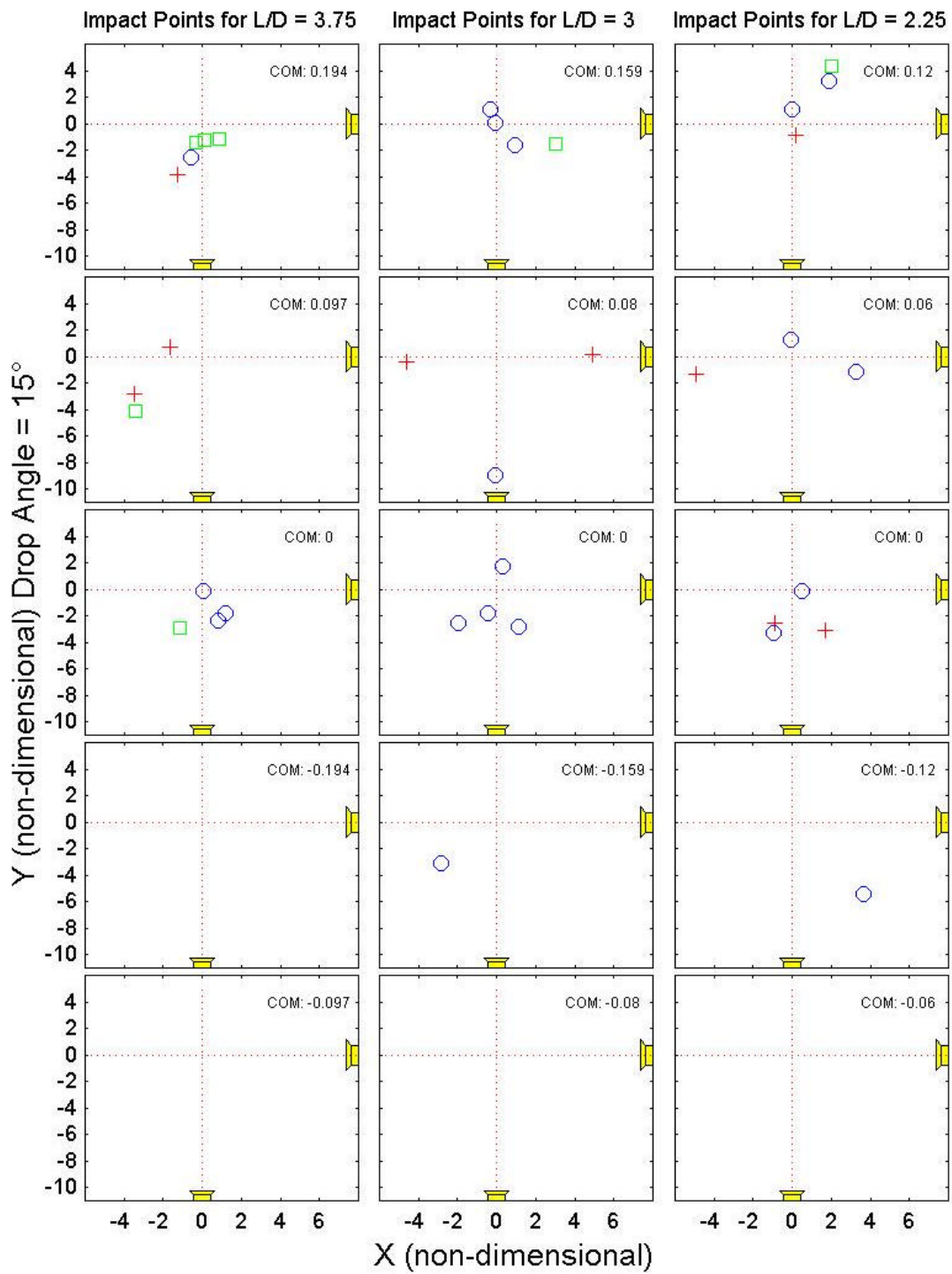
## APPENDIX C. IMPACT POINTS

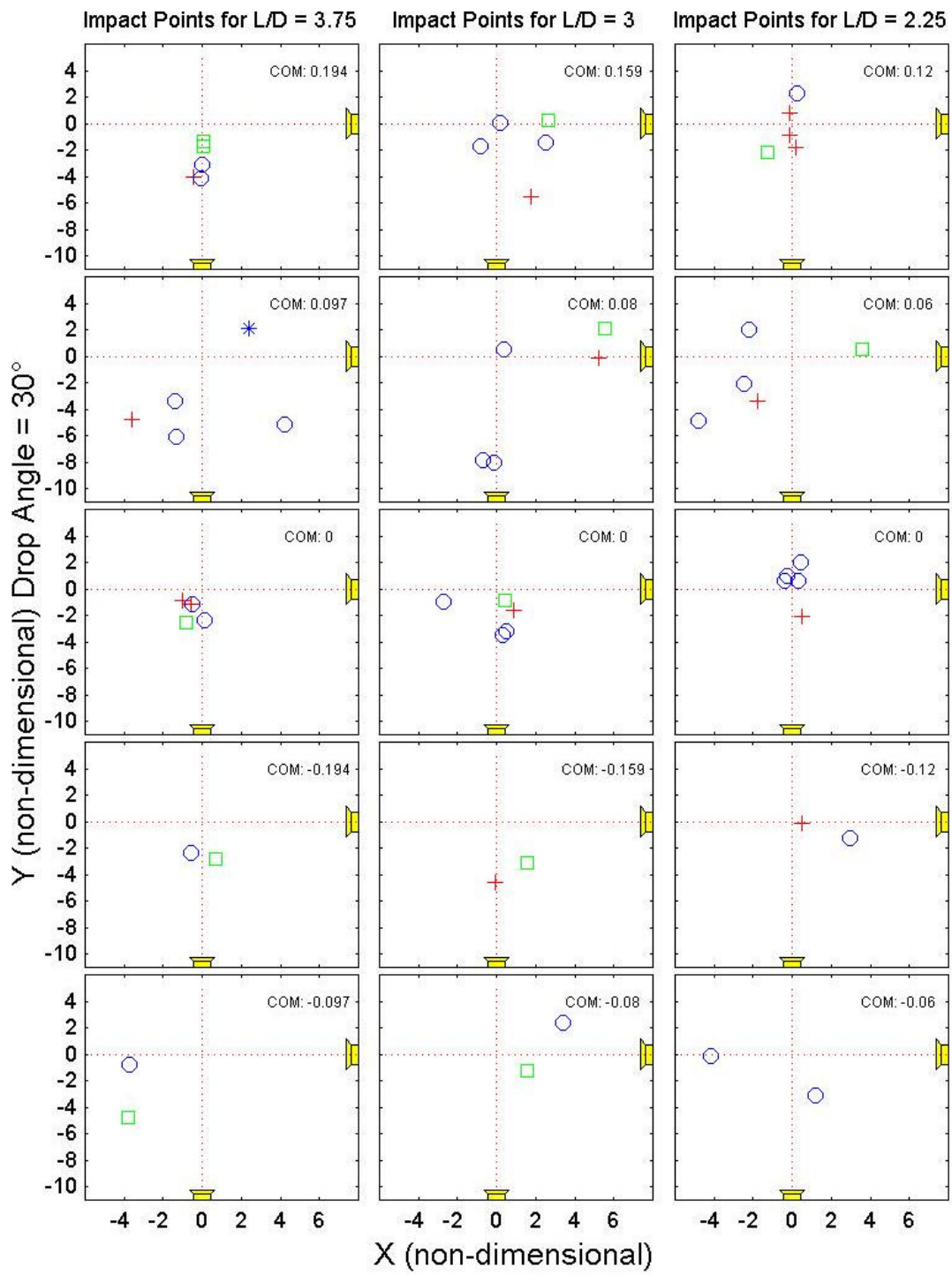
Appendix C contains all of the x-y plane impact points. The impact points are derived from the mine's volumetric center x and y coordinates and is presented in three columns and five rows. The columns correspond to mine length, while the rows represent the COM positions beginning with position 2 to position -2. There are two sets of plots, one for all drop angles and another set for each drop angle. Each of the individual plots is assigned a symbol based upon the mine's  $V_{int}$ . The velocity ranges used are in m/s and are provided in the legend below:

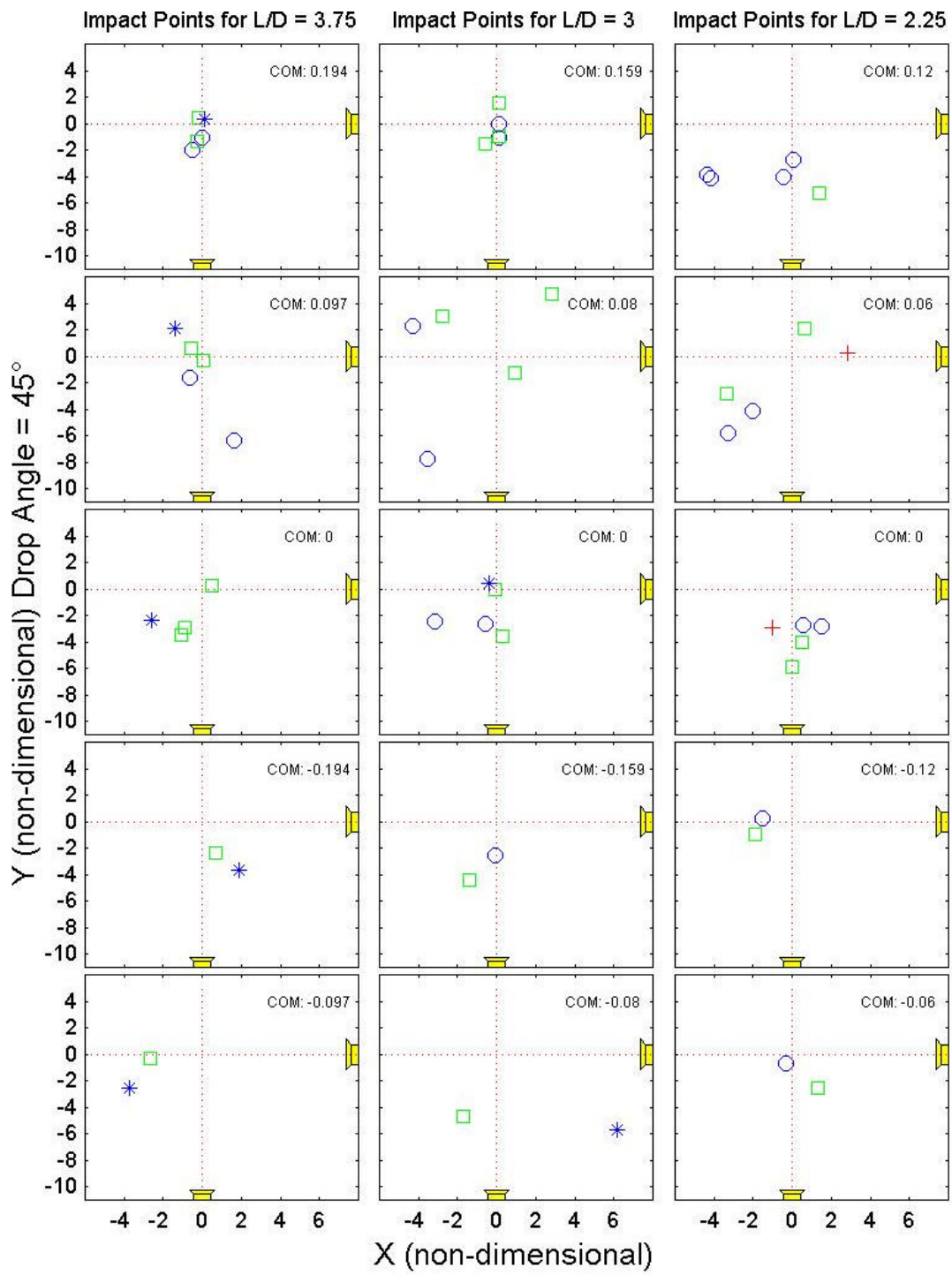
+	.7-1.5
○	>1.5-2.5
□	>2.5-3.5
*	>3.5-4.8

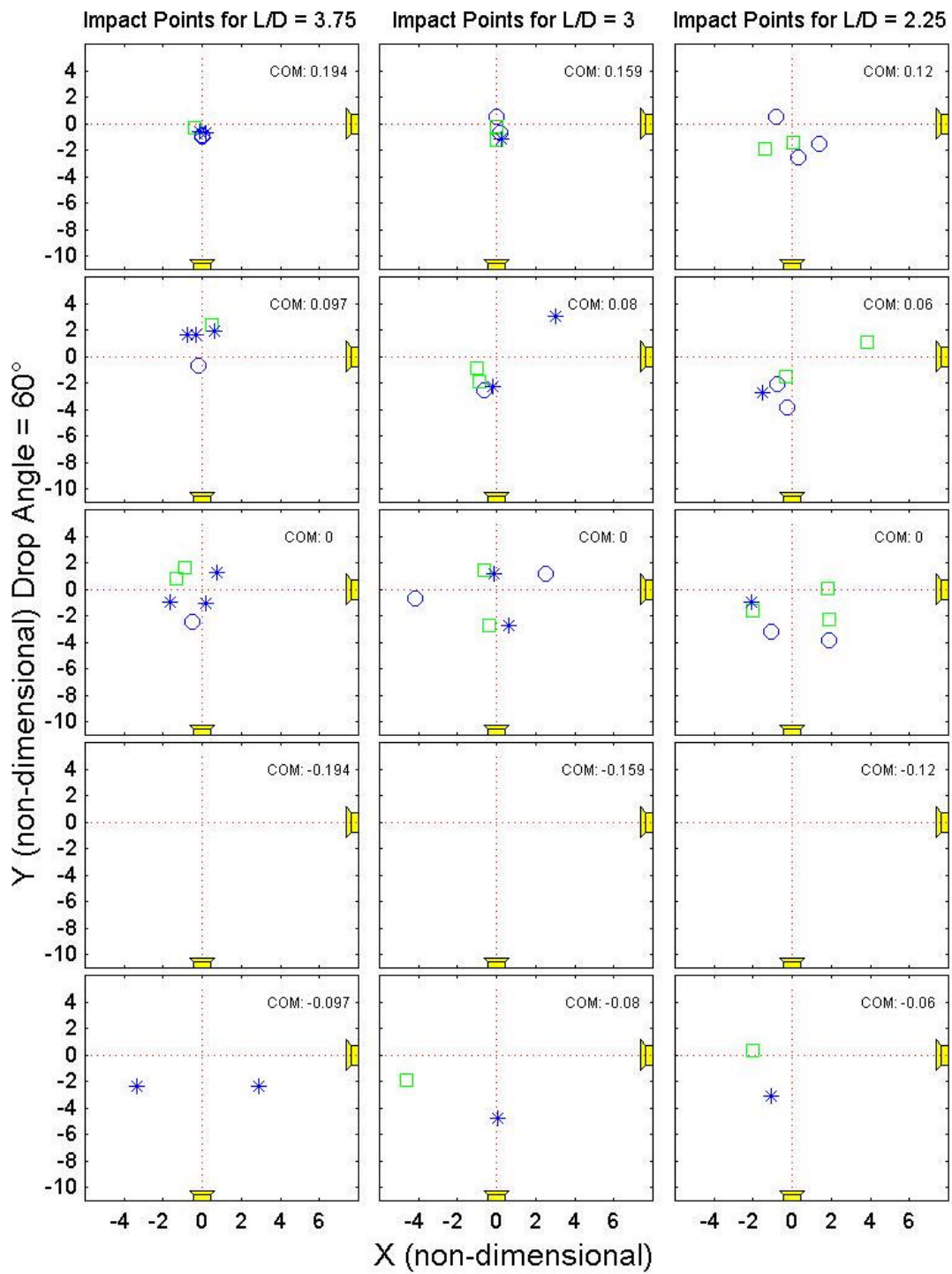


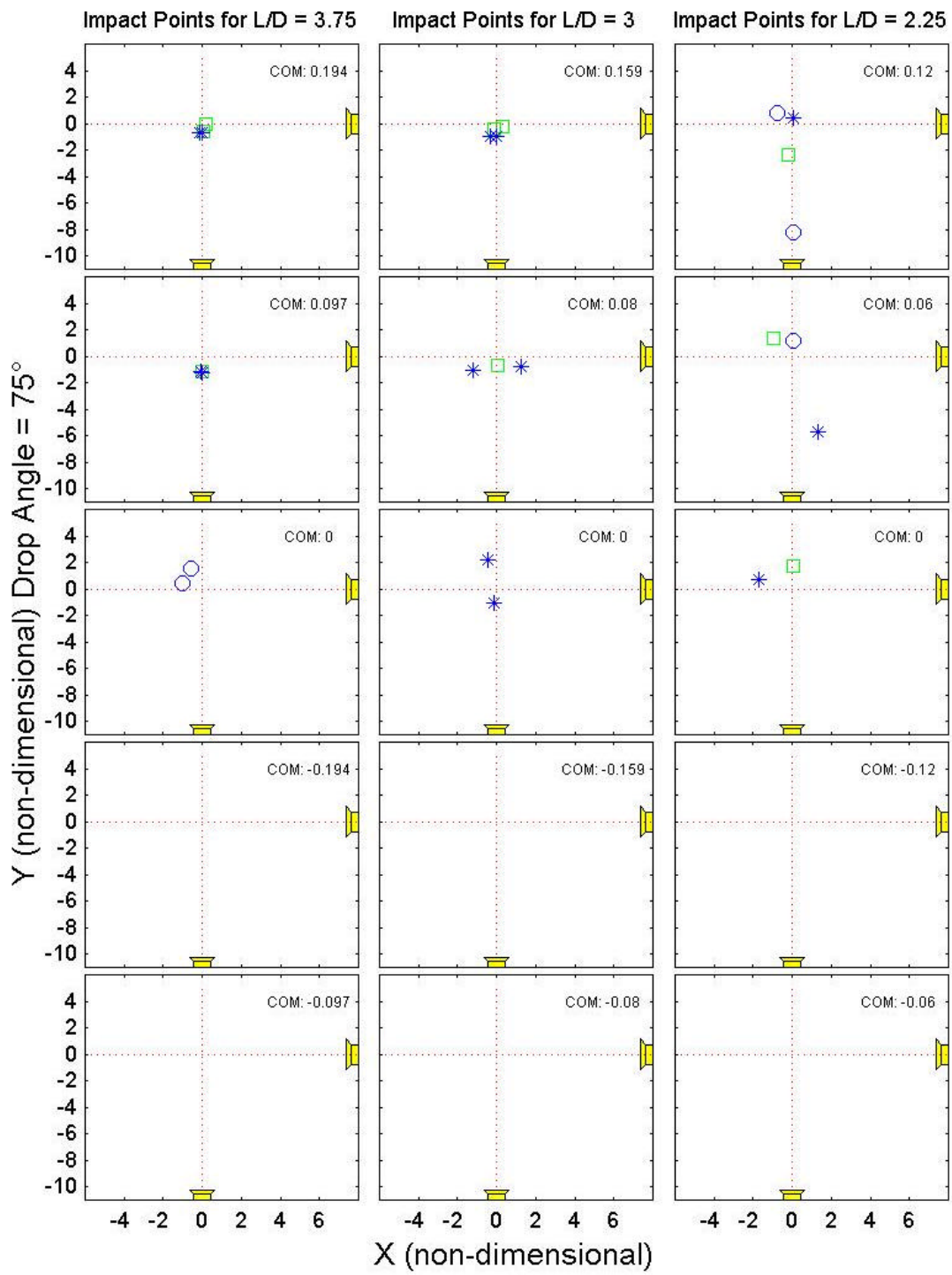












THIS PAGE INTENTIONALLY LEFT BLANK

## APPENDIX D. IMPACT DATA TABLES

This appendix contains all of the impact point data used in the multiple linear regression calculations, impact angle histograms and impact point scatter plots. The last recorded point was considered to be the point at which the mine moved outside of the background grid's boundaries. The first four columns are the input parameters, t represents time and the last seven columns are the output parameters. The data has been organized by drop angle, decreasing mine length and decreasing COM position. All of the data contained has been made non-dimensional by the conversions listed earlier.

ang	L/D	Vind	COM	t	xm	ym	zm	Psi	u	v	w
15	3.75	2.708	.194	48.2	0.10	-1.29	-14.03	169.6	0.09	0.07	-1.38
15	3.75	1.467	.194	53.2	-1.29	-3.82	-13.50	179.1	0.00	0.04	-1.59
15	3.75	2.346	.194	47.0	-0.55	-2.54	-14.15	180	0.04	-0.04	-1.73
15	3.75	3.261	.194	48.2	0.85	-1.20	-13.93	177.9	0.05	0.04	-1.36
15	3.75	2.847	.194	48.2	-0.30	-1.45	-14.01	176.9	-0.05	0.05	-1.32
15	3.75	1.286	.097	61.8	-1.67	0.75	-14.48	126.8	-0.35	0.40	-0.84
15	3.75	1.31	.097	53.2	-3.49	-2.79	-9.30	137.8	-0.62	-0.22	-1.04
15	3.75	2.884	.097	44.5	-3.41	-4.10	-11.24	132.3	-0.66	-0.05	-1.11
15	3.75	1.711	.000	120.0	1.17	-1.81	-14.91	69	0.00	-0.13	-0.60
15	3.75	1.705	.000	108.8	0.04	-0.12	-15.01	93.3	-0.09	-0.13	-0.62
15	3.75	2.696	.000	103.9	-1.14	-2.95	-14.73	90	-0.09	0.00	-0.73
15	3.75	2.372	.000	107.6	0.79	-2.35	-14.92	94.3	0.05	-0.13	-0.77
15	3	1.555	.159	46.5	0.92	-1.61	-17.37	163.7	0.05	0.58	-1.33
15	3	2.121	.159	53.1	-0.09	0.06	-17.95	169.7	-0.05	0.21	-1.59
15	3	3.054	.159	54.2	2.99	-1.52	-17.88	169.2	0.10	0.21	-1.55
15	3	1.601	.159	48.7	-0.30	1.12	-16.74	167.7	0.00	0.30	-1.28
15	3	1.34	.080	73.0	4.93	0.16	-18.36	144.8	0.15	0.40	-0.91
15	3	1.237	.080	74.1	-4.58	-0.39	-16.17	144.9	-0.35	-0.05	-0.91
15	3	2.095	.080	70.8	-0.09	-9.00	-17.48	135.7	-0.15	-0.54	-0.91
15	3	1.729	.000	99.5	-0.45	-1.80	-19.04	90	-0.30	0.10	-0.69
15	3	2.406	.000	81.8	0.33	1.76	-18.57	141.6	0.10	0.15	-0.91
15	3	2.325	.000	83.0	-1.98	-2.53	-17.45	115	-0.05	0.05	-0.72
15	3	2.094	.000	92.9	1.12	-2.84	-18.61	90	0.10	0.00	-0.86
15	3	2.475	-.159	57.5	-2.84	-3.12	-17.59	11	0.25	0.00	-1.40
15	2.25	1.448	.120	48.9	0.16	-0.86	-24.79	163.6	0.00	-0.34	-1.64
15	2.25	2.296	.120	51.7	1.90	3.23	-23.47	160.5	0.23	0.13	-1.59
15	2.25	2.572	.120	55.6	2.00	4.32	-24.31	145	0.46	0.53	-1.32
15	2.25	1.647	.120	47.9	0.02	1.05	-23.09	155.5	0.00	-0.29	-1.11
15	2.25	1.446	.060	56.5	-4.92	-1.31	-23.66	128.1	0.40	-0.34	-0.80
15	2.25	1.637	.060	71.8	3.29	-1.15	-25.36	60.6	-0.69	-0.06	-0.71
15	2.25	1.801	.060	68.0	-0.10	1.23	-24.37	135.5	0.00	-0.06	-0.91
15	2.25	1.489	.000	69.9	-0.91	-2.54	-24.73	39	0.17	-0.06	-1.00
15	2.25	1.587	.000	69.0	-0.93	-3.25	-24.70	129.6	-0.28	-0.23	-1.28
15	2.25	2.414	.000	69.9	0.48	-0.10	-25.01	93.6	0.00	0.11	-0.85
15	2.25	1.456	.000	69.0	1.71	-3.10	-24.79	84.6	-0.05	-0.23	-0.74
15	2.25	2.126	-.120	53.6	3.65	-5.41	-23.69	9	0.23	0.00	-1.39

ang	L/D	Vind	COM	t	xm	ym	zm	Psi	u	v	w
30	3.75	2.574	.194	45.8	0.08	-1.72	-13.93	172.9	0.04	0.04	-1.44
30	3.75	2.855	.194	48.2	0.02	-1.35	-14.15	176.4	-0.05	0.34	-1.45
30	3.75	1.886	.194	49.5	0.01	-3.12	-14.36	177.4	0.00	-0.31	-1.26
30	3.75	1.538	.194	51.9	-0.06	-4.11	-14.17	178	0.00	0.13	-1.39
30	3.75	1.426	.194	54.4	-0.46	-4.04	-14.66	173	0.05	0.05	-1.37
30	3.75	3.807	.097	65.5	2.38	2.07	-14.66	132.6	0.31	0.22	-0.84
30	3.75	2.314	.097	55.6	-1.32	-6.05	-13.75	134.5	0.00	-0.40	-0.84
30	3.75	2.374	.097	47.0	-1.39	-3.39	-13.70	175.7	0.00	-0.13	-1.30
30	3.75	1.666	.097	74.2	4.23	-5.13	-14.35	144.5	0.31	-0.22	-0.97
30	3.75	1.134	.097	58.1	-3.62	-4.75	-9.78	133.9	-0.27	-0.05	-0.93
30	3.75	2.819	.000	100.2	-0.86	-2.54	-14.49	86.6	0.05	0.00	-0.73
30	3.75	2.215	.000	107.6	0.13	-2.37	-14.80	64.8	0.09	-0.09	-0.84
30	3.75	1.323	.000	111.3	-0.57	-1.19	-15.16	91.6	-0.05	-0.04	-0.66
30	3.75	1.594	.000	113.8	-0.51	-1.19	-15.07	90	0.31	-0.05	-0.62
30	3.75	0.709	.000	110.1	-1.01	-0.83	-15.09	109.3	-0.09	-0.05	-0.55
30	3.75	2.853	-.097	66.8	-3.76	-4.75	-12.69	41.8	-0.22	-0.35	-0.77
30	3.75	1.919	-.097	63.1	-3.70	-0.80	-12.42	29.2	-0.05	0.05	-0.97
30	3.75	2.955	-.194	58.1	0.68	-2.83	-14.28	2.1	0.00	0.09	-1.30
30	3.75	1.92	-.194	56.9	-0.57	-2.38	-14.20	0	0.00	0.00	-1.50
30	3	3.013	.159	54.2	2.66	0.21	-18.13	173.1	-0.10	-0.21	-1.25
30	3	1.981	.159	48.7	2.53	-1.40	-17.75	175.2	0.15	-0.08	-1.68
30	3	2.16	.159	46.5	-0.82	-1.71	-17.20	146.9	-0.20	-0.35	-1.21
30	3	1.689	.159	50.9	0.18	0.07	-18.23	144.7	0.10	0.45	-0.94
30	3	1.392	.159	55.3	1.74	-5.54	-17.78	166	0.10	-0.20	-1.21
30	3	3.007	.080	68.6	5.55	2.08	-17.93	138.5	0.40	-0.30	-0.89
30	3	1.966	.080	65.3	-0.68	-7.87	-17.51	130.3	0.20	-0.10	-0.99
30	3	1.985	.080	53.1	0.36	0.52	-18.10	128.4	0.10	0.35	-0.94
30	3	1.774	.080	67.5	-0.15	-8.05	-17.69	141.9	-0.15	-0.64	-1.46
30	3	1.369	.080	76.3	5.21	-0.09	-18.59	131.3	0.20	0.50	-0.96
30	3	2.94	.000	84.1	0.46	-0.83	-18.30	61.5	-0.20	-0.15	-0.84
30	3	2.172	.000	84.1	-2.72	-1.01	-18.22	90	0.00	0.05	-0.69
30	3	1.849	.000	87.4	0.48	-3.21	-18.36	109.4	0.05	0.00	-0.67
30	3	1.636	.000	92.9	0.31	-3.48	-18.51	66.5	0.05	0.05	-0.62
30	3	0.898	.000	97.3	0.86	-1.64	-18.97	90	0.10	-0.10	-0.74
30	3	2.707	-.080	59.7	1.58	-1.24	-18.48	7.4	0.05	-0.15	-1.21
30	3	2.022	-.080	76.3	3.42	2.38	-18.74	50.2	0.05	0.35	-0.84
30	3	2.773	-.159	58.6	1.59	-3.08	-18.26	9.4	0.05	0.00	-1.46
30	3	1.413	-.159	58.6	-0.04	-4.58	-17.45	2	0.00	-0.15	-1.33
30	2.25	2.63	.120	45.0	-1.27	-2.22	-23.35	171.4	-0.17	0.29	-1.48
30	2.25	2.106	.120	51.7	0.22	2.32	-24.83	133	-0.51	-0.10	-1.33
30	2.25	1.496	.120	49.8	-0.16	0.75	-24.21	162	-0.23	0.51	-1.22
30	2.25	1.207	.120	50.8	-0.14	-0.85	-24.71	142.7	0.40	0.28	-1.14
30	2.25	1.075	.120	48.9	0.18	-1.79	-24.58	145.1	-0.12	-0.23	-1.14
30	2.25	2.854	.060	67.1	3.61	0.54	-25.02	137.8	0.00	-0.23	-0.80
30	2.25	1.9	.060	66.1	-2.22	2.02	-24.14	130.5	-0.12	0.40	-0.86
30	2.25	1.696	.060	60.3	-2.44	-2.10	-24.06	121.1	-0.40	-0.17	-0.91
30	2.25	1.519	.060	61.3	-4.78	-4.90	-24.13	124.6	-0.17	0.06	-1.00
30	2.25	1.153	.060	70.9	-1.81	-3.35	-24.07	132.2	-0.40	0.00	-0.91
30	2.25	2.343	.000	70.9	-0.42	0.57	-25.46	100.2	0.00	0.05	-1.03
30	2.25	1.759	.000	69.0	0.46	1.98	-25.11	104.1	0.00	0.00	-0.86
30	2.25	1.751	.000	67.1	-0.28	0.95	-24.86	94.5	0.00	0.12	-1.14
30	2.25	1.503	.000	68.0	0.30	0.60	-25.47	92.4	0.12	-0.23	-1.06
30	2.25	0.985	.000	72.8	0.48	-2.04	-24.72	94.5	-0.34	-0.17	-1.03
30	2.25	2.163	-.060	65.1	1.21	-3.14	-24.73	36.8	0.34	-0.34	-0.97
30	2.25	1.738	-.060	63.2	-4.17	-0.14	-25.06	54.9	-0.40	0.00	-0.91
30	2.25	2.197	-.120	53.6	2.98	-1.23	-24.65	99.8	0.00	0.68	-1.28
30	2.25	1.355	-.120	52.7	0.50	-0.16	-24.97	11.8	0.34	0.12	-1.34



ang	L/D	Vind	COM	t	xm	ym	zm	Psi	u	v	w
45	3.75	3.575	.194	50.7	0.12	0.32	-14.26	172.3	0.00	0.09	-1.13
45	3.75	3.319	.194	51.9	-0.20	0.38	-14.59	167.7	0.35	0.22	-1.15
45	3.75	2.758	.194	47.0	-0.24	-1.35	-14.32	167.8	0.00	0.05	-1.48
45	3.75	2.265	.194	48.2	-0.04	-1.08	-14.51	167.9	-0.05	0.13	-1.35
45	3.75	1.642	.194	48.2	-0.49	-2.04	-14.36	175.6	-0.09	-0.09	-1.50
45	3.75	3.642	.097	60.6	-1.42	2.08	-14.48	122.8	-0.13	0.35	-0.73
45	3.75	3.243	.097	54.4	-0.56	0.58	-14.36	134.2	-0.27	0.49	-0.82
45	3.75	2.724	.097	48.2	0.06	-0.32	-14.11	168	-0.05	0.13	-1.24
45	3.75	2.106	.097	47.0	-0.64	-1.64	-14.33	174.5	-0.05	-0.05	-1.41
45	3.75	1.805	.097	61.8	1.64	-6.38	-14.00	135.8	0.35	-0.49	-1.10
45	3.75	3.52	.000	81.6	-2.60	-2.35	-14.29	82.2	0.09	0.00	-0.71
45	3.75	3.441	.000	79.1	0.49	0.21	-14.64	132.8	0.05	0.13	-0.66
45	3.75	2.787	.000	48.2	-1.10	-3.50	-13.99	150.8	-0.09	0.04	-1.37
45	3.75	2.505	.000	96.5	-0.89	-2.92	-14.60	110.7	0.00	0.49	-0.69
45	3.75	3.717	-.097	63.1	-3.73	-2.57	-11.97	44.8	-0.13	-0.40	-0.95
45	3.75	2.892	-.097	66.8	-2.68	-0.35	-12.99	27.5	-0.18	0.31	-0.95
45	3.75	3.554	-.194	58.1	1.88	-3.62	-14.14	1.4	0.04	0.05	-2.03
45	3.75	2.884	-.194	59.4	0.68	-2.39	-14.49	3.2	0.09	0.05	-1.17
45	3	3.454	.159	53.1	0.09	1.50	-17.46	176.7	-0.05	0.10	-1.28
45	3	2.93	.159	47.6	-0.60	-1.55	-17.91	173.6	-0.10	0.00	-1.36
45	3	2.544	.159	46.5	0.13	-0.97	-17.33	170.1	0.05	-0.25	-1.53
45	3	2.031	.159	46.5	0.13	-1.07	-17.35	170.2	0.35	0.30	-1.19
45	3	1.731	.159	49.8	0.15	0.00	-17.86	160.5	0.00	0.25	-1.31
45	3	3.084	.080	67.5	2.84	4.67	-17.98	132.4	0.45	0.20	-0.82
45	3	3.1	.080	68.6	-2.75	2.99	-18.02	136.9	-0.15	0.25	-0.84
45	3	2.549	.080	48.7	0.94	-1.27	-18.00	176.2	0.30	0.10	-1.46
45	3	2.315	.080	67.5	-4.29	2.29	-18.08	139.9	-0.69	0.15	-0.81
45	3	1.64	.080	68.6	-3.57	-7.74	-17.43	151.6	-0.15	0.25	-0.91
45	3	3.564	.000	85.2	-0.36	0.42	-18.67	113.5	0.05	-0.05	-0.59
45	3	2.959	.000	85.2	-0.07	-0.04	-18.62	50.2	0.05	0.00	-0.74
45	3	2.597	.000	55.3	0.28	-3.60	-18.65	92.7	-0.05	-0.05	-0.74
45	3	2.036	.000	55.3	-3.16	-2.46	-18.30	82.1	0.00	0.15	-0.52
45	3	1.522	.000	88.5	-0.58	-2.68	-18.30	80	0.55	0.05	-0.54
45	3	3.566	-.080	76.3	6.18	-5.69	-18.27	53.6	0.40	-0.35	-0.79
45	3	2.722	-.080	69.7	-1.68	-4.64	-18.25	40.1	-0.05	-0.45	-0.79
45	3	3.293	-.159	54.2	-1.41	-4.36	-16.93	5.2	-0.05	0.10	-1.26
45	3	2.208	-.159	57.5	-0.05	-2.53	-18.07	11.6	0.05	-0.10	-1.14
45	2.25	2.828	.120	50.8	1.37	-5.20	-23.77	144.9	0.28	0.17	-1.40
45	2.25	2.402	.120	51.7	-4.19	-4.13	-23.86	140.4	0.12	-0.12	-1.20
45	2.25	2.147	.120	49.8	-0.48	-3.99	-23.43	153.1	0.05	0.12	-1.31
45	2.25	1.746	.120	51.7	-4.37	-3.87	-23.57	149	0.00	0.51	-1.51
45	2.25	1.557	.120	50.8	0.08	-2.72	-24.15	151.1	-0.12	0.06	-0.94
45	2.25	2.996	.060	65.1	-3.37	-2.84	-23.39	144.3	0.00	0.17	-0.68
45	2.25	2.624	.060	57.5	0.63	2.06	-24.93	147.5	0.40	0.00	-1.20
45	2.25	2.296	.060	62.3	-2.04	-4.17	-24.32	141	-0.17	0.12	-0.97
45	2.25	1.947	.060	52.7	-3.27	-5.75	-23.56	144.5	0.05	-0.34	-1.05
45	2.25	1.488	.060	66.1	2.82	0.26	-24.43	124.6	0.34	-0.12	-0.74
45	2.25	3.289	.000	60.3	0.50	-3.99	-24.27	79.2	0.23	0.12	-0.85
45	2.25	2.831	.000	65.1	0.00	-5.85	-24.11	107	-0.17	0.12	-1.17
45	2.25	2.177	.000	60.3	0.56	-2.72	-24.74	88.6	0.00	0.00	-1.06
45	2.25	2.033	.000	61.3	1.51	-2.86	-24.90	77.9	0.12	-0.06	-0.94
45	2.25	1.497	.000	63.2	-0.99	-2.96	-23.96	143.4	-0.12	0.00	-0.94
45	2.25	2.902	-.060	64.2	1.29	-2.50	-23.80	34.5	0.17	-0.17	-0.63
45	2.25	2.22	-.060	60.3	-0.30	-0.65	-22.83	37.8	0.23	-0.12	-1.14
45	2.25	2.773	-.120	52.7	-1.90	-0.95	-24.51	26.6	0.06	0.11	-1.31
45	2.25	2.175	-.120	51.7	-1.55	0.26	-23.37	38.3	0.63	0.40	-1.03

ang	L/D	Vind	COM	t	xm	ym	zm	Psi	u	v	w
60	3.75	4.204	.194	44.5	-0.11	-0.56	-13.79	177.3	0.18	-0.09	-1.10
60	3.75	3.629	.194	43.3	0.17	-0.71	-13.62	176	-0.09	0.05	-1.26
60	3.75	3.35	.194	47.0	-0.39	-0.33	-14.29	175.4	-0.22	0.09	-1.46
60	3.75	2.269	.194	45.8	-0.02	-0.86	-14.01	174.9	0.00	0.27	-1.66
60	3.75	1.938	.194	47.0	0.00	-0.93	-14.53	171.8	0.00	0.00	-1.48
60	3.75	4.412	.097	55.6	0.61	1.93	-14.44	133.1	0.13	0.31	-0.75
60	3.75	3.69	.097	53.2	-0.77	1.66	-14.20	132.8	0.18	0.62	-0.73
60	3.75	3.601	.097	54.4	-0.33	1.61	-14.60	124.5	0.27	0.40	-0.80
60	3.75	2.986	.097	59.4	0.52	2.35	-14.64	138.8	0.05	0.40	-0.73
60	3.75	2.226	.097	47.0	-0.18	-0.70	-14.23	178.2	0.05	0.00	-1.50
60	3.75	4.292	.000	69.3	0.73	1.24	-14.57	129.3	0.27	-0.09	-0.57
60	3.75	3.711	.000	85.3	-1.64	-1.01	-14.33	72.2	0.00	-0.09	-0.53
60	3.75	3.257	.000	66.8	-0.88	1.66	-14.45	131.5	-0.44	0.09	-0.53
60	3.75	2.795	.000	59.4	-1.33	0.83	-14.83	86.5	-0.13	0.22	-0.53
60	3.75	1.758	.000	96.5	-0.54	-2.45	-14.40	90.7	0.13	-0.27	-0.44
60	3.75	4.157	.000	75.4	0.17	-1.10	-14.77	104.4	0.05	-0.40	-0.42
60	3.75	4.154	-.097	63.1	-3.37	-2.33	-12.82	31.6	-0.05	-0.18	-1.04
60	3.75	3.661	-.097	63.1	2.91	-2.33	-13.46	52	0.71	-0.18	-1.04
60	3	3.92	.159	44.2	0.27	-1.15	-17.72	169.5	0.30	0.15	-1.09
60	3	3.277	.159	46.5	0.02	-0.18	-17.63	158.1	-0.05	0.10	-1.14
60	3	2.816	.159	46.5	-0.02	-1.28	-18.07	159	0.00	-0.05	-1.36
60	3	1.905	.159	48.7	0.21	-0.69	-18.21	160.3	-0.10	-0.05	-1.38
60	3	1.889	.159	48.7	0.00	0.51	-18.04	167.7	0.05	0.05	-1.28
60	3	3.868	.080	46.5	-0.21	-2.29	-17.57	159.1	-0.25	0.05	-1.46
60	3	4.077	.080	57.5	3.01	3.07	-17.95	136.3	0.59	0.40	-1.01
60	3	3.239	.080	47.6	-0.88	-1.88	-18.01	146.6	-0.30	-0.15	-1.16
60	3	2.758	.080	47.6	-1.01	-0.83	-17.55	171.2	0.15	0.15	-1.21
60	3	2.063	.080	49.8	-0.66	-2.56	-18.04	141	-0.15	-0.30	-1.19
60	3	3.831	.000	79.6	-0.10	1.15	-17.79	139.2	0.00	-0.25	-0.69
60	3	3.346	.000	78.5	-0.63	1.49	-18.50	89	-0.05	-0.20	-0.84
60	3	2.978	.000	48.7	-0.39	-2.74	-18.11	131.5	-0.40	-0.55	-0.74
60	3	2.421	.000	73.0	-4.18	-0.69	-18.35	72.7	0.00	0.05	-0.72
60	3	1.756	.000	84.1	2.53	1.15	-18.32	124.8	-0.25	0.05	-0.79
60	3	3.702	.000	77.4	0.60	-2.69	-17.70	128.1	-0.20	-0.05	-0.49
60	3	4.196	-.080	65.3	0.07	-4.79	-17.83	44.2	0.00	-0.59	-0.89
60	3	3.085	-.080	61.9	-4.58	-1.90	-16.24	53.4	-0.45	-0.74	-0.83
60	2.25	3.455	.120	44.1	0.04	-1.43	-24.20	146.3	0.00	-0.29	-1.22
60	2.25	3.085	.120	46.0	-1.37	-1.90	-24.13	154.1	-0.28	-0.12	-1.28
60	2.25	2.406	.120	46.9	-0.83	0.54	-24.31	157	0.40	-0.06	-1.37
60	2.25	1.76	.120	52.7	0.28	-2.52	-24.50	134.4	0.00	0.34	-1.14
60	2.25	1.86	.120	47.9	1.37	-1.55	-24.43	160.3	0.28	0.06	-1.43
60	2.25	3.554	.060	49.8	-1.55	-2.74	-24.16	141.3	0.11	-0.40	-1.03
60	2.25	3.15	.060	65.1	-0.34	-1.57	-24.04	141.3	-0.63	-0.12	-0.88
60	2.25	2.808	.060	57.5	3.87	1.07	-24.57	123.1	0.00	-0.45	-0.91
60	2.25	2.374	.060	59.4	-0.28	-3.81	-23.90	147.1	0.28	0.57	-0.77
60	2.25	1.864	.060	70.9	-0.75	-2.06	-24.12	139.4	0.06	0.11	-1.00
60	2.25	3.5	.000	62.3	-2.02	-1.65	-23.98	102.5	0.12	0.12	-1.17
60	2.25	2.996	.000	63.2	1.90	-2.22	-24.86	72.6	0.06	0.00	-0.97
60	2.25	2.6	.000	61.3	1.83	0.06	-24.59	36.6	0.06	0.23	-1.06
60	2.25	2.251	.000	62.3	1.90	-3.87	-24.55	61.7	0.00	0.06	-0.94
60	2.25	1.715	.000	61.3	-1.11	-3.23	-24.39	77.2	-0.23	-0.12	-0.97
60	2.25	3.542	.000	60.3	-2.08	-1.01	-23.83	145.7	-0.06	0.00	-1.03
60	2.25	3.649	-.060	66.1	-1.11	-3.10	-24.04	54.5	-0.17	0.12	-0.74
60	2.25	2.818	-.060	66.1	-2.00	0.32	-24.64	58.1	-0.11	0.00	-1.00

ang	L/D	Vind	COM	t	xm	ym	zm	Psi	u	v	w
75	3.75	4.51	.194	42.0	-0.01	-0.69	-14.17	178.7	0.00	0.04	-1.17
75	3.75	4.099	.194	42.0	-0.13	-0.71	-14.29	177	-0.04	0.18	-1.50
75	3.75	2.984	.194	45.8	0.20	-0.01	-14.50	176.9	-0.05	0.05	-1.17
75	3.75	3.303	.194	42.0	0.02	-0.57	-13.64	177.1	-0.09	0.04	-1.81
75	3.75	4.717	.097	40.8	-0.06	-1.16	-13.65	172.4	-0.05	-0.09	-1.52
75	3.75	4.004	.097	42.0	-0.04	-1.26	-13.46	178.2	0.22	-0.04	-1.20
75	3.75	2.916	.097	45.8	0.00	-1.16	-14.46	175.5	-0.13	0.05	-1.19
75	3.75	1.735	.000	68.0	-1.02	0.42	-14.35	100.2	0.09	-0.49	-0.64
75	3.75	1.855	.000	79.1	-0.58	1.58	-14.27	128.3	0.35	0.40	-0.80
75	3	4.16	.159	45.4	-0.31	-0.92	-17.76	161.2	0.20	-0.10	-1.21
75	3	3.549	.159	44.2	0.02	-0.92	-17.66	174.5	-0.05	0.00	-1.33
75	3	2.564	.159	46.5	0.30	-0.22	-17.98	165	-0.10	-0.05	-1.38
75	3	2.673	.159	48.7	-0.16	-0.40	-18.05	157.6	0.40	-0.15	-1.16
75	3	4.322	.080	46.5	-1.22	-1.07	-17.99	165.9	0.20	-0.05	-1.28
75	3	3.706	.080	46.5	1.25	-0.80	-17.75	147.9	0.50	-0.20	-1.21
75	3	2.747	.080	45.4	0.03	-0.71	-17.65	171.4	0.15	0.10	-1.51
75	3	4.351	.000	43.1	-0.13	-1.10	-17.88	147.3	-0.05	-0.15	-1.09
75	3	3.507	.000	60.8	-0.46	2.19	-18.14	73.1	0.05	-0.05	-0.81
75	2.25	3.598	.120	43.1	0.04	0.40	-24.43	156.5	0.00	-0.17	-1.20
75	2.25	3.107	.120	46.0	-0.22	-2.38	-24.00	143.7	-0.23	-0.46	-1.14
75	2.25	2.155	.120	54.6	0.08	-8.21	-23.97	129	-0.11	-0.34	-1.14
75	2.25	2.391	.120	46.0	-0.77	0.81	-24.64	147.3	0.40	0.28	-1.20
75	2.25	3.845	.060	52.7	1.31	-5.73	-22.82	124.4	-0.05	-0.05	-1.11
75	2.25	3.137	.060	60.3	-0.97	1.31	-24.39	136	-0.23	0.34	-0.71
75	2.25	2.326	.060	65.1	0.04	1.21	-25.33	127.3	0.23	0.00	-0.74
75	2.25	3.98	.000	56.5	-1.69	0.69	-24.58	90	0.17	0.06	-0.97
75	2.25	3.172	.000	60.3	0.08	1.69	-24.86	92.2	-0.06	-0.17	-0.66

THIS PAGE INTENTIONALLY LEFT BLANK

## LIST OF REFERENCES

Arnone, R. A., and Bowen, Prediction Model of the Time History Penetration of a Cylinder through the Air-Water-Sediment Phases. NCSC letter report T34, Naval Coastal Systems Center, Panama City, FL, 1980.

Boorda, J. M., "Mine Countermeasures - An Integral Part of our Strategy and our Forces." Federation of American Scientists.

(<http://www.fas.org/man/dod-101/sys/ship/weaps/docs/cnopaper.htm>)

Chu, P.C., V. Taber, and S.D. Haeger, Environmental Sensitivity Study on Mine Impact Burial Prediction Model. Proc. of the Fourth International Symposium on Technology and the Mine Problem, April 2000, Naval Postgraduate School.

Department of the Navy. U.S. Naval Mine Warfare Plan Fourth Edition, Programs for the Millennium. Washington, D.C., January 2000.

Fischer, Ben B. At Cold War's End: US Intelligence on the Soviet Union and Eastern Europe, 1989-1991. Springfield: National Technical Information Service, 1999.

Hurst, R.B. Mine Impact Burial Prediction Model - Technical Description of Recent Changes and Developments. Defense Scientific Establishment, Auckland, New Zealand, Report 149.

Lehr, S.E., Mine Warfare: To Enable Maneuver, Amphibious Warfare Conference, 26 April 2000. PowerPoint Presentation.

(<http://www.exwar.org/awcfinal/6th/n852mines.ppt>)

Lott, D.F., K. Williams, and D. Jackson, Mine Burial in Carbonate Sediments. Proc. of the Technology and Mine Problem Symposium, November 1996, Naval Postgraduate School.

Rhodes, J.E., G. Holder, Concept for Future Naval Mine Countermeasures in Littoral Power Projection, 1 May 1998.

(<http://192.156.75.102/mcm.htm>)

Satkowiak, L. J., User's Guide for the Modified Impact Burial Prediction Model. NCSC TN 884-87. Naval Coastal Systems Center, Panama City, FL, 1987.

Smith, T., Mine Burial Impact Prediction Experiment. *Master Thesis*, Naval Postgraduate School, Monterey, CA, 2000.

Taber, V., Environmental Sensitivity Study on Mine Impact Burial Prediction Model. *Master Thesis*, Naval Postgraduate School, Monterey, CA, 1999.

Walpole, Ronald, Raymond Myers and Sharon Myers. Probability and Statistics for Engineers and Scientists, Sixth Edition. New Jersey, Prentice Hall, 1998.

THIS PAGE INTENTIONALLY LEFT BLANK

## INITIAL DISTRIBUTION LIST

1. Defense Technical Information Center.....2  
8725 John J. Kingman Road, Suite 0944  
Ft. Belvoir, VA 22060-6218
2. Dudley Knox Library.....2  
Naval Postgraduate School  
411 Dyer Road  
Monterey, CA 93943-5101
3. Dr. Richard Bennett  
SEAPROBE, Inc.  
Picayune, MS  
rbennett@datastar.net
4. LCDR Jim Berdeguez  
Chief of Naval Operations N75  
Washington, D.C.  
berdeguez.james@hq.navy.mil
5. CDR Jeff Best  
Commander Naval Meteorology and Oceanography  
Stennis Space Center, MS  
bestj@nmopdc.navy.mil
6. Dr. Wayne Dunlap  
Off Shore Technology Research Center  
College Station, TX  
wad2094@zeus.tamu.edu
7. Dr. Peter Fleischer  
Naval Oceanographic Office  
Stennis Space Center, MS  
fleischerp@navo.navy.mil
8. Dr. Steve Haeger  
Naval Oceanographic Office  
Stennis Space Center, MS  
haegers@navo.navy.mil
9. Dr. Yuming Liu  
Department of Ocean Engineering Massachusetts Institute of Technology  
Cambridge, MA  
liu@turbulence.mit.edu

10. LCDR Paul Oosterling  
Chief of Naval Operations N96  
Washington, D.C.  
oosterling.paul@hq.navy.mil
11. Dr. Mike Richardson  
Naval Research Laboratory  
Stennis Space Center, MS  
mike.richardson@nrlssc.navy.mil
12. Dr. Richard Spinrad  
Chief of Naval Operations N96  
Washington, D.C.  
spinrad.richard@hq.navy.mil
13. Dr. Robert Stoll  
Columbia University  
Palisades, N.Y.  
stoll@deo.Columbia.edu
14. Dr. Philip Valent  
Naval Research Laboratory  
Stennis Space Center, MS  
phil.valent@nrlssc.navy.mil
15. Dr. Linwood Vincent  
Office of Naval Research  
Arlington, VA  
vincenc@onr.navy.mil
16. Dr. Roy Wilkins  
Office of Naval Research  
Arlington, VA.  
wilkinr@onr.navy.mil
17. Dr. Dick Yue  
Department of Ocean Engineering Massachusetts Institute of Technology  
Cambridge, MA  
yue@mit.edu